Cardiovascular toxicity of combined administration of ethanol and combination antiretroviral therapy in HIV naïve diabetic Sprague Dawley male rats

Mcebo Treasure Zwane

Student number: 1473425

A dissertation submitted to School of Anatomical Sciences Faculty of Health Sciences University of the Witwatersrand, in fulfilment of the requirement for the degree of Master of Science in Medicine

Supervisors
Prof Ejikeme Mbajiorgu
Dr Jaclyn Johnson

DECLARATION

I, the undersigned hereby declare that the work contained in this thesis is my own original work and that I have not previously in its entirety or in part submitted it at any university for a degree.

Signature

Name in full

Mcebo Treasure Zwane

Date

20 / 09 / 2024

DEDICATION

To my mother, the reason I started, and the only reason I made it through. I love you.

ABSTRACT

Atripla, a combination antiretroviral drug (cART) was the first once daily antiretroviral treatment to be approved by FDA in 2008. Since then, Atripla has been the first line of treatment in HIV/AIDS management, and one of widely used medications, with 76% of people living with HIV on medication. The incidence of diabetes in Africa has increased, owing to decreased mobility and increasing urbanization in the continent. Excessive alcohol consumption on the continent, especially in South Africa is common across all age groups, with ethanol (alcohol) often taken concomitantly with antiretroviral drugs. This results in co-presence of cART and alcohol in a diabetic condition.

Adult male Sprague-Dawley rats divided into 8 groups were used: untreated (negative control), diabetic (diabetes, diabetes + alcohol, diabetes + Atripla, and diabetes + Alcohol + Atripla), and treated (alcohol alone, alcohol and Atripla, and Atripla alone). Harvested hearts' morphology was investigated (surface area and weight) before being processed and histological investigations were carried out (H&E for structural differences, Pentachrome for collagen and muscle profile, and Verhoeff Van Gieson for collagen and elastic fiber profiling). Fasting glucose levels were measured and recorded throughout the study. Enzyme-linked immunosorbent assays for troponin I&T (myocardial degeneration), MDA, and GPx (oxidative stress) were performed. Additionally, immunohistochemistry for expression of eNOS (as a marker for endothelial homeostasis) and c-reactive protein CRP (as a marker for inflammation) were performed.

The fasting glucose was significantly increased in diabetes + Alcohol + Atripla group (DBALCARV) throughout the study period ($p=0.001$), and morphological examination revealed a decrease in body weight ($p=0.001$) and total surface area of the heart ($p=0.01$). The coronary

artery had a significant decrease in tunica media thickness ($p=0.02$), while the aorta was increased ($p=0.001$). The collagen in the coronary arteries was significantly increased when examined with Pentachrome special stain ($p=0.032$). The collagen was also significantly increased in both ventricle ($p=0.015$) and atrium ($p=0.013$). Qualitative analysis of c-reactive protein and endothelial nitric oxide synthase immunohistochemistry showed a reduction in localization of both antibodies.

In conclusion, combination of cART, diabetes, and alcohol resulted in changes in cardiac and vascular morphology, fasting glucose, body weight, oxidative stress, myocardial degradation markers, and collagen expression.

ACKNOWLEDGEMENTS

With all my thanks to:

- My wonderful family, whose irrational belief in me that kept me going through the more impossible times.
- My mother, for her emotional presence and support and her financial support in funding both my studies and a portion of the research.
- My supervisors, who believed in both me and the research and encouraged me through the most stressful and difficult disappointments. Your passion for science is inspiring, and I am truly appreciative.
- My co-researcher Mr. Mmotong Mahloko for being an amazing teammate through and through.
- Mrs. Hasiena Ali for answering the silliest of questions with so much kindness and care, and for imparting her wealth of knowledge with so much grace.
- My colleagues in the Fishbowl for making me smile during the most stressful year of my life. I appreciate you.

Table of contents

List of figures

List of tables

ABBREVIATIONS

CVD – cardiovascular disease

CVS – cardiovascular system

cART – combination antiretroviral therapy

ART – antiretroviral therapy

HAART – highly active antiretroviral therapy

PEP – pre-exposure prophylaxis

NNRTI – non-nucleoside reverse transcriptase inhibitor

NRTI – nucleoside reverse transcriptase inhibitor

PI – protease inhibitor

HIV/AIDS – human immunodeficiency virus/acquired immunodeficiency syndrome

PLWHA – people living with HIV/AIDS

ARV – antiretroviral

T2DM – type 2 diabetes mellitus

T1DM – type 1 diabetes mellitus

ALC – alcohol

DB – diabetes

FDA – food and drug administration

ALCARV – alcohol and antiretroviral

DBARV – diabetes and antiretroviral

DBALC – diabetes and alcohol

DBALCARV – diabetes and alcohol and antiretroviral

NC – negative control

eNOS – endothelial nitric oxide synthase

NOS – nitric oxide synthase

NO – nitric oxide

MDA – Malondialdehyde

GPx – glutathione peroxidase

CRP – c-reactive protein

TNF-α – tumor necrosis factor alpha

LDL – low density lipoprotein

HDL – high density lipoprotein

CYP – cytochrome p450

ROS – reactive oxygen species

CT – connective tissue

DTG – dolutegravir

H&E – haematoxylin and eosin

CAS – central animal services

APES – 3-aminopropyltriethoxysilane

OD – optical density

AF – area fraction

AFM – area fraction muscle

AFC – area fraction collagen

AFE – are fraction elastic fibers

AFA – area fraction atrium

AFV – area fraction ventricle

IHC – immunohistochemistry

ELISA – enzyme-linked immunosorbent assay

SEM – standard error of the mean

AREC – Animal Ethics and Research Committee facility

CHAPTER 1

INTRODUCTION

Cardiac diseases resulting from structural disturbances are common and directly cause defects in cardiac function (Schwinger, 2021). The vascular system, particularly the large and coronary vessels, also has cardiac associations that involve functional issues like endothelial dysfunction, hypertension, and damage to cardiomyocytes (Hadi and Suwaidi, 2007; Jia and Sowers, 2021; Wei *et al.*, 2022). As a result, cardiovascular diseases (CVD) have become widespread and are a major contributor to morbidity and mortality (Roth *et al.*, 2020). While there are numerous studies and investigations exist in the literature on CVD implicated in nephropathy (Jankowski *et al.*, 2021), neuropathy (Serhiyenko and Serhiyenko, 2018), and retinopathy (Simó *et al.*, 2019), limited information is available on cardiovascular toxicity caused by pharmaceutical drugs and lifestyle agents.

Cardiotoxicity has been reported for pharmaceutical agents such as chemotherapeutic and anti-infection medication (Dong and Chen, 2018; Birkhoelzer, Cowan and Guha, 2021)**.** However, the impact of combination antiretroviral therapy (cART) on CVD has only been studied in individuals infected with human immunodeficiency virus (HIV) (Antony *et al.*, 2020; Jia and Sowers, 2021; Xu *et al.*, 2021; Kovacs, Kress and Belin de Chantemèle, 2022). Therefore, it is necessary to investigate the direct cardiovascular toxic effects of cART in HIV-naïve individuals as a reference for better-managing patients who may receive cART as pre-exposure prophylaxis (PEP).

Additionally, medications like cART can have multiple and divergent effects, such as insulin insensitivity and the potential induction of type 2 diabetes (T2D) (da Cunha *et al.*, 2020),. This

makes individuals on cART more susceptible to developing T2D as a co morbidity. Moreover, alcohol consumption is prevalent among adult males in South Africa and Sub-Saharan Africa (Mpinganjira *et al.*, 2023), with South Africa having one of the highest rates of alcohol consumption globally (Morojele *et al.*, 2006). The high caloric levels in individuals who frequently consume alcohol also predispose them to developing T2D (Polsky and Akturk, 2017), These factors contribute to an increased number of diabetic individuals on cART PEP regimen who frequently consume alcohol. Therefore, it is invaluable to document cardiac toxicity of concomitant use of cART and alcohol in diabetic individuals.

The independent effects of alcohol, diabetes, and cART-treated HIV-positive state on cardiovascular system have been extensively investigated. These effects are associated with redox imbalance characterized by elevated oxidants and depleted antioxidants (Laonigro *et al.*, 2009; Bhatt *et al.*, 2015; Doody *et al.*, 2017). Therefore, it is important to study redox imbalance in combination with these parameters (cART, alcohol, and diabetes).

Oxidative stress resulting from these factors has been linked to structural perturbations in the coronary artery and aortic vascular walls (Sena *et al.*, 2018). These vascular perturbations have been reported independently in cART-treated HIV-positive patients (Kovacs, Kress and Belin de Chantemèle, 2022), alcohol use (Noflatscher *et al.*, 2020), and diabetic condition (Bhatt *et al.*, 2015). Furthermore, they induce an inflammatory response, leading to elevated expression of inflammatory markers in cardiomyocytes and coronary vessels (Shikuma *et al.*, 2011; Iakunchykova *et al.*, 2020; Mirza *et al.*, 2012). This indicates endothelial toxicity and cardiac damage.

In addition, the regulation of cardiomyocyte cytoskeleton degradation and protection against fibrosis and hypertrophy relies on endothelial nitric oxide synthase (eNOS), which is independently decreased in cART-treated HIV positive individuals, alcohol and diabetes. (Kovacs *et al.*, 2021; Toda and Ayajiki, 2010; Felaco *et al.*, 2001). Moreover, the disassembly of dying or dysfunctional cardiomyocyte sarcomere leads to an elevation of plasma cardiac troponin (I and T) levels. This has been reported independently in cART-treated HIV-positive individuals, alcohol, and diabetes (Foster *et al.*, 2019; Hammarsten *et al.*, 2018; Fernández-Solà, 2020; Segre *et al.*, 2015).

Therefore, it is crucial to investigate the cardiotoxic effects of cART in HIV-naive individuals when comorbidities such as diabetes and alcohol use are present.

CHAPTER 2

LITERATURE REVIEW

2.1 Antiretroviral therapy

The number of people living with HIV/AIDS (PLWHA) in Eastern and Southern Africa is reported to continually increase in recent decades (UNAIDS, 2022). The national health anti-HIV/AIDS program is so huge that it puts a strain on public health systems and has led to an increase in antiretroviral therapy (ART) programs in these African regions (Vandormael *et al.*, 2019). The introduction of highly active antiretroviral therapy (HAART) in 1996 has successfully and significantly reduced the mortality of PLWHA (Melhuish and Lewthwaite, 2018; Vandormael *et al.*, 2019), with the incidence rate of HIV in this region dropping by 43% between 2012 and 2017 (Vandormael *et al.*, 2019). Atripla® was the first one-pill daily HIV treatment regimen that was approved by Food and Drug Administration (FDA) in 2006, combining the active ingredients of a Non-nucleoside reverse transcriptase inhibitor (NNRTI) (efavirenz) and two Nucleoside reverse transcriptase inhibitors (NRTI), consisting of Tenofovir disoproxil fumarate and emtricitabine, into one convenient pill (Julg and Bogner, 2008). Despite its success in controlling opportunistic infections in HIV infected individuals, a correlation has been established between chronic use of Atripla, a combination Antiretroviral drug therapy (cART), and the development of type 2 diabetes mellitus (T2DM) metabolic syndrome (da Cunha *et al.*, 2020). Studies have reported that T2DM is two to five times more prevalent in cART treated PLWHA compared to untreated cohort (Mbanya *et al.*, 2010; Husain *et al.*, 2017). Additionally, Protease inhibitors (PI) and NNRTIs interfere with transportation of GLUT-4 from

cytosol to cell surface thereby inhibiting glucose uptake (Husain *et al.*, 2017), culminating in increased body fat, lipodystrophy and subsequently insulin resistance, insufficiency, or both (da Cunha *et al.*, 2020). These metabolic perturbations reported in type 2 Diabetes Mellitus (T2DM), HIV/AIDS, and cART are further independently implicated in cardiovascular toxicity (Randell and Moyle, 2009; Polsky and Akturk, 2017) which is a major health problem and calls for attention.

2.2 Diabetes

Diabetes is a metabolic condition characterized either by pancreas inability to produce insulin (type 1 diabetes mellitus), the body's inability to utilize insulin during metabolism (T2DM), or both (Bastaki, 2005). While type 1 diabetes mellitus (T1DM) is typically congenital, type 2 diabetes mellitus (T2DM) is more commonly an acquired illness, influenced not only by genetics but by factors such as lifestyle choices, urbanization, decrease in physical activity, and change in dietary composition which have significantly increased the incidence of T2DM in Southern Africa (Mbanya *et al.*, 2010). According to International Diabetes Federation, an estimated 24 million adults are living with diabetes in Africa as of 2021, and that number is estimated to escalate to 55 million individuals by 2045 (International Diabetes Foundation, 2021). Diabetes results in hyperglycemia, low-grade inflammatory perturbations, endothelial dysfunction, and an imbalance in redox reactions (Hadi and Suwaidi, 2007; Bhatt *et al.*, 2015; Sharif *et al.*, 2021) which has led to recent attention and research into diabetes-induced metabolic disruptions, endocrine and systemic organ pathologies (Brunová, 2004; Cheung and Wong, 2008; Lehrke and Marx, 2017). However, cardiovascular diseases, as a predictor of mortality in PLWHA or diabetic individuals (Dubé *et al.*, 2008; Raghavan *et al.*, 2019) is often underestimated and may contribute to lack of needed attention towards implementation of early intervention strategies

necessary to improve the quality of lives of these individuals. Therefore, the rising epidemiology of diabetes in addition to diabetogenic effect of cART warrants that cardiovascular impact of chronic cART medication in a diabetic model be further investigated.

2.3 Diabetes epidemic and alcohol abuse

In addition to diabetic epidemic and prevalent cART programs due to high HIV/AIDS incidence, South Africa is also plagued with excessive alcohol use, and recorded as having one of the highest amounts of alcohol consumption across different age groups in the world (Morojele *et al.*, 2006). In 2019, South Africa's consumption of alcohol per capita was 11 liters (Cupido, 2021), and heavy alcohol drinking has been shown to increase the possibility of HIV infection and incidence of T2DM due to high caloric content of alcohol (Polsky and Akturk, 2017), with attendant lipodystrophy (a change in fat distribution) (Cheng *et al.*, 2009), insulin resistance and gestational diabetes (Howard, Arnsten and Gourevitch, 2004; Ehehalt *et al.*, 2015). Combination anti-retroviral therapy, alcohol, and diabetes independently alter lipid and cholesterol profiles leading to vascular dysfunction and consequently cardiovascular pathologies (Funderburg and Mehta, 2016; Minzer, Losno and Casas, 2020; Wang *et al.*, 2022). Therefore, this study is designed against this backdrop to investigate potential cardiovascular histopathology that may arise due to chemo toxic effects of diabetes, cART, alcohol, and their combinations.

2.4 The cardiovascular system

The mammalian cardiovascular system (CVS) is made of a four chambered muscular heart and blood vessels; coronary vessels are abundant on the outer pericardium of the heart and are essential for maintaining cardiac tissue (Ross, 2018; Arackal and Alsayouri, 2022). These coronary vessels are muscular arteries with unusually thick walls, consisting of an outer

collagenous tunica adventitia, middle vascular smooth muscle tunica media and, innermost layer consisting of connective tissue and endothelium called tunica intima (Taylor and Bordoni, 2022). The endothelium expresses a variety of surface adhesion molecules and receptors for low density lipoprotein (LDL), and insulin (Galley and Webster, 2004) in response to different stimuli and maintaining blood homeostasis (Chia, Teo and Yeo, 2020). The endothelium and myocytes are sensitive cells which respond to perturbation in lipids, hypoxia (Galley and Webster, 2004) and reactive oxygen species (ROS) (Marincowitz *et al.*, 2019), which are common factors independently associated with diabetes, cART, and alcohol. Furthermore, oxidative stress and endothelial pathology induced by diabetes, cART, and or alcohol cumulates in structural modification of cardiac tissue resulting in dysfunctional cardiovascular health (Hijmering *et al.*, 2007; Odegaard *et al.*, 2016; Watanabe *et al.*, 2016).

2.4.1 Oxidative stress as a mechanism for cardiotoxicity

Alcohol is metabolized by dehydrogenase and cytochrome-P (CYP) enzymes which may lead to generation of reactive oxygen species (ROS), both enzymatic pathways lead to elevated acetaldehyde levels with attendant impact on oxidative stress (Laonigro *et al.*, 2009; Doody *et al.*, 2017). Additionally, cART is reported to impair mitochondrial function and induce redox imbalance (Doody *et al.*, 2017). Remarkably, cART is also metabolized by CYP enzyme (Walubo, 2007), therefore it is vital to investigate the impact of alcohol-cART interaction on oxidative stress. Furthermore, hyperglycemia in diabetes induces a redox reaction imbalance with oxidative stress implications in cardiac and vascular tissue (Bhatt *et al.*, 2015; Yan, 2018). Considering the independent effects of diabetes, cART, and alcohol on oxidative stress induced endothelial dysfunction and cardiac toxicity, it is important to evaluate the combinatorial effect of these factors on systemic oxidative stress.

2.4.2 Role of lipids in atherosclerosis

Diabetes, cART, and alcohol are independently associated with formation of atherosclerotic plaques (Funk, Yurdagul and Orr, 2012; Noflatscher *et al.*, 2020; Kovacs, Kress and Belin de Chantemèle, 2022) which arise due to accumulation of low density lipoproteins (LDL) which are oxidized by increased reactive oxygen species (ROS), engulfed by macrophages, transformed into foam cells and often contain a fibrous cap of smooth muscle cells (Rafieian-Kopaei *et al.*, 2014). The treatment of PLWHA with cART is associated with a higher incidence of metabolic conditions such as obesity, dyslipidemia, hypertension, elevated LDL cholesterol and high-density lipoprotein (HDL) cholesterol (Funderburg and Mehta, 2016) compared to their cART naïve counterparts (Masenga *et al.*, 2020; Sapuła *et al.*, 2022). Additionally, alcohol use has mixed reported effects, with heavy alcohol intake and low alcohol intake contributing to elevated LDL and HDL levels respectively with associated atherosclerotic plaque formation or cardio-protective effects respectively (Hong *et al.*, 2015; Minzer, Losno and Casas, 2020). Furthermore, diabetes is associated ROS production, dyslipidemia which leads to LDL uptake by immune cells forming foam cells and atherosclerotic plaques (Wang *et al.*, 2022). While LDL cholesterol may increase formation of atherosclerotic lesions, HDL cholesterol has preventative effects on formation of atherosclerotic lesions (Huff, Boyd and Jialal, 2022). Therefore, these scenarios warrant investigation into the interactive effects of diabetes, cART, and alcohol on vascular wall perturbation in coronary and aortic vessels.

2.4.3 Cardiovascular effects of inflammatory response

Independently, alcohol, diabetes and cART induce accumulation of engulfed LDLs by macrophages (Funk, Yurdagul and Orr, 2012; Noflatscher *et al.*, 2020; Kovacs *et al.*, 2021).

These macrophages are stimulated to secrete inflammatory cytokines during atherosclerotic plaque formation (Graves and Kayal, 2008; Piano, 2017; Osuji *et al.*, 2018). However, the combinatorial effects of alcohol use, cART, and diabetes on this inflammatory response remain undocumented. The quantity of alcohol consumed as well as age and gender are mostly reported to induce mixed effects on cardiovascular system (Hvidtfeldt *et al.*, 2010; Brien *et al.*, 2011; Piano *et al.*, 2020). However, heavy alcohol consumption is directly implicated in elevation of pro-inflammatory protein TNF-α and plasma proteins, C-reactive protein (CRP) (Alvarez Cooper *et al.*, 2020; Iakunchykova *et al.*, 2020). An increased amount of TNF-α is produced by myocardial and coronary intima macrophages and implicated in cardiac damage, remodeling, apoptosis, and endothelial dysfunction while CRP is produced by cardiomyocytes as a downstream indicator for cardiac inflammatory response and cardiovascular injury with attendant coronary endothelial toxicity (Joshi *et al.*, 2012; Urschel and Cicha, 2015). Similarly, alcohol induced inflammation is often accompanied by reduction of anti-inflammatory mediators such as IL-10 (Imhof and Koenig, 2003), therefore alcohol use may induce a net inflammatory state and myocardial cell death (Wang and Ren, 2018). Additionally, cART therapy in HIV infected patients is associated with reduced IL-10, increased serum levels of TNF-α and consequently elevation of CRP levels (Shikuma *et al.*, 2011; Osuji *et al.*, 2018). However, chemo-toxic effects of cART on inflammatory response in HIV naïve model remains unclear. Furthermore diabetes is generally considered as a state of low-grade inflammation resulting in reduced IL-10 (Abhilasha *et al.*, 2021) and increased TNF-α and CRP production in vascular tissue and cardiac Interstitium (Mirza *et al.*, 2012) which induces tissue damage and fibrosis, leading to stiffening of the heart wall and consequent impairment of cardiac contractility (Ng, 2016; Bajpai and Tilley, 2018). Hence, evaluation of the effects of co-presence of cART, alcohol

and diabetes considering their independent roles in inflammatory processes and coronary vessel occlusion, both of which are implicated in cardiovascular ischemia and atrophy.

2.4.4 Alcohol, cART, and Diabetes induced apoptosis in cardiovascular tissue

Death of cardiac tissue reported in an earlier study on heavy alcohol intake suggested the presence of both necrosis and apoptosis (Capasso, *et al*., 1992). Myocyte necrosis involves enzymatic induced degradation of myocyte sarcomere releasing different subunits of myocyte contractile proteins, troponin (I and T), into the blood stream (Hammarsten *et al.*, 2018; Fernández-Solà, 2020a). In another study alcohol-induced loss of myocytes and endothelial cells are also associated with apoptotic elevated Caspase-3 expression in these cells (Rodriguez *et al.*, 2015). Additionally, cART components may induce diabetogenic effects in PLWHA with attendant myocyte injury and necrosis which may account for elevated serum troponin T in HIV positive individuals receiving cART compared to non-treated patients (Dubé *et al.*, 2008; Foster *et al.*, 2019). However, chemo-toxic effect of cART on cardiovascular Caspase-3 expression (apoptosis) and serum troponin (I and T) in the absence of HIV remains unclear. Diabetes has also been shown to elevate Caspase-3 expression in myocytes and endothelial cells of the vascular wall (Sun *et al.*, 2021) in response to diabetogenic factors such as ROS and inflammation (Mirza *et al.*, 2012; Volpe *et al.*, 2018). This diabetes induced myocyte injury is implicated in increased serum troponin T (Segre *et al.*, 2015), warranting the need to investigate the combined effects of diabetes, cART and alcohol on myocardial cardiovascular Caspase-3 and troponin levels as an indicator of cardiovascular injury and apoptosis.

2.4.5 Perturbation of cardiovascular tissue with treatment

Another mechanism for endothelial and myocardial dysfunction involves impairment of eNOS, which is an important enzyme required for time-sensitive production of nitric oxide (NO) (Marincowitz *et al.*, 2019) for functional homeostatic regulation of vascular wall or lumen (Soccal *et al.*, 2016). Of the three isoforms of nitric oxide synthase (NOS), the eNOS is localized in both vascular and cardiac tissue (Tirziu and Simons, 2008). In cardiac tissue, eNOS protects against myocyte hypertrophy and fibrosis (Moncada and Higgs, 1993; Tran *et al.*, 2022). Diabetes decreases eNOS deposition in cardiac endothelial cells but not in myocytes of rat models (Felaco *et al.*, 2001), resulting in coronary vasodilation and microvascular damage, which subsequently results in collagen deposition, inducing diabetic cardiomyopathy (Lehrke and Marx, 2017), a form of hypertrophic cardiomyopathy in diabetic patients, which may present without the associated risk factors (Mohan *et al.*, 2021). Diabetic cardiomyopathy is characterized by interstitial fibrosis, which leads to connective tissue (CT) infiltration leading to ventricular hypertrophy, apoptosis of myocardium, and atrial enlargement (Russo and Frangogiannis, 2016; Frati *et al.*, 2017). Similarly, the role of cART induced reduction of eNOS expression in coronary endothelial cells is reported in mice (Marincowitz *et al.*, 2019; Kovacs *et al.*, 2021), but effects of cART on myocyte eNOS remain unclear. Likewise, cART components may induce diabetogenic effects in PLWHA, further increasing their risk of developing diabetic cardiomyopathy (daCunha, *et al.*, 2020). On the other hand, high alcohol intake has been reported to impair eNOS (Wu and Cederbaum, 2003; Toda and Ayajiki, 2010), with attendant endothelial dysfunction, altered cardiac tissue structure leading to heart diseases such as atherosclerosis and hypertrophic cardiomyopathy (McCalister *et al.*, 2015). Studies on alcohol-induced cardiac effects are mixed with reports of cardio-protective effects following moderate

consumption of alcohol, such as wine (Laonigro *et al.*, 2009; Minzer, Losno and Casas, 2020), while heavy alcohol use are associated with cardio-toxic effects, such as alcoholic cardiomyopathy, a form of dilated cardiomyopathy characterized by a reduced thickness of left ventricle and myocyte loss (Laonigro *et al.*, 2009). Thus, it is vital to examine the effect that may arise with combinatorial administration of cART and alcohol in diabetes on eNOS in coronary vessels and cardiac tissue and evaluate the possible pathological effects due to possible attendant myocardial structural modifications.

Diabetes, cART, and alcohol have all been independently implicated in mechanisms associated with cardiovascular diseases (Fig. 1), however their combined effects have not been well documented, warranting a need for further inquiry into their combinatorial effects on cardiomyopathy, fibrosis, and atherosclerotic lesions using histological techniques. Additionally, combined effects of diabetes, cART, and alcohol will be analyzed for serum indicators of oxidative stress, and biochemical degradation of myocytes using immunoassay. Finally, the combined effects of diabetes, cART, and alcohol will be investigated for apoptotic, inflammatory, and functional homeostatic markers in coronary and cardiac tissue using immunohistochemistry.

2.5 Choice of animal model and treatment

Although dolutegravir (DTG) has been recently introduced and recommended as a first-line treatment option in HIV management, its rollout in low income settings, pregnant women and tuberculosis co-infection in South Africa and globally is not wide spread (Vitoria *et al.*, 2018; Wilson and Mapesi, 2020). On the other hand, Atripla's proven long-term efficacy makes its use common as a first line treatment (Vitoria *et al.*, 2018) and therefore selected as antiretroviral

treatment for this study. Additionally, an HIV naïve model was chosen to investigate the effects of diabetes, alcohol and cART and their combinations on heart and cardiovascular tissue in absence of HIV. The HIV naïve model is important because cART prophylaxis among prostitutes, individuals indulging in casual sex/over the night lifestyle practices, persons with multiple sex partners without condone and medical workers due to accidental needle pricks and consequent antiretroviral therapy. Furthermore, male rats were utilized to reduce variability of the study results (Sert *et al.*, 2020) due to conflicting effects that may be imposed by hormonal cycle in female rats (Smarr *et al.*, 2017).

2.6 Rationale

Diabetes remains a significant public health concern and burden on the South African public health system. It contributes to various cardiac events, including coronary artery diseases. In addition to diabetes, alcohol use and cART is also prevalent in South Africa due to the increasing rates of HIV infection and alcohol abuse. Consequently, several independent studies have focused on examining the effects of alcohol use or cART on the brain, endocrine system, and various organs. However, despite the individual implications of alcohol, cART, and diabetes on mechanisms that affect coronary and cardiac health, their direct and combined effects on cardiac morphology have not been sufficiently explored. Therefore, further investigation is necessary, which makes this study relevant. The findings obtained from this study will provide invaluable insights into the diagnosis and management of cardiovascular conditions in diabetic individuals who are on cART and regularly consume alcohol.

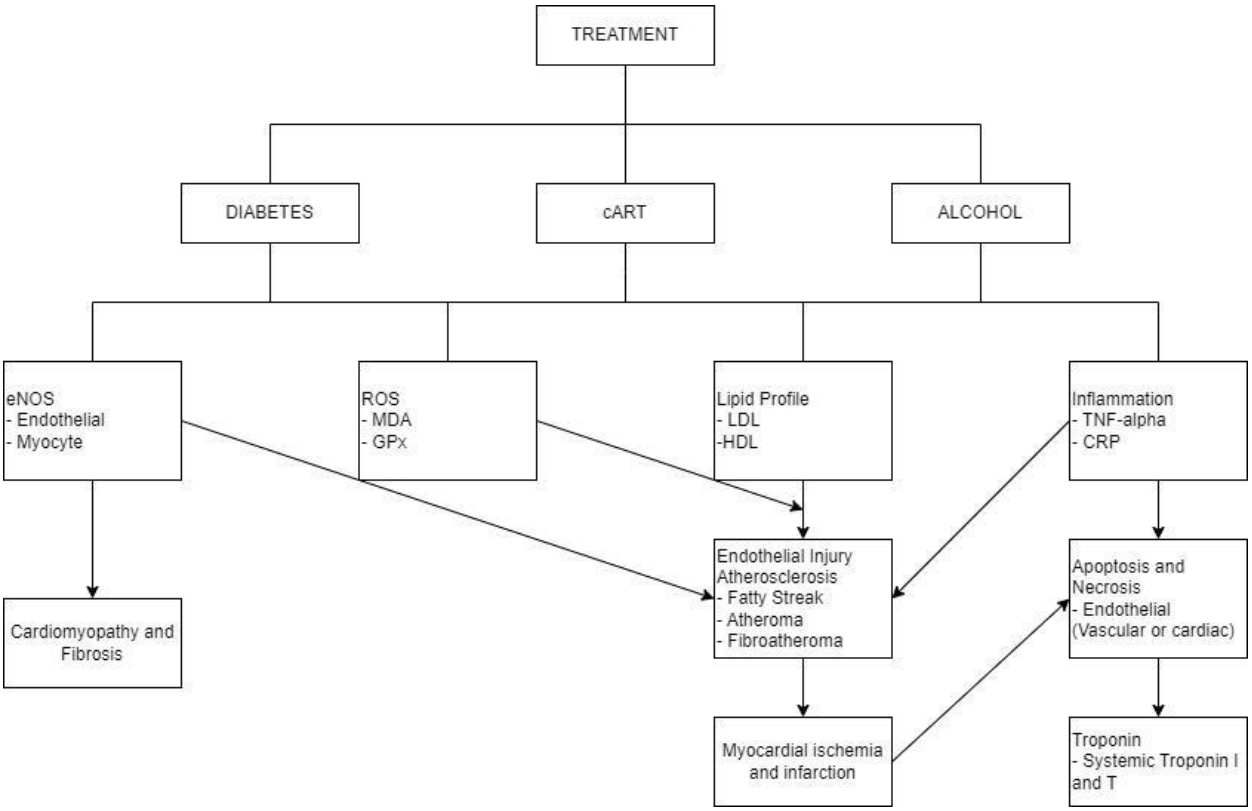

Figure 1 Schematic diagram illustrating relationship between Diabetes, cART, and alcohol independently, and cardiovascular pathologies

2.7 Aim

To investigate the cardiovascular toxicity of combined administration of ethanol and combination anti-retroviral therapy in HIV naïve diabetic male Sprague Dawley rats.

2.8 Objectives

To investigate the effects of the interactions between ethanol, cART, and diabetes on:

- The heart weight, size differences, and organ-body ratio using sensitive weighing scale and stereo microscope respectively.
- Serum levels of oxidative stress markers (MDA and GPx), and coronary disease-associated protein (Troponin I and T) using immunoassay technique.
- Cardiomyopathy (dilated and hypertrophic) by assessing histomorphology of atrial and ventricular myocyte interstitium, vascular tunica thickness in Hematoxylin and Eosin (H&E) staining, using morphometric technique and Image J software.
- Coronary artery pathology by evaluating histomorphology area of vascular wall layers using the Van-Gieson stain for elastic fibers using Image J software.
- Cardiac and coronary vasculature fibrosis, by quantifying percentage area fraction collagen profile as an indicator for heart failure, myocardial, and interstitial fibrosis using Masson and Trichrome staining technique and Image J software.
- Cardiac and vascular apoptosis (Caspase-3), functional homeostasis (eNOS), and inflammatory response (TNF-α, IL-10, and CRP), using immunohistochemistry and Image J software.

CHAPTER 3

MATERIALS AND METHODS

3.1 Animals

Samples from an already conducted study were used to reduce operational costs and minimize animal suffering. Adult male Sprague Dawley rats used for this study were kept at Central Animal Services (CAS) at University of the Witwatersrand under sterile conditions. The animals were housed in individual plastic cages 430 millimeters (mm) long, 220mm wide, and 200mm in height and kept at approximately 21-23 degrees Celsius and a 12-hour light-dark cycle. Water was available *ad libitum*, and the rats were fed a standard rodent diet.

3.2 Diabetes induction

The animals were fed a 20% fructose diet made from ground rodent chow (Lab Chef, Roodent Breeder, Stellenbosch, South Africa) mixed with fructose (Nature's Choice, Dischem pharmacies, Durban, South Africa) for two weeks. Thereafter, a once-off intra-peritoneal injection of Streptozotocin (Sigma, St. Louis, MO, United States of America) at 40mg/kg was used also to induce diabetes (Wilson and Islam, 2012). Animals with fasting glucose values above 7.5 mmol/L were deemed diabetic at the end of week three. The animals in the diabetic group were subjected to a monthly oral glucose tolerance test (OGTT), following 12 12-hour fast before the test. The animals were also weighed daily and a biweekly fasting glucose test (FGT) (12 hours before test) was taken to ensure that diabetic conditions were maintained during the experiment.

3.3 Experimental groups

The study used 48 adult male Sprague Dawley rats aged 12 weeks at the commencement of experiment, divided into three major groups: non-diabetic (Alcohol, Alcohol + Atripla, and Atripla), untreated (negative control group), and diabetic groups (Diabetes, Diabetes + Atripla, Diabetes + Alcohol and, Diabetes + Alcohol + Atripla). The non-diabetic group consisted of three subgroups, each with 6 rats. The Atripla subgroup (ARV) received antiretroviral daily. Atripla (Bristol-Myers Squibb & Gilead Sciences LLC, United States of America) was administered at a daily extrapolated dose of 23.22 mg/Kg body weight, administered orally via 2ml gelatin cubes (Pick'n'Pay, South Africa). The Alcohol subgroup (ALC) received 10% ethanol administered in drinking water bottles, which consisted of 10:90 distilled water available ad libitum diluted in distilled water to make 10% ethanol. The alcohol + Atripla subgroup (ALCARV) received both a daily dose of Atripla and 10% ethanol in their drinking water.

The untreated group consisted of one subgroup: the negative control group, with 6 rats receiving no treatment.

The diabetic group, consisting of diabetic rats, was further divided into four sub-groups each containing 6 rats: the diabetic subgroup (DB) received no further treatment, the diabetes and Atripla subgroup (DBARV) was treated with 10% ethanol, administered in their drinking water ad libitum. The diabetes + alcohol + Atripla sub-group (DBALC) was diabetic and treated with a daily dose of Atripla, administered in gelatin cubes and diabetes + alcohol + Atripla subgroup (DBALCARV) was diabetic and treated with both Atripla daily and 10% ethanol in their drinking water.

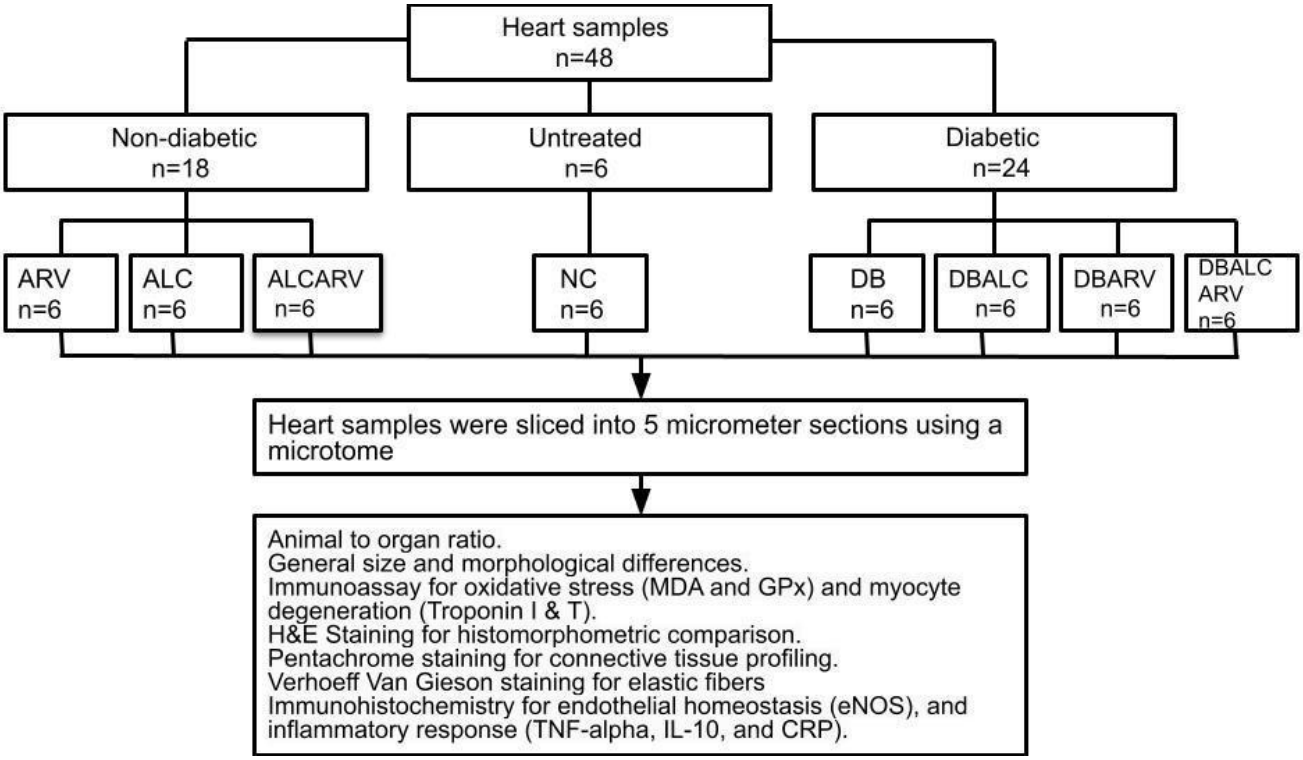

Figure 2 Experimental flow chart illustrating the different groups, treatments and laboratory analyses used in the study.

3.4 Termination

At the end of 90-day treatment period, animals were weighed and then anesthetized with a 9.1mg/ml dose of pentobarbitone, blood was collected for serum analysis, thereafter the heart was harvested.

3.5 Gross Morphology

The heart and other internal organs were weighed after harvesting and their weights recorded. The dorsal and ventral surface area of the heart was examined using Nikon-Model C-DSS230 stereomicroscope coupled to an Olympus EP50 camera (Fig 3A and B), gross morphological images of the heart was captured, and area of the heart was obtained using free-hand tool in Image J software, as depicted in figure 3. Measurements of dorsal and ventral surface areas were measured, and the total surface area was obtained by summing them up.

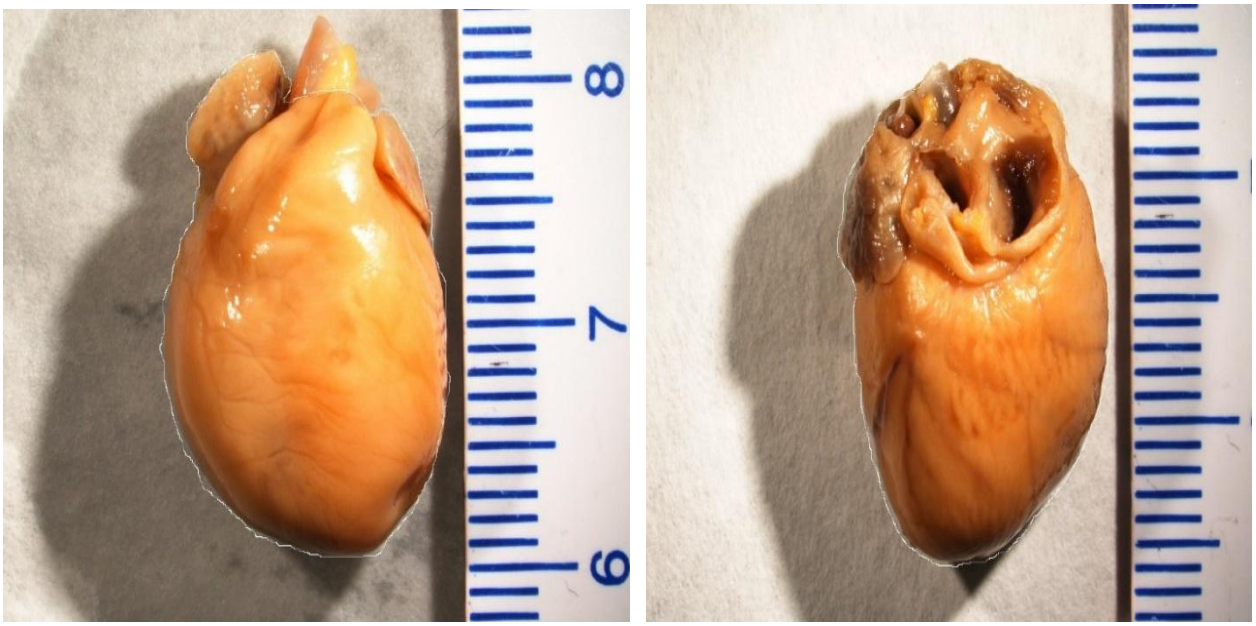

Figure 3 Measurement of the dorsal and ventral surface area of the heart.

Photomicrographs of the dorsal (A) and ventral (B) surface area of the heart. Arrows indicate the line traces with the free hand tool in image J.

3.6 Enzyme Linked Immunosorbent Assay and Bio-chemicals

3.6.1 Troponin I and Troponin T

Serum samples stored at -80°C were used for immunoassay of Troponin I and T according to manufacturer's protocol (appendix), using an Elabscience ELISA Rat TNNI3/cTn-I and cTnT/TNNT2 respectively, with catalogue numbers E-EL-R1253 and E-EL-R0151 respectively (Texas, United States). Results were evaluated by optical density (OD) on a microplate reader at 450nanometers (nm), and concentration of Troponin I and T were calculated using Origin pro software as recommended by the manufacturer (appendix).

3.6.2 Glutathione Peroxidase (GPx)

The concentration of GPx in stored serum samples was determined according to the manufacturer's protocol (appendix) using an ELISA kit obtained from Elabscience (E-EL-R249, Texas, United States). Results were evaluated by OD on a microplate reader at 450nm and concentration of GPx was calculated using Origin pro software as recommended by the manufacturer.

3.6.3 Malondialdehyde (MDA)

Malondialdehyde (MDA) colorimetric assay was done on serum samples stored at -80°C according to manufacturer's protocol (appendix) using a colorimetric assay kit obtained from Elabscience (E-BC-K025-M, Texas, United States). Results were evaluated by OD on a microplate reader at 450nm and concentration of MDA was calculated using

Origin pro software as recommended by the manufacturer.

3.7 Histology

The rat hearts were fixed in 10% buffered formalin from termination (2019), until this study (2022). After fixation, the hearts were routinely processed in an automatic processor (Citadel 2000, Thermo Fischer) through a graded series of alcohols of different percentages and embedded vertically in

paraffin wax, such that the ventricle and atrium are both represented in each section. The tissue was then sectioned at a 5 micrometer (µm)thickness using a rotary microtome (Leica RM2125 RTS, Germany). The sections were picked up on glass slides coated in 3% 3-aminopropyltriethoxysilane (APES) in acetone (silane coated slides) (Appendix 1), dried, and stained with Hematoxylin and Eosin (H&E), and other special stains listed below.

3.7.1 Modified Pentachrome Stain for collagen to cardiac muscle profiling

Cardiac tissue sections mounted on silane coated slides were stained in modified Pentachrome stain for analysis of cardiac muscle and connective tissue. After de-waxing, they were pre-treated in nitric acid, stained in toluene blue for five minutes and picric acid for five minutes. They were then dehydrated in a series of graded alcohols, mounted in entellen and visualized under a light microscope. The protocol results in collagen fibers stained pinky-red, red blood cells stained yellow, and muscle fibers stained in an orange yellow. Due to their prominent nuclei, leukocytes stain green.

3.7.2 Modified Verhoeff Van Gieson stain for elastic to collagen profiling

Sections mounted on silane coated slides were de-waxed subjected to Modified Verhoeff Van Gieson stain. They were stained in modified Verhoeff working elastic solution, differentiated in ferric chloride and counter-stained in Van Gieson solution. They were then dehydrated and mounted in entellen before visualization under light microscopy. The nuclei stain grey-ish black, elastic fibers stain bluish black, collagen fibers stain pinky red, and muscle fibres stains greenish-yellow.

3.8 Histomorphometry

Imaging of routinely stained slides were captured using Leica DM750 camera coupled to a Leica ICC50w camera and captured using LAS EZ software at 10x and 40x magnification. Image J software was used for measurements.

3.8.1 Collagen to smooth muscle profiling for coronary arteries and aorta

A total of six fields of view per group were used for coronary arteries and six fields of view for aorta, from Modified Pentachrome stained sections. In total, 48 fields of view of the vessels were used to determine total percentage area fraction (AF) occupied by smooth muscle (AFM) and collagen (AFC). This was determined using grid method and cell counter plugin on Image J. AFM and AFC were calculated using the following equation: $AFM\ or\ AFC = (App \times \sum p)/(A\ slide) \times 100$. Where *App=area per point, ∑p=sum of points, and A slide=area of slide.*

3.8.2 Elastic to collagen profiling for coronary arteries and aorta

A total of 6 fields of view per group were used for both the coronary arteries and aorta from the Verhoeff Van Gieson stained sections, totaling 48 fields of view. These were used to determine the AF occupied by smooth muscle and collagen using the grid method and the cell counter plugin on Image J, with the area fraction calculated using the equation: $AFE\ or\ AFC = (App \times \sum p)/(A\ slide) \times 100$. Where App=area per point, ∑p=sum of points, and A slide=area of slide.

3.8.3 Nuclei cell count

A total of two longitudinal fields of view per H&E section were captured at x40 magnification for atrium and ventricle. The cardiac myocyte was imaged, beginning from two lateral ends of heart apex and proceeding towards the lumen for ventricle. In the atrium, due to limited fields of view, area of best fit was captured. A total of 96 fields of view were used each for atrium and ventricle in order to determine myocyte cell count using cell counter plugin on Image J software. An average of measurements was used such that each group had a total of six measurements before statistical analysis.

3.8.4 Interstitial spaces profiling

A total of two transverse fields of view per H&E section were captured at x40 magnification for atrium and ventricle. The cardiac myocyte was imaged, beginning from two lateral ends of heart apex and

proceeding towards lumen for ventricle. In the atrium, due to limited field of view, area of best fit was captured. A total of 96 fields of view were used each for atrium and the ventricle in order to determine total AF of interstitial spaces in atrium (AFA) and ventricle (AFV), and grid method and cell counter plugin on Image J were used. The AF was calculated using the equation: $AFA\ or\ AFV = (App \times \sum p)/(A\ slide) \times 100$. Where *App=area per point, ∑p=sum of points, and A slide=area of slide.*

3.8.5 Coronary artery and aorta vessel thickness

Two fields of view per H&E section of coronary arteries and aorta each were captured at x40 magnification, a total of 96 fields of view were used to determine thickness of tunica media, tunica adventitia and total thickness of coronary arteries and aorta, using straight tool of Image J software. Measurements were averaged, such that each group had a total of 6 measurements before statistical analysis.

3.8.6 Characterization of myocyte width at bifurcation

A total of 2 transverse fields of view per Modified Pentachrome section were captured at x40 magnification for atrium and ventricle. The cardiac myocyte was imaged, beginning from the two lateral ends of the heart apex and proceeding towards lumen for ventricle. In the atrium, due to limited fields of view, area of best fit was captured. A total of 96 fields of view were used for atrium and ventricle each to determine width of myocytes at bifurcation using straight tool plugin on Image J software. Measurements were averaged, such that each group had a total of 6 measurements before statistical analysis.

3.8.7 Scoring for waviness

The longitudinal images captured on Modified Pentachrome stain were used to score the myocytes for waviness according to this scale: 1= straight (typical), 2= somewhat wavy, and 3= very wavy.

3.9 Immunohistochemistry (IHC)

3.9.1 Endothelial Nitric Oxide Synthase (eNOS)

Cardiac tissue sections mounted on silane-coated slides were subjected to an immunohistochemistry protocol for paraffin sections (appendix). Normal goat serum diluted at 5% in phosphate-buffered saline (PBS; PH 7.4) was used, with a rabbit polyclonal anti-eNOS antibody (Abcam, ab5589, Massachusetts, United States) as primary antibody, diluted to ratio of 1:50 and a biotinylated goat anti-rabbit antibody as secondary antibody, diluted to ratio 1:1000. In control sections, primary antibody was replaced with 5% normal goat serum. Sections were then dehydrated, cleared, mounted and viewed under a light microscope. Two sections per slide and one slide per animal, with six animals per group were imaged for NOS, totaling 18 sections per group. A total of 5 fields of view was captured for atrium and ventricle per section for cardiac and coronary endothelium and myocyte from which counts of nuclei with immunolocalized NOS were made using click point tool on image j. In total, 90 fields of view of atrium and ventricle each were analyzed for NOS localization.

3.9.2 C - reactive protein (CRP)

Cardiac tissue sections mounted on silane-coated slides were subjected to an immunohistochemistry protocol for paraffin sections. Normal goat serum was used, diluted to 5% using PBS at PH=7.4. The slides were incubated in a rabbit polyclonal anti-CRP antibody (Abcam, ab227507, Massachusetts, United States) diluted to ratio of 1:50. A biotinylated goat anti-rabbit antibody was used as secondary antibody, diluted to ratio of 1:1000. Control sections were incubated in 5% normal goat serum in place of primary antibody. Sections were, dehydrated, cleared, mounted, then viewed under a light microscope. Two sections per slide and one slide per animal, with six animals per group were imaged for CRP, totaling 18 sections per group. A total of five fields of view were captured for atrium and ventricle per section for cardiac myocyte and grid method with multi point click tool on Image J was used. In total 90 fields of view of atrium and ventricle each were analyzed for CRP localization.

3.9.3 Tumor Necrosis Factor-alpha (TNF-α)

Cardiac tissue sections mounted on silane-coated slides were subjected to an immunohistochemistry protocol for paraffin sections. Normal goat serum was used, diluted to 5% using PBS at PH=7.4. The slides were incubated in a rabbit polyclonal anti-TNF-α antibody (Abcam, ab205587, Massachusetts, United States) diluted to ratio of 1:250. A biotinylated goat anti-rabbit antibody was used as secondary antibody, diluted to ratio of 1:1000. Control sections were incubated in 5% normal goat serum in place of primary antibody. Sections were, dehydrated, cleared, mounted, then viewed under a light microscope. Two sections per slide and one slide per animal, with six animals per group were imaged for TNF-α, totaling 18 sections per group. A total of five fields of view was captured for atrium and ventricle per section for cardiac myocyte and grid method with point click tool on Image J was used. In total, 90 fields of view of atrium and ventricle each were analyzed for TNF-α localization.

3.9.4 Caspase-3

Cardiac tissue sections mounted on silane-coated slides were subjected to immunohistochemistry protocol for paraffin sections. Normal goat serum was used, diluted to 5% using PBS at PH=7.4. The slides were incubated in a rabbit polyclonal anti-Caspase-3 antibody (Abcam, ab184787, Massachusetts, United States) diluted to ratio of 1:250. A biotinylated goat anti-rabbit antibody was used as secondary antibody, diluted to a ratio of 1:1000. Control sections were incubated in 5% normal goat serum in place of the primary antibody. Sections were, dehydrated, cleared, mounted, then viewed under a light microscope. Two sections per slide and one slide per animal, with six animals per group was imaged for caspase-3, totaling 18 sections per group. A total of five fields of view was captured for atrium and ventricle per section for cardiac myocyte and grid method with the point click tool on Image J was used. In total, 90 fields of view of the atrium and ventricle each were analyzed for caspase-3 localization.

3.10 Statistical analysis

All data were recorded as standard error of mean (SEM). Data was tested for normality using Shapiro-Wilks test, parametric data was analyzed by One-way ANOVA and a Bonferroni post hoc test was conducted to determine difference between groups. Non-parametric data were analyzed using Kruskal-Wallis test and a Mann-Whitney post hoc test was conducted to determine differences between groups. IBM SPSS version 29.0 was used to perform statistical analysis. Results with $p<0.05$ were considered significant.

3.11 Ethics

The ethical clearance for this study was obtained from Animal Research Ethics Committee (AREC) at University of the Witwatersrand, clearance number 2018/011/58C. A Modifications and extensions clearance was submitted and granted by AREC to include this study to originally approved ethics (Appendix).

CHAPTER 4

RESULTS

For easier understanding and interpretation, results for treatment groups were divided into two general themes, one describing antiretroviral toxicity and the other detailing diabetes and alcohol interaction.

4.1 ANTIRETROVIRAL TOXICITY

4.1.1 Fasting Glucose Test

After the induction of diabetes, a fasting glucose test was conducted biweekly, and the results are shown in Figure 4. The control group and non-diabetic groups treated with cART and alcohol (NC, ARV, and ALCARV) and diabetic groups treated with ARV (DBARV and DBALCARV) recorded average fasting glucose levels of 4.8; 5.38; and 4.72mmol/L respectively, while DBARV and DBALCARV diabetic treated groups recorded elevated fasting glucose levels (8.52mmols/L and 10.98mmols/L respectively) at the end of second week (Fig. 4). Generally, non-treated control (NC), and non-diabetic negative control (ARV and ALCARV) groups recorded similar fasting glucose levels which were not significantly different from control (NC) value at the end of week two (NC vs ARV, NC vs ALCARV, and ARV vs ALCARV: $P < 0.05$ respectively), as against diabetic treated (DBALC and DBALCARV) groups which recorded similar/non-significant values (DBARV vs DBALCARV: $P < 0.05$), but showed elevated levels relative to non-diabetic groups (NC, ARV, ALCARV) at the end of week two, and remained significantly elevated against these groups until week 12 (NV, ARV, ALCARV vs DBARV, DBALCARV: $P < 0.05$ in all comparisons respectively). The mean fasting glucose level increased considerably between week two and week twelve in the DBARV compared to rest of the groups ($p<0.05$), but while it was also increased in DBALCARV group, the increases were significantly ($p < 0.05$) less than values recorded in DBARV.

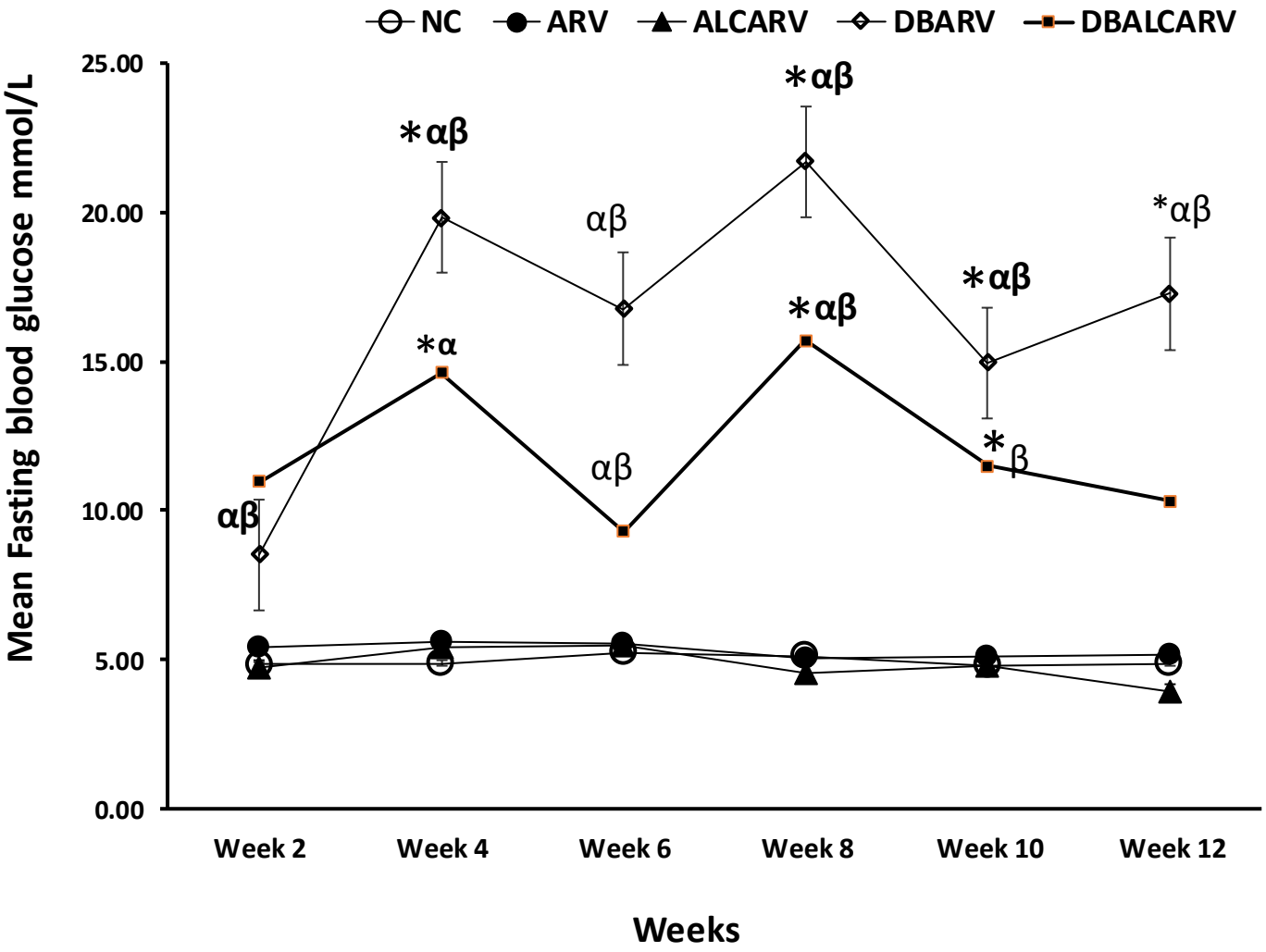

Figure 4 Bi-weekly mean oral glucose tolerance test

Significantly increased FG in DBARV: DBARV vs ARV and DBARV vs ALCARV groups, end of the second week (p= 0.011 and 0.008 respectively). At the end of the 4th week, the DBARV group FG, significantly increased relative to NC, ARV, and ALCARV groups (p= 0.01, 0.001, and 0.001 respectively), but in ALCARV group, mean FG level non-significantly decreased in comparison to ARV group (p= 0.08). At end of 6 weeks, mean FG significantly increased in DBARV, and DBALCARV groups, compared to ARV and ALCARV groups (p= 0.014 and 0.023; and p= 0.013 and 0.017 respectively). At week 8, the DBALCARV group mean FG level significantly increased versus NC, ARV, and ALCARV groups (p= 0.024, 0.023, and 0.019 respectively), the DBARV group also showed increased mean FG level versus NC, ARV, and ALCARV groups (p=0.001 across all 3 groups), and the ALCARV group mean FG level showed significant increase against NC and ARV groups (p= 0.008 and 0.031 respectively). The mean FG level at the end of the 10th week increased in DBALCARV group versus NC, ARV, and ALCARV groups (p= 0.002 across all three groups) and was also increased in DBARV group compared to NC (p=0.023) and the ALCARV (p=0.023) groups. The mean FG level at week 12 increased significantly in DBARV group compared to NC, ARV, and ALCARV groups (p=0.004, 0.004, and 0.003 respectively). '*'denotes a significant difference when

compared to the NC group, ‘α’ denotes a significant difference when compared to the ARV group, and ‘β’ denotes a significant difference when compared to the ALCARV group. Key: NC: control (non-treated; ARV: cART treated; ALCARV: Alcohol + cART; DBARV: diabetic + cART; DBALCARV: diabetic + alcohol + cART.

4.1.2 Body and Heart weight

The mean terminal body and heart weights were as shown in figures 5A & B, while body-organ weight ratio is shown in figure 5C. The ARV group had significantly reduced mean body weight compared to control group (Fig. 5A, $p<0.05$). Also, DBARV and DBALCARV groups had significant decreases in mean body weight compared to NC, ARV and ALCARV groups (Fig. 5A, <0.05). The mean heart weight for DBARV group was significantly decreased compared to NC, ARV, and ALCARV groups (Fig. 5B, $p<0.05$). The mean body-heart weight ratio for DBALCARV group was significantly decreased compared to rest of treatment groups (Fig. 5C, $p<0.05$).

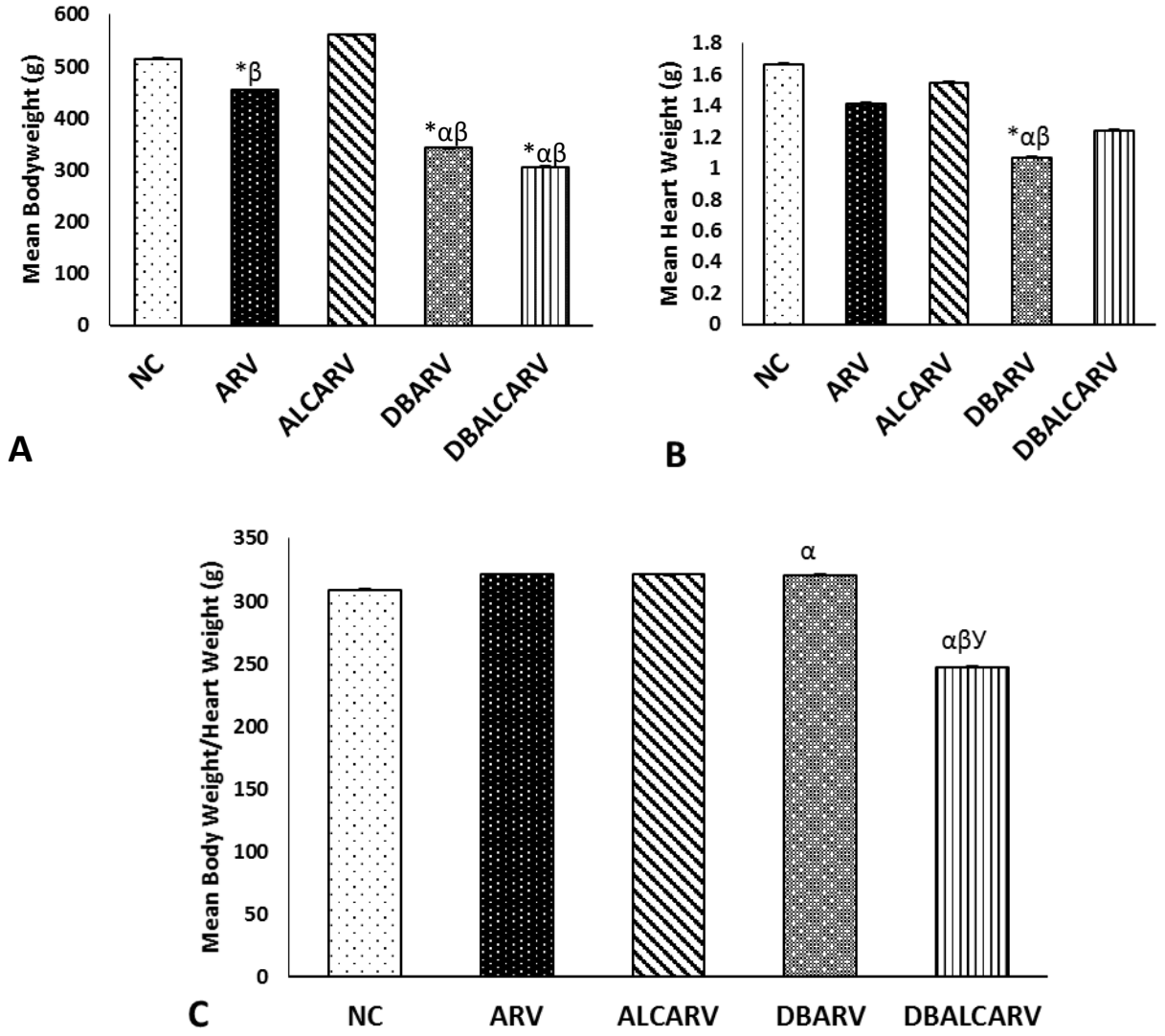

Figure 5 Body and Heart weight and their ratio

A) The body weight for the ARV group was significantly decreased against the NC, ALCARV, but significantly higher than DBARV, and DBALCARV groups (p=0.021, 0.001, 0.001, and 0.001 respectively). The ALCARV group's mean bodyweight recorded a significant increase compared to the NC, DBARV, and DBALCARV groups (p=0.006, 0.001, and 0.001 respectively). The mean bodyweight of DBARV and DBALCARV groups both significantly decreased against NC group (p= 0.001 and 0.001 respectively). **B)** The mean heart weight in the DBARV group decreased significantly compared to the NC, ARV, and ALCARV groups (p= 0.003, 0.001, and 0.033 respectively). **C)** The body-heart weight ratio in the DBALCARV group was significantly decreased compared to all treatment groups (p= 0.005, 0.045, all respectively). '*' indicates significant difference when compared to the NC group, 'α' denotes a significant difference when compared to the ARV group, 'β' denotes a significant difference compared to the ALCARV group, and 'ϒ' denotes significant difference compared to the DBARV group. Key: NC: control (non-treated; ARV: cART treated; ALCARV: Alcohol + cART; DBARV: diabetic + cART; DBALCARV: diabetic + alcohol + cART

4.1.3 Surface area of the heart

The results of mean surface area of heart are as presented in Figure 6. The total surface area of ARV, ALCARV, DBARV, and DBALCARV groups were all significantly reduced compared to NC group (Fig 6A, $p<0.05$). The ventricular, dorsal and ventral aspects of heart samples appear tapered in control (NC) in contrast to other treatment groups which appeared rounded (Fig. 6). The atrium (black arrows: ventral view, broken arrows: insert: dorsal view) in control group (NC) also appeared prominent or widened compared to other treatment groups (Fig 6).

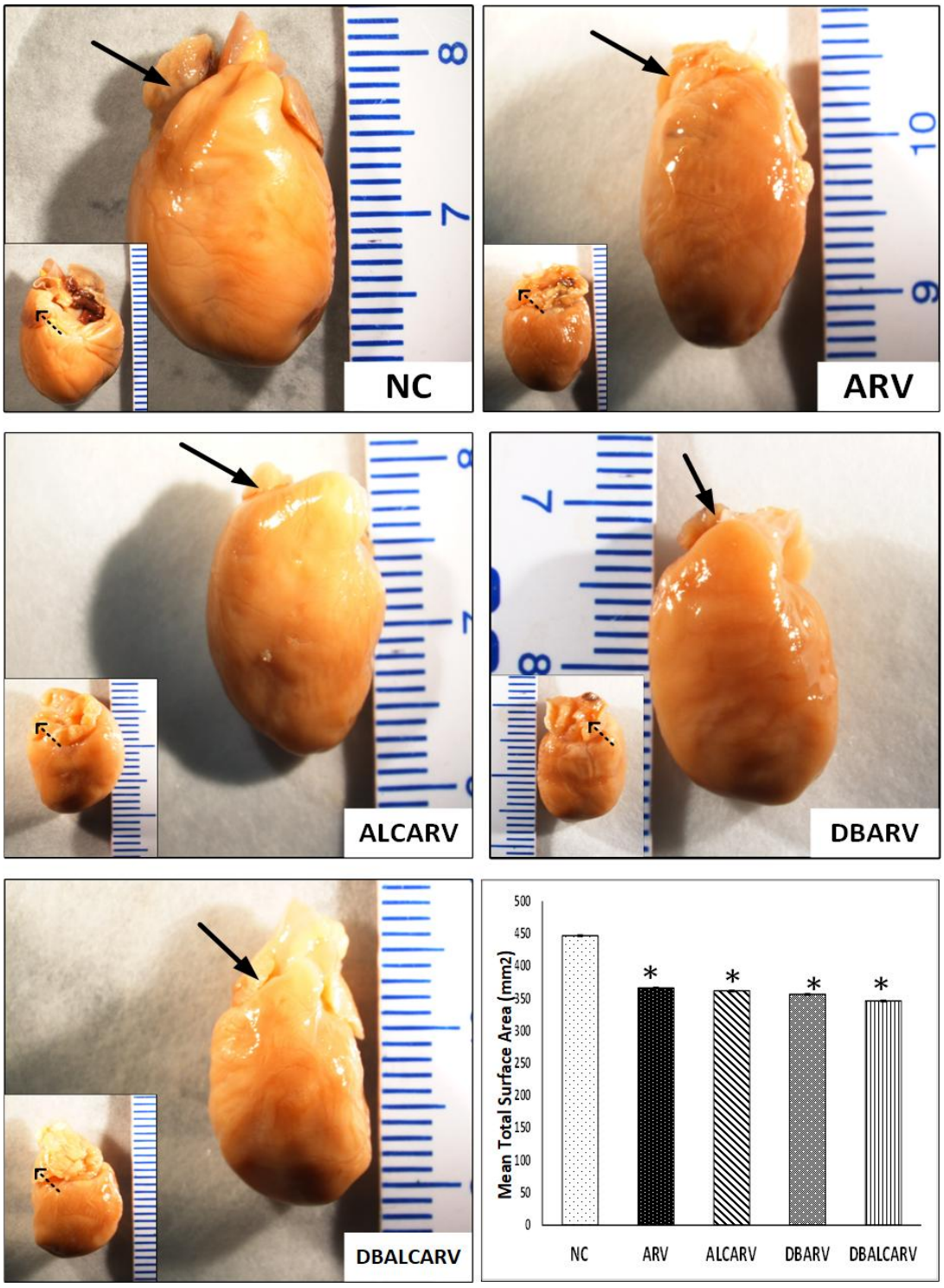

Figure 6 Mean surface area of the heart.

The total surface area in the ARV, ALCARV, DBARV, and DBALCARV groups are significantly decreased compared to the NC group (p=0.022, 0.018, 0.015, and 0.01 respectively, Fig. 6E). '*' denotes significant difference when compared to the NC group. Black arrows: atrium: dorsal heart surface, broken arrow: atrium: ventral surface. Key: NC: control (non-treated; ARV: cART treated; ALCARV: Alcohol + cART; DBARV: diabetic + cART; DBALCARV: diabetic + alcohol + cART.

4.1.4 Serum MDA and GPx

The concentration of serum MDA and GPx were measured, and the results were as presented in figure 7. The DBARV group showed a significant increase in MDA concentration when compared to NC, ALC ALCARV, DBARV and DBALCARV groups ($p<0.05$, Fig. 7A), while ARV group exhibited a significant decrease when compared to NC, ALCARV, and DBALCARV groups ($P < 0.05$ across all groups). The GPx concentration significantly decreased in DBARV group comparec against NC, ARV, and ALCARV groups ($p<0.05$, Fig. 7B). In ARV group, GPx concentration was significantly higher compared to NC, DBARV and DBALCARV groups ($p<0.05$, Fig. 7B).

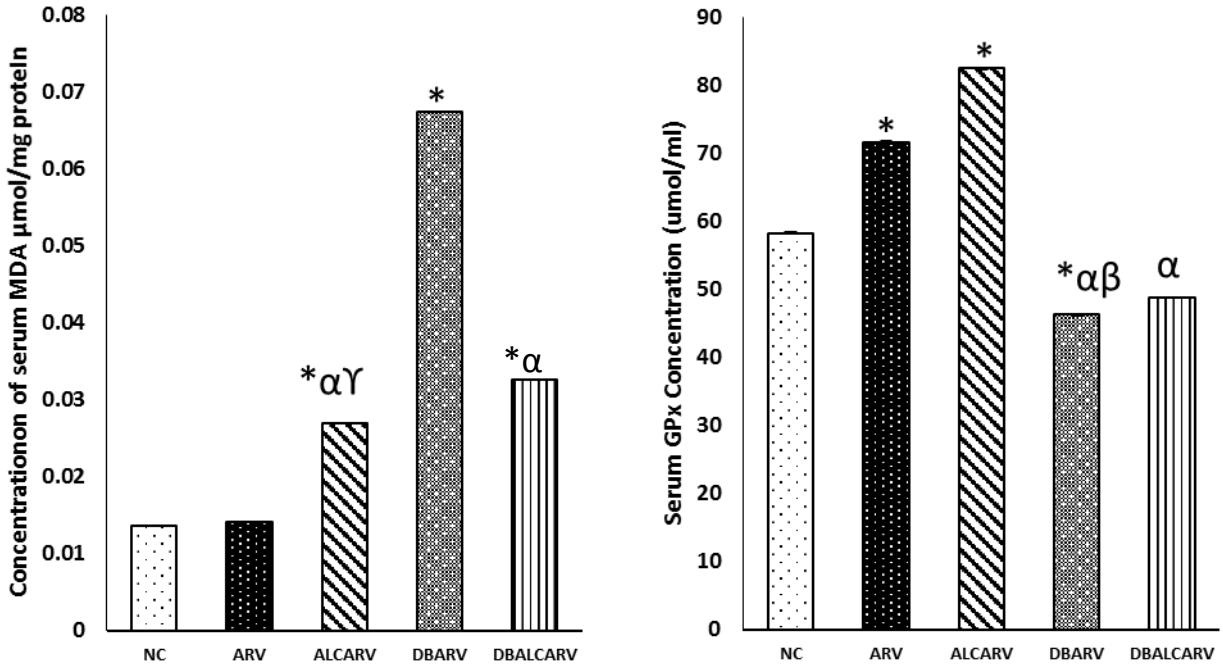

Figure 7 Mean Serum MDA and GPx

A) Serum concentration of MDA in the ALCARV, DBARV and DBALCARV groups significantly increased in comparison to the NC (p=0.034, 0.009, and 0.039 respectively), while MDA levels significantly increased in DBARV versus ALCARV and DBALCARV groups (p=0.015 and 0.016 respectively). **B)** The concentration of GPx significantly decreased in the DBARV group when compared to the NC, ARV and ALCARV groups (p=0.017, 0.001, and 0.045 respectively). The ARV group showed a significant increase in GPx concentration against the NC group (p=0.037), and the DBALCARV group had a significant decrease against the ARV group (p=0.002 respectively). '*' denotes a significant difference in comparison to the NC group, 'α' denotes a significant difference in comparison to the ARV group, 'β' denotes a significant difference when compared to the ALCARV group, and 'ϒ' denotes a significant difference in comparison to the DBARV group. Key: NC: control (non-treated; ARV: cART treated; ALCARV: Alcohol + cART; DBARV: diabetic + cART; DBALCARV: diabetic + alcohol + cART.

4.1.5 Serum Troponin T and I

The mean serum concentrations of troponin T and I are illustrated in figure 8A & B. The troponin T concentration was significantly increased in DBALCARV group in comparison to all the other groups ($p<0.05$, Fig. 8A). The concentration of troponin T also significantly ($p < 0.05$) decreased in DBARV against NC, ARV and ALCARV. Troponin I concentration recorded significant ($P < 0.05$) increases in

ARV and DBARV compared to NC, ALCARV and DBALCARV groups (Fig. 8B). Also, ALCARV and DBALCARV troponin I concentrations, decreased significantly against NC group ($p < 0.05$).

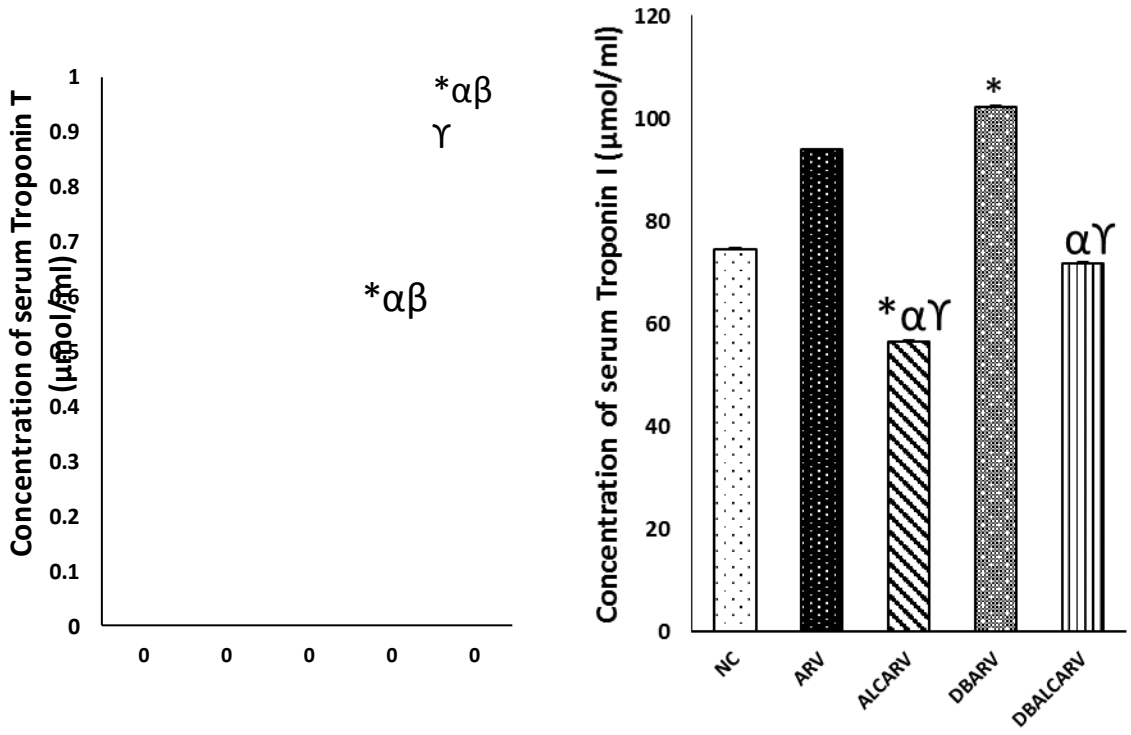

Figure 8 Mean Serum Troponin T and I Concentrations

A) Troponin T is significantly elevated in the DBALCARV group against the other groups (p=0.001) and reduced in the DBARV compared to the NC, ARV, and ALCARV groups (p=0.008, 0.013, and 0.33). **B)** Troponin I significantly elevated in ARV and DBARV and depleted in the ALCARV against NC (p=0.007, 0.046, and 0.038 respectively), the ALCARV and DBALCARV both decreased against the ARV and DBARV group (p=0.001). '*' denotes a significant difference when compared to the NC group, 'α' denotes a significant difference when compared to the ARV group and 'ϒ' denotes a significant difference when compared to the DBARV group. Key: NC: control (non-treated; ARV: cART treated; ALCARV: Alcohol + cART; DBARV: diabetic + cART; DBALCARV: diabetic + alcohol + cART.

4.1.6 Coronary artery and aorta tunica morphology

The results of thickness of tunica media in coronary and aortic vessels are presented in Figure 9. The tunica media in aorta (double-headed long arrows) and coronary arteries (double-headed short arrows) are shown in figure 9. The endothelium and tunica intima (arrowheads) were seen in these vessels,

while tunica adventitia (broken double arrows) of varying morphologies were observed (Fig. 9). The tunica media (double-headed long arrows) of aorta in the ALCARV and DBALCARV groups were significantly thicker when compared to that in NC, ARV, and DBARV groups ($p<0.05$, Fig. 9A), while in the coronary arteries, the thickness of the tunica media in the ALCARV and DBALCARV groups was significantly decreased in comparison to the NC group ($p<0.05$, Fig. 9B).

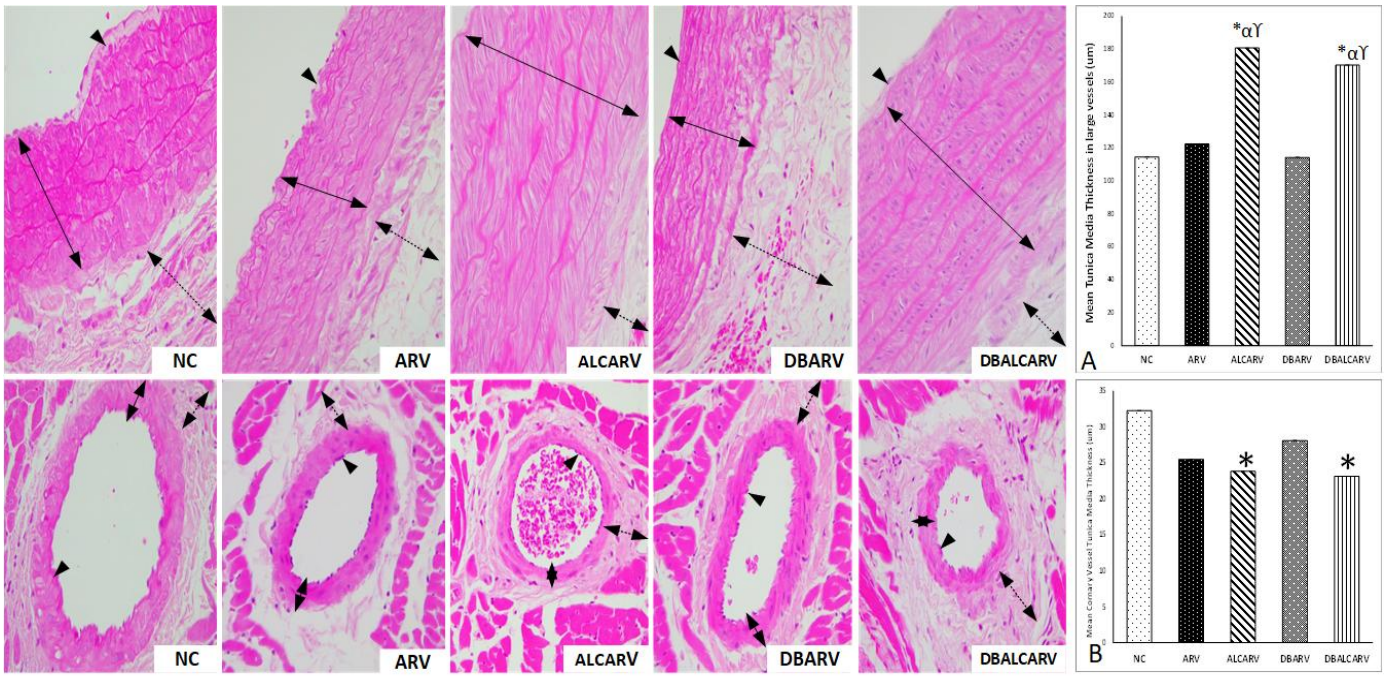

Figure 9 Thickness of vascular tunica media (H & E stain) of aorta and coronary arteries

A) Aorta tunica media thickness (double-headed long arrows) of the ALCARV and DBALCARV groups were significantly increased when compared to the NC, ARV, and DBARV groups (For ALCARV: p=0.016, 0.049, and 0.021 respectively; For DBALCARV: P = 0.001, 0.014, and 0.002). B) decreased coronary tunica media thickness (double-headed short arrows) was significantly decreased in ALCARV and DBALCARV groups against NC group (p=0.02 and 0.02 respectively). '*' denotes a significant difference in comparison to the NC group, 'α' denotes a significant difference in comparison to the ARV group, and 'ϒ' denotes a significant difference in comparison to the DBARV group. Key: NC: control (non-treated; ARV: cART treated; ALCARV: Alcohol + cART; DBARV: diabetic + cART; DBALCARV: diabetic + alcohol + cART.

4.1.7 Area of smooth muscle and collagen in coronary arteries

The results of the smooth muscle and collagen fibre percentage area fraction area are presented in Figure 10. The smooth muscle (the double arrows) and collagen fibres (broken double arrows) are shown. The DBALCARV and DBARV groups showed a significant increase in collagen area against ALCARV group ($p<0.05$), DBARV group increased against ARV group ($p<0.05$) and DBALCARV groups increased against NC group ($p<0.05$, Fig. 10A). The muscle to collagen ratio was significantly decreased against ALCARV group ($p<0.05$), while also showing an insignificant decrease against other groups (Fig. 10 C).

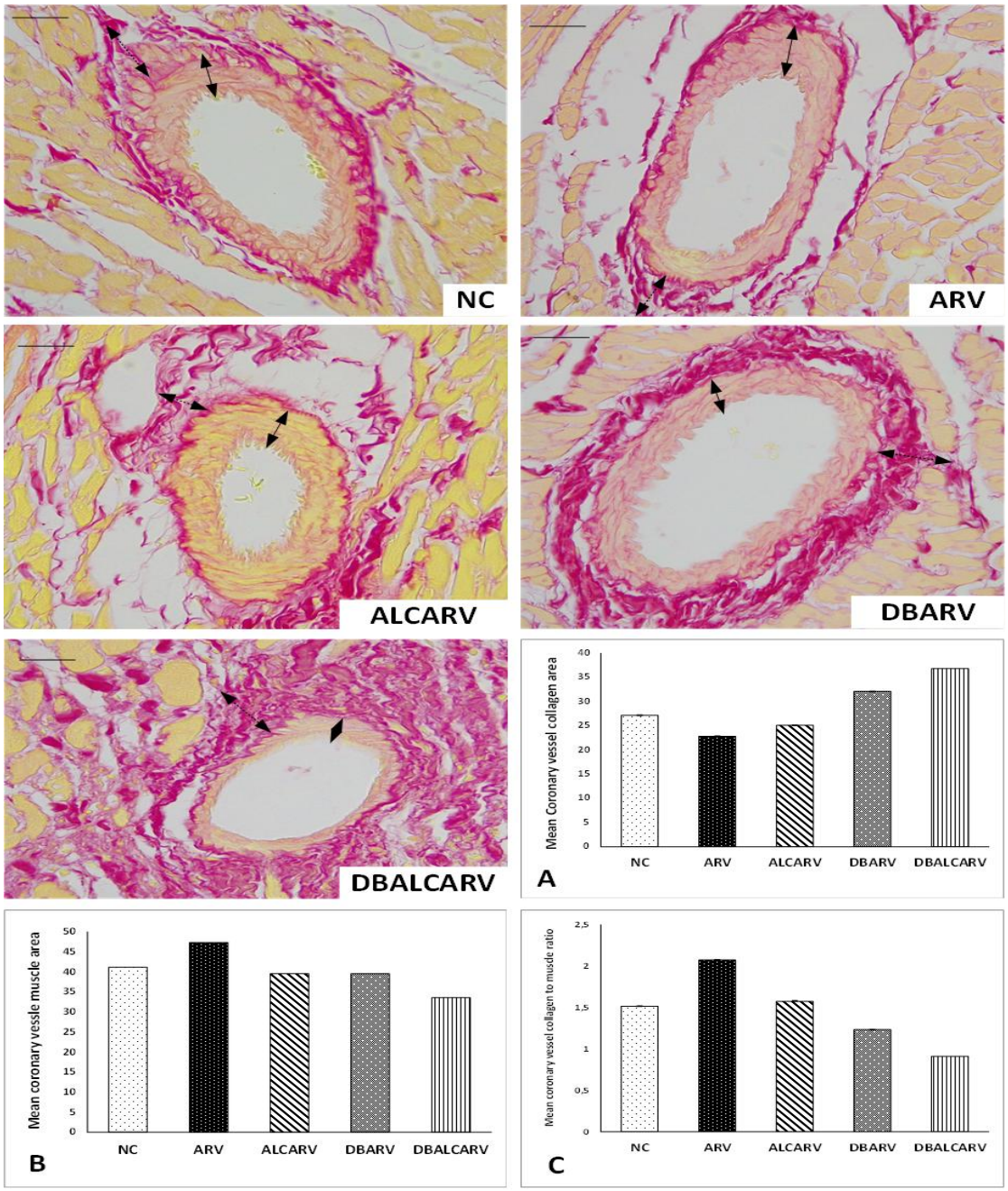

Figure 10 Collagen and smooth muscle area in coronary arteries (Pentachrome stain)
Significant differences in collagen expression (ANOVA, p=0.024). **A)** The DBALCARV and DBARV groups showed a significant increase in collagen area against the ALCARV group (p=0.032 and 0.033 respectively), the DBALCARV group showed a significant increase against the NC group (p=0.032), and the DBARV group showed a significant increase against the ALCARV group (p=0.038). **B)** The muscle area showed no significant differences between groups. **C)** The DBALCARV group showed a significant increase against the ALCARV group (0.037). '*' denotes a significant difference to the NC group, 'α' denotes a significant difference to ARV, and 'β' denotes a significant difference against the ALCARV group. Smooth muscle (the double arrows) and the collagen fibres (broken double arrows)

Key: NC: control (non-treated); ARV: cART treated; ALCARV: Alcohol + cART; DBARV: diabetic + cART; DBALCARV: diabetic + alcohol + cART

4.1.8 Area of Elastic Fibres and Collagen fibres in coronary arteries

The percentage area fraction of coronary artery collagen and elastic fibres are shown in Figure 11. The elastic fibres (arrowheads) and collagen fibres (broken double arrows) are illustrated in their varying morphologies between groups. The collagen fibre area decreased significantly in ARV and DBALCARV groups against NC group, and also significantly decreased in DBALCARV group against the ALCARV and DBARV groups ($p<0.05$, Fig. 11A). The DBALCARV group had a decreased elastic fibre (Fig. 11B) and collagen to elastic fibre ratio ($p<0.05$, Fig. 11B) when compared to the NC group.

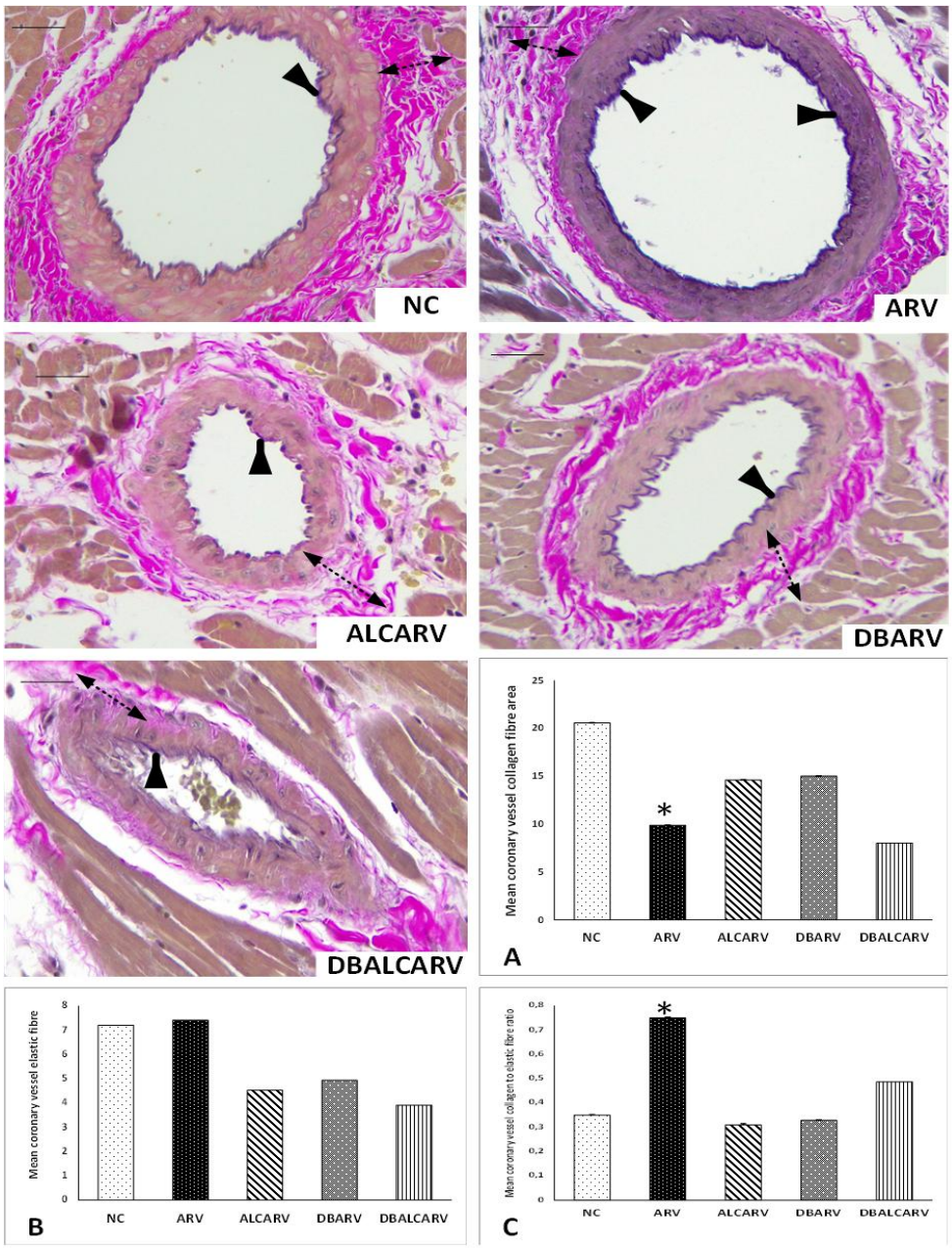

Figure 11 Area of collagen and elastic fibres

(Modified Van Gieson stain) Significant differences in collagen expression (ANOVA, p=0.004). **A)** The area of collagen expression was significantly decreased in the ARV group against the NC group (p=0.003), and the DBALCARV group was significantly decreased against the NC (p=0.001), ALCARV (p=0.032), and DBARV (p=0.009). **B)** The elastic fibre area was significantly increased in the ARV group (p=0.039), but significantly decreased in the DBALCARV group (p=0.012) against the NC group. **C)** The DBALCARV group showed significant increase against the NC group (p=0.022). '*' denotes a significant difference in comparison to the NC group, 'β' denotes a significant difference when compared to the ALCARV group, and 'ϒ' denotes a significant difference in comparison to the DBARV group. Key: NC: control (non-treated; ARV: cART treated; ALCARV: Alcohol + cART; DBARV: diabetic + cART; DBALCARV: diabetic + alcohol + cART.

4.1.9 Aorta smooth muscle and collagen

The collagen and smooth muscle fibres of aorta are shown in Figure 12. The collagen fibres (broken double arrow heads) appear increased in ARV and DBARV groups while smooth muscle (single arrowheads) is slightly increased in DBALCARV groups. However, no significant differences were reported between groups ($p<0.05$, Fig.12).

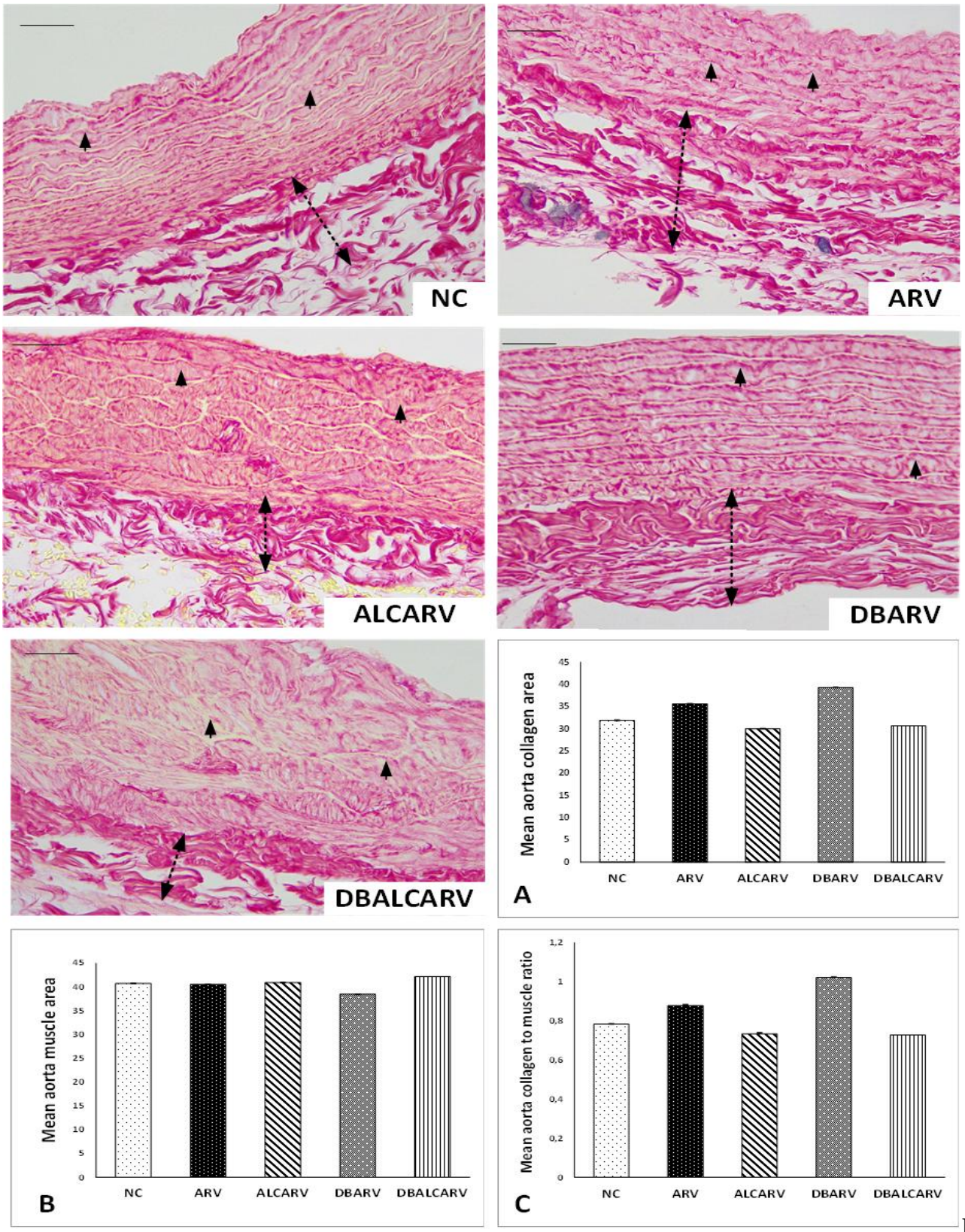

Figure 12 Collagen and Muscle presentation (Pentachrome stain)

Collagen fibres (broken double arrow), smooth muscle (arrowheads), no significant difference between groups.

4.1.10 Aorta elastic and collagen fibre area

The percentage area fraction of elastic and collagen fibres are shown in Figure 13. The elastic fibres (arrowheads) and collagen fibres (broken double arrowheads) are shown in their differing morphologies across different groups. The collagen fibre area in ALCARV, DBARV, and DBALCARV groups were all significantly increased against NC groups ($p<0.05$, Fig. 13A). The elastic fibre area was significantly increased in ALCARV group against ARV group ($p<0.05$, Fig. 13B), and collagen to muscle ratio in ALCARV, DBARV, and DBALCARV groups was significantly increased against the ARV group ($p<0.05$, Fig. 13B).

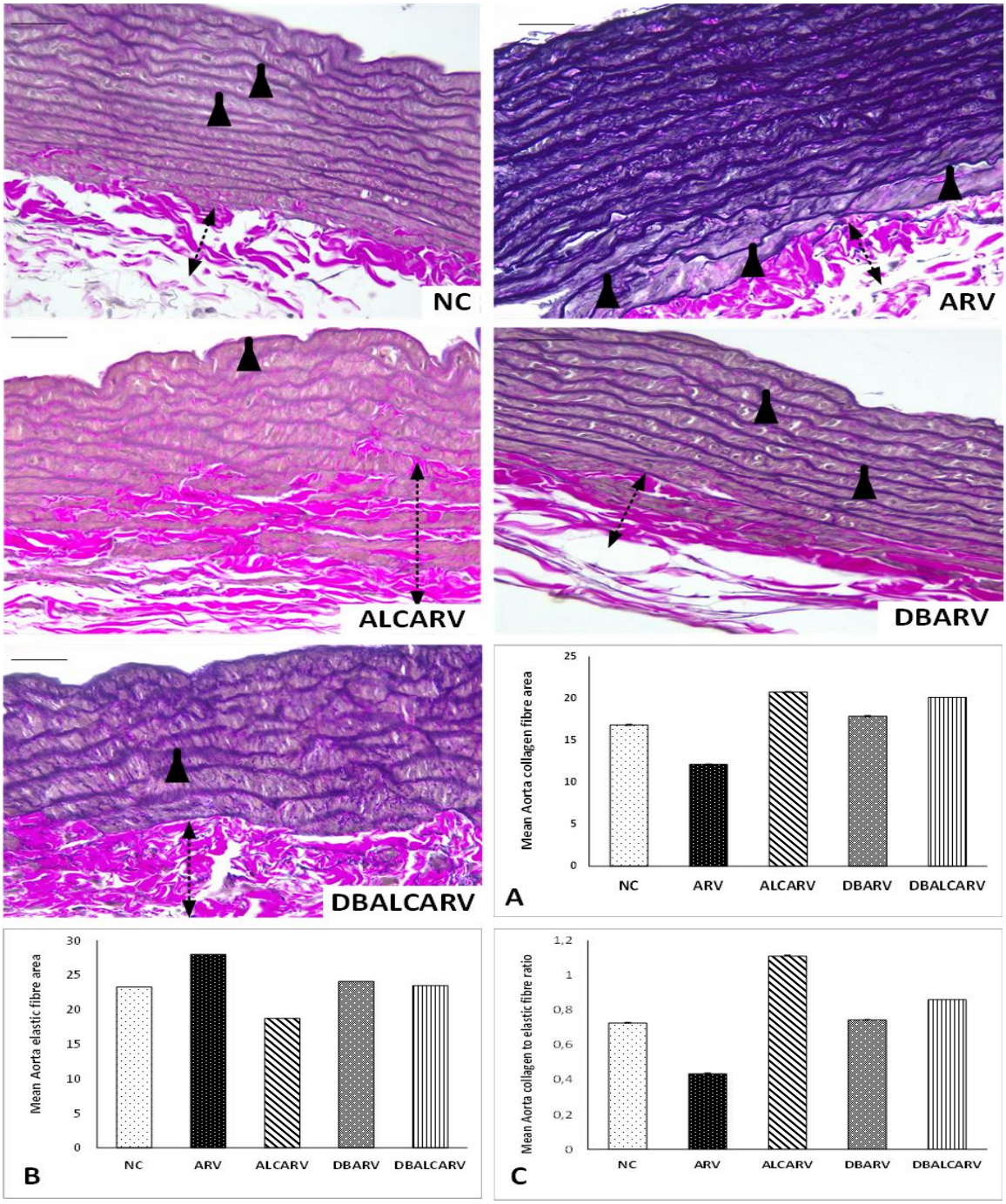

Figure 13 Elastic fibre and collagen area

Significant differences in collagen expression (ANOVA, p=0.038). **A)** Collagen fibre percentage area fraction was significantly increased in the ALCARV, DBARV and DBALCARV groups against the ARV group (p=0.014, 0.02, and 0.02 respectively). **B)** the ALCARV group had a significantly decreased elastic fibre area against the ARV group (p=0.032). **C)** The collagen to elastic fibre ratio in the ALCARV, DBARV, and DBALCARV groups were significantly increased (p=0.006, 0.024, 0.011). 'α' denotes a significant difference against ARV. (Van Gieson stain) Key: NC: control (non-treated;

ARV: cART treated; ALCARV: Alcohol + cART; DBARV: diabetic + cART; DBALCARV: diabetic + alcohol + cART.

4.1.11 Atrium interstitial cells and spaces

The interstitial cells (encircled) and interstitial spaces (asterisks) are presented in Figure 14 in their varying morphologies across groups. The score of interstitial cells and percentage area fraction of interstitial spaces in atrium are presented Figure 14A & B. The DBALCARV and ARV groups had an increased number of interstitial cells nuclei compared to NC, ALCARV, and DBARV groups ($p<0.05$, Fig. 14A). The ARV, DBARV and DBALCARV groups' atrial percentage area fraction was significantly increased when compared to NC group ($p<0.05$, Fig.14B).

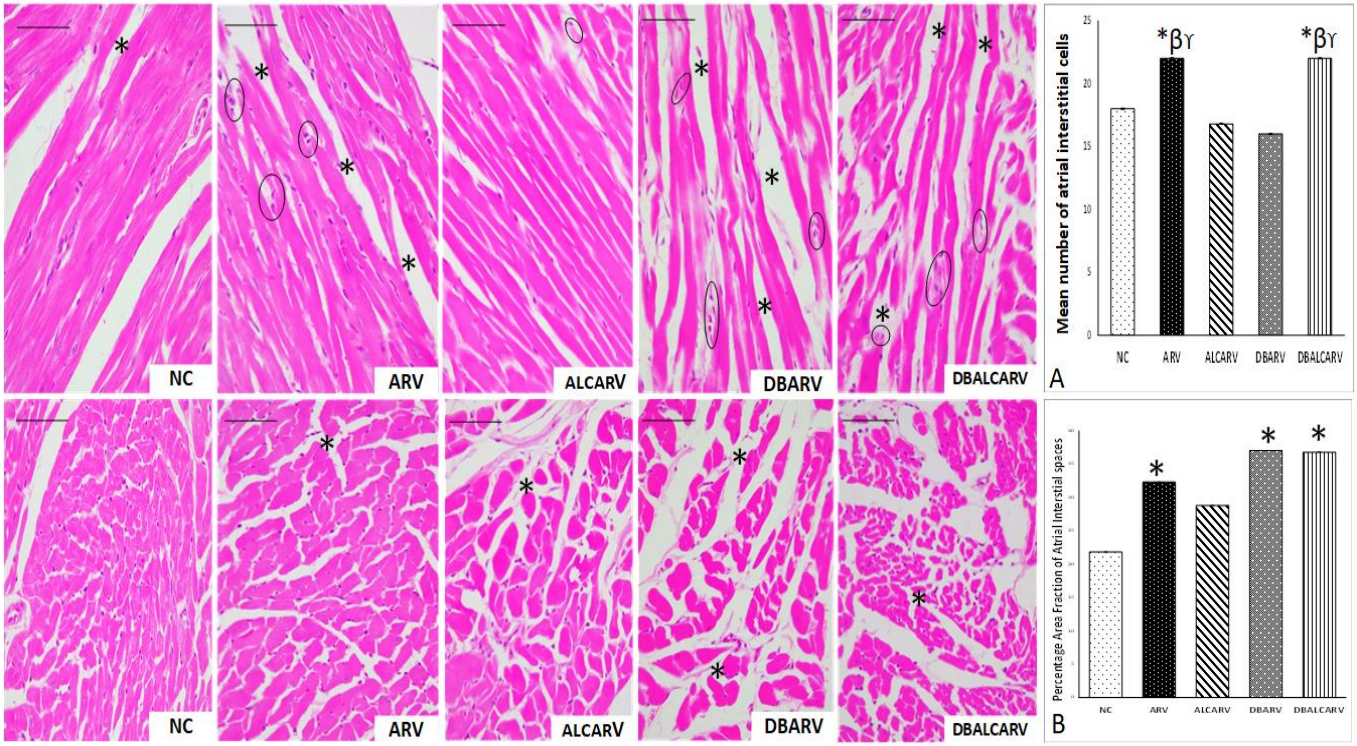

Figure 14 Atrial interstitial nuclei and interstitial percentage area fraction (H&E stain)

A) mean number of interstitial cells nuclei (encircled) in DBALCARV group, significantly increased relative to NC, ARV, ALCARV, and DBARV groups (p *=0.042).* **B)** The atrial percentage area fraction of the interstitial spaces (asterisk) in ARV, DBARV and DBALCARV groups, significantly increased relative to the NC group (p=0.041, 0.017, and 0.009 respectively). '*' denotes a significant difference in comparison to the NC group, 'β' denotes a significant difference when compared to the ALCARV group, and 'ϒ' denotes a significant difference in comparison to the DBARV group Key: NC: control (non-treated; ARV: cART treated; ALCARV: Alcohol + cART; DBARV: diabetic + cART; DBALCARV: diabetic + alcohol + cART.

4.1.12 Atrium histomorphology

The percentage area fraction of collagen and muscle, muscle waviness scoring, and muscle fibre width at the point of bifurcation is shown in Figure 15. The muscle fibre width (straight line), muscle fibre (arrowheads), and collagen fibres (broken arrows) are illustrated in their varying morphologies across groups. The ALCARV, DBARV, and DBALCARV groups had significantly thinner muscle fibre width against NC group, and DBALCARV group's width was also thinner than ARV and DBARV groups ($p<0.05$, Fig. 15A). The muscle fibres are significantly wavier in DBALCARV group against NC, ARV, ALCARV, and DBARV groups ($p<0.05$, Fig. 15B). The ALCARV and DBALCARV groups had a significantly higher collagen area against NC group ($p<0.05$, Fig. 15C). The DBALCARV group had a significantly higher muscle fibre area against ARV, ALCARV, and DBARV groups ($p<0.05$, Fig. 15D).

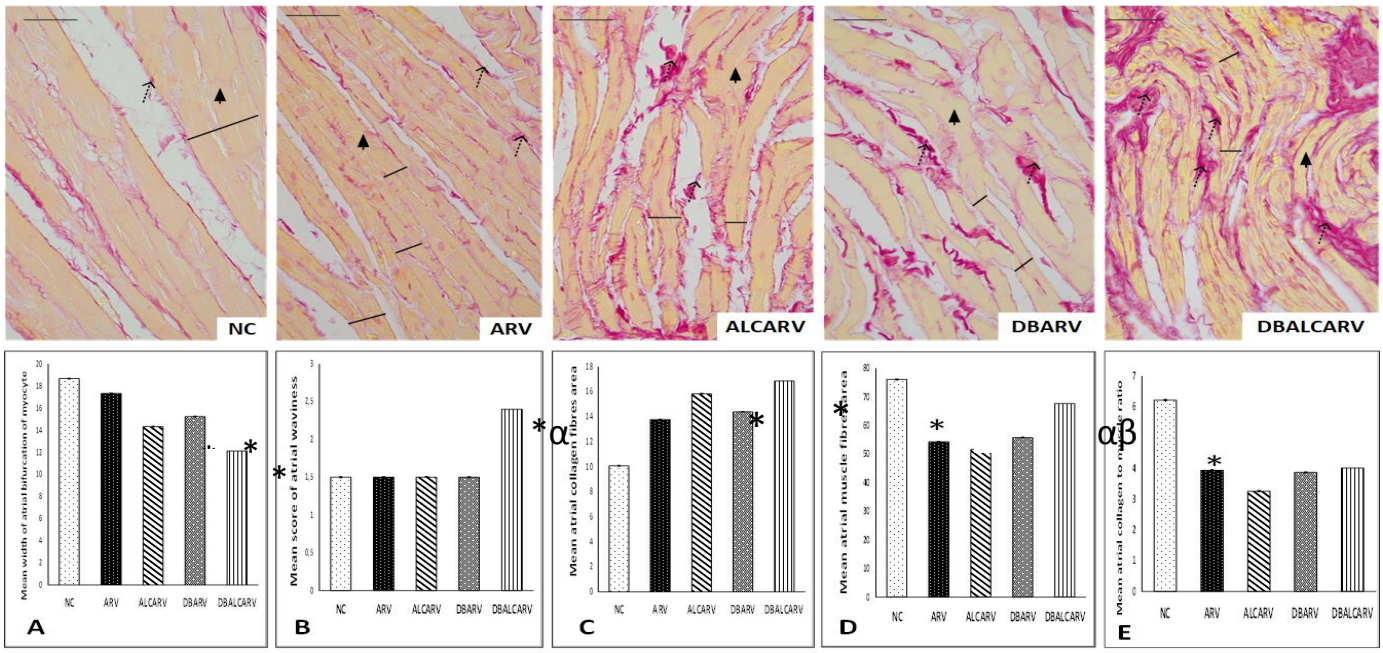

Figure 15 Atrial histomorphology

A) The bifurcation of the ALCARV, DBARV, and DBALCARV groups was significantly thinner against the NC group (p=0.015, 0.007, and 0.002 respectively). The DBALCARV group was also significantly thinner than the ARV and DBARV groups (p=0.012 and 0.033 respectively). **B)** the DBALCARV group was significantly wavier than the NC, ARV, ALCARV, and DBALCARV group (p=0.037, 0.023, 0.023, and 0.043 respectively). **C)** The ALCARV and DBALCARV groups have a significantly higher collagen area against the NC group (0.021 and 0.013 respectively). **D)** The muscle fibres in the DBALCARV group had a significantly higher area than the ARV, ALCARV, and DBARV groups (p=0.04, 0.006, and 0.027 respectively). '*' denotes a significant difference in comparison to the NC group, 'α' denotes a significant difference in comparison to the ARV group, 'β' denotes a significant difference when compared to the ALCARV group, and 'ϒ' denotes a significant difference in comparison to the DBARV group Key: NC: control (non-treated; ARV: cART treated; ALCARV: Alcohol + cART; DBARV: diabetic + cART; DBALCARV: diabetic + alcohol + cART.

4.1.13 Ventricle interstitial cells and spaces

The interstitial cells (encircled) and interstitial spaces (asterisks) are presented in Figure 16, in their varying morphologies across groups. The score of interstitial cells and percentage area fraction of interstitial spaces in atrium are presented Figure 16A & B. The interstitial cells in ARV and DBARV groups had a significant difference against NC group ($p<0.05$, Fig. 16A).

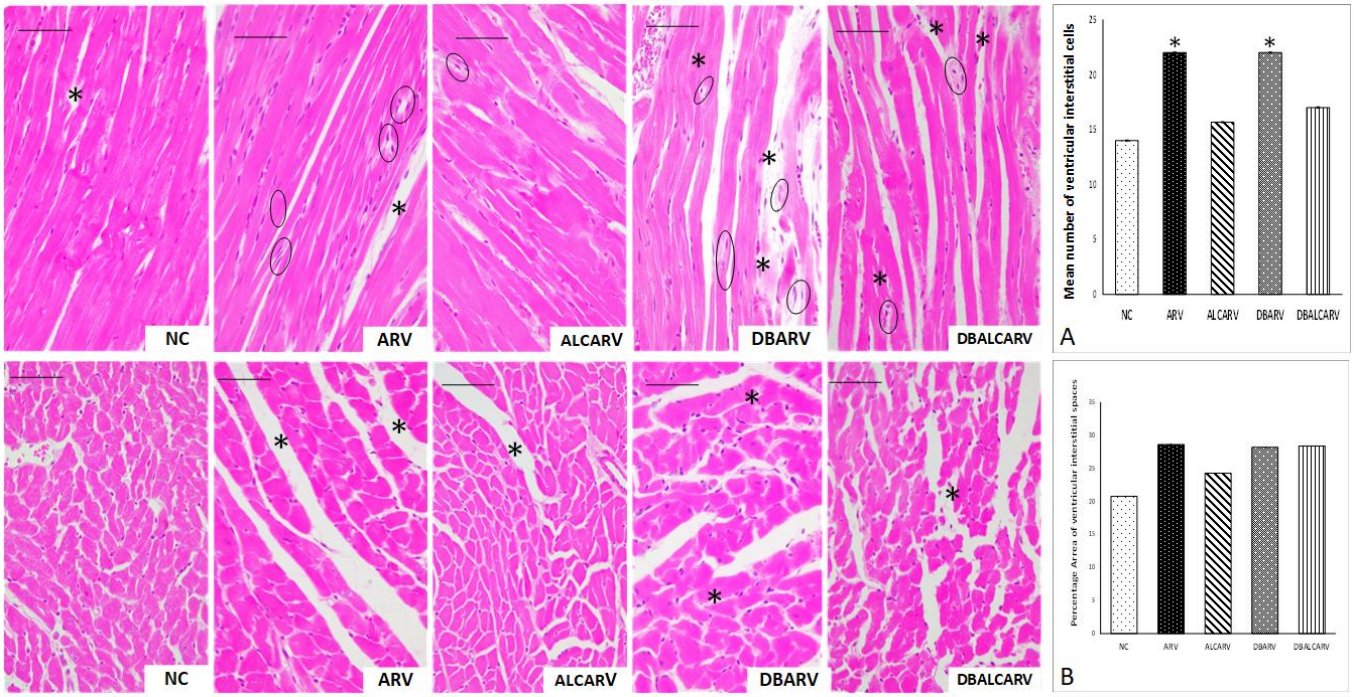

Figure 16 Ventricular interstitial nuclei and interstitial percentage area fraction

A) The interstitial nuclei in the ARV and DBARV groups are significantly increased against the NC group (p=0.03) **B)** No significant difference in ventricular percentage area fraction. '*' denotes a significant difference in comparison to the NC group. Key: NC: control (non-treated; ARV: cART treated; ALCARV: Alcohol + cART; DBARV: diabetic + cART; DBALCARV: diabetic + alcohol + cART.

4.1.14 Ventricle histomorphology

The percentage area fraction of collagen and muscle, muscle waviness scoring, and muscle fibre width at point of bifurcation is shown in Figure 17. The muscle fibre width (straight line), muscle fibre (arrowheads), and collagen fibres (broken arrows) are illustrated in their varying morphologies across groups. The muscle fibre width at point of bifurcation is significantly increased in DBARV group against ARV group and significantly decreased in DBALCARV group against DBARV group ($p<0.05$, Fig 17A). The DBALCARV group had significantly wavier muscle fibres than DBARV group ($p<0.05$, Fig. 17B). The collagen area is significantly increased in ALCARV and DBALCARV against NC group, DBALCARV group was also significantly increased against DBARV group, while DBARV group was significantly decreased against ARV and ALCARV groups ($p<0.05$, Fig. 17C). The ARV and ALCARV groups have a significantly decreased muscle area against NC group, DBARV group was significantly increased against ARV and ALCARV groups, and DBALCARV group was significantly increased against ARV and ALCARV groups ($p<0.05$, Fig. 17D). The ARV, ALCARV and DBALCARV groups have a significantly decreased collagen to muscle ratio against NC group, DBARV group is significantly increased against ARV and ALCARV groups, and DBALCARV group is significantly increased in ALCARV and DBARV groups ($p<0.05$, Fig. 17E).

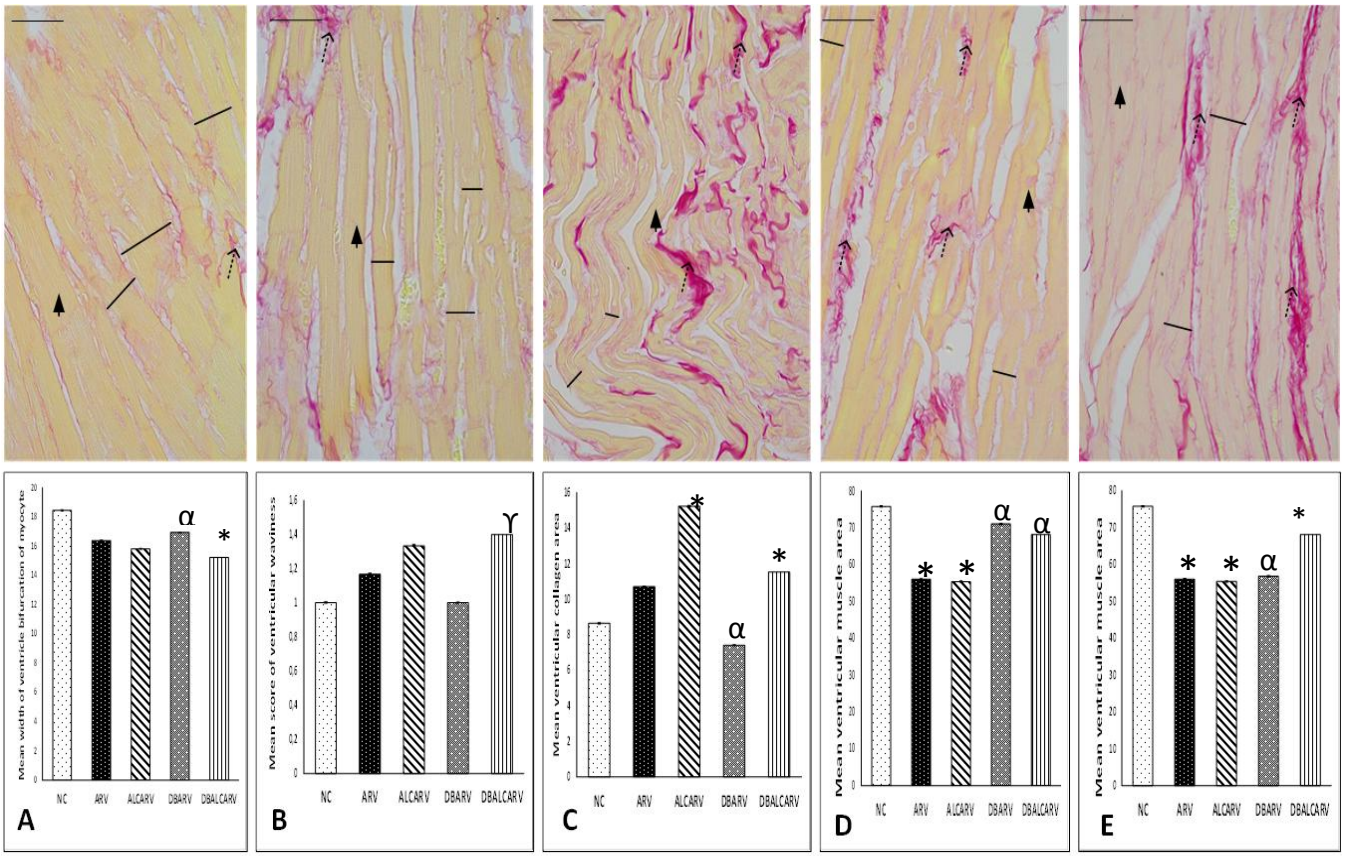

Figure 17 Ventricle histomorphology

A) The muscle fibre width at the point of bifurcation is significantly increased in the DBARV group against the ARV group and significantly decreased in the DBALCARV group against the DBARV group (p=0.046 and 0.023 respectively). **B)** The DBALCARV group had significantly wavier muscle fibres against the DBARV group (p<0.037). C) The collagen area is significantly increased in the ALCARV and DBALCARV against the NC group (p=0.019 and 0.015 respectively), the DBALCARV group was also significantly increased against the DBARV group (p=0.004), while the DBARV group was significantly decreased against the ARV and ALCARV groups (p=0.037 and 0.01 respectively). **D)** The ARV and ALCARV groups have a significantly decreased muscle area against the NC group (p=0.003 and 0.005 respectively), the DBARV group was significantly increased against the ARV and ALCARV groups (p=0.009 and 0.015 respectively), and the DBALCARV group was significantly increased against the ARV and ALCARV groups (p=0.005 and 0.014 respectively). **E)** The ARV, ALCARV and DBALCARV groups have a significantly decreased collagen to muscle ratio against the NC group (p=0.016, 0.003 and 0.022 respectively), the DBARV group is significantly increased against the ARV and ALCARV groups (p=0.008 and 0.002 respectively), and the DBALCARV group is significantly increased in the ALCARV and DBARV groups (p=0.031 and 0.01 respectively). '*' denotes a significant difference in comparison to the NC group, 'α' denotes a significant difference in comparison to the ARV group, 'β' denotes a significant difference when compared to the ALCARV group, and 'ϒ' denotes a significant difference in comparison to the DBARV group Key: NC: control (non-treated; ARV: cART treated; ALCARV: Alcohol + cART; DBARV: diabetic + cART; DBALCARV: diabetic + alcohol + cART.

4.1.15 C- Reactive Protein

C-reactive protein (CRP) is expressed with varying observations in the epicardium (Fig. 18A-E), interstitial spaces (Fig. 18F-J), and coronary arteries (Figure 18K-O). In the epicardium, NC group showed no presentation (Fig. 18A), ARV and DBARV (Fig. 18B&D) groups showed a higher expression (solid arrows), and ALCARV and DBARV (Fig. 18C&E) groups showed least amount of expression. The interstitial spaces in NC group (Fig. 18F) showed no presentation, and ARV and DBARV (Fig. 18G&I) groups showed the most expression in interstitium (broken arrows), while ALCARV (Fig. 18H) group have less expression in interstitium (broken arrows). The DBALCARV group (Fig. 18I) showed no expression in interstitial spaces but showed a little presentation in myocytes (solid arrow). The coronary arteries in NC group (Fig. 18K) showed no CRP expression, while ARV, ALCARV, DBARV, and DBALCARV (Fig. 18F, L, M&O) groups showed more CRP expression in interstitial spaces and cells surrounding the artery (broken arrows).

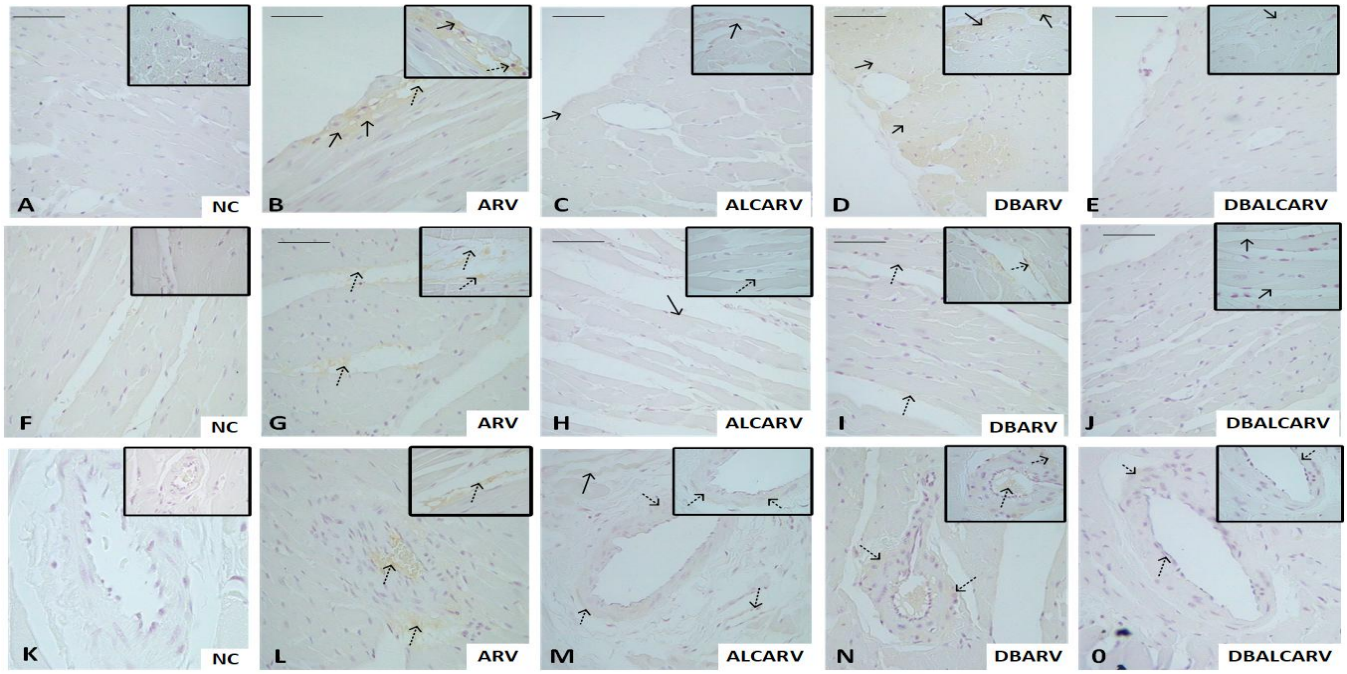

Figure 18 C-Reactive Protein expression in the epicardium, Interstitium and coronary artery

A-E), The expression of CRP in the epicardium with the NC group showing no presentation and the ARV and DBARV showing the most expression (solid arrows). CRP expression in the interstitium . F-J) No expression in the NC group, the most expression in the ARV (broken arrows) group and less expression in the ALCARV, DBARV, and DBALCARV groups (broken arrows). CRP expression in and around the coronary arteries, with no expression in the NC group and varying levels of CRP expression in the ARV, ALCARV, DBARV and DBALCARV groups (broken arrows). Key: NC: control (non-treated; ARV: cART treated; ALCARV: Alcohol + cART; DBARV: diabetic + cART; DBALCARV: diabetic + alcohol + cART.

4.1.16 Endothelial Nitric Oxide Synthase

Endothelial nitric oxide synthase (eNOS) is expressed in epicardium (Fig. 19A-E), myocardium (Fig. 19F-J) and coronary arteries (Fig. 19K-O) across the treated groups. The epimysium in the NC group (Fig. 19A) showed more eNOS expression (solid arrows), ARV group (Fig. 19B) showing both myocyte (solid arrows) and nuclear expression (broken arrows), and ALCARV group (Fig. 19C) showing myocyte expression (solid arrows). The DBARV and DBALCARV groups showed very little to no eNOS expression (Fig. 19D&E). The NC and ARV groups (Fig. 19A&B) showed a substantial amount of eNOS expression in myocardium (solid arrows) and nuclei (broken arrows). The myocardium of ALCARV and DBARV groups (Fig. 19H&J) showed little to no eNOS expression (solid arrows), while DBARV group (Fig. 19I) showed no expression of eNOS. The coronary artery endothelium (broken arrows) and myocytes around it (solid arrows) in NC group (Fig. 19K) expressed eNOS. The myocytes in ARV and ALCARV groups (Fig. 19L&M) also showed eNOS expression, with the endothelium of ALCARV group also showing very little expression. The DBARV and DBALCARV groups (Fig. 19N&O) showed no eNOS expression.

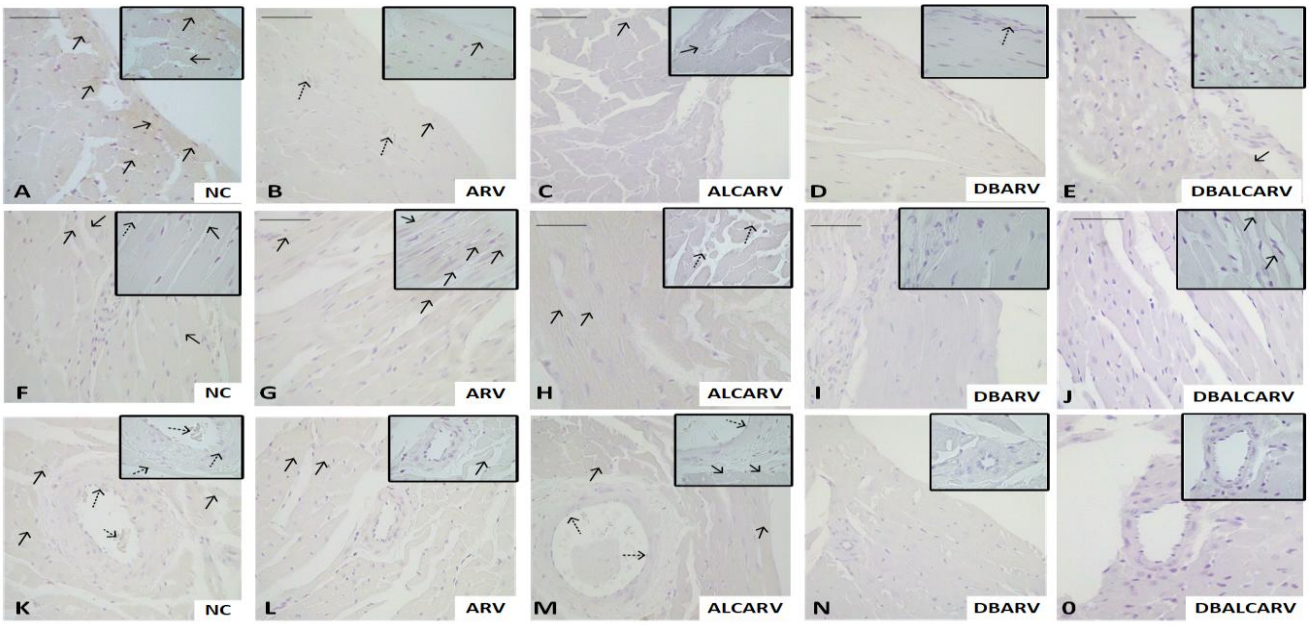

Figure 19 eNOS expression in the epicardium, myocardium, and coronary artery

The expression of eNOS in the epicardium with the NC group showed the most presentation (solid arrows), and the ARV, ALCARV, DBARV and DBALCARV groups showed little to no expression. eNOS expression in the myocardium with the NC group showing the most myocyte (solid arrows) and nuclear expression (broken arrows), the ARV and ALCARV groups showing less presentation and the DBARV and DBALCARV groups showing very little to no presentation. eNOS presentation in the coronary arteries) with the NC group showing the most expression in the endothelium (broken arrows) and myocyte (solid arrow), the ARV and ALCARV groups showing less presentation of eNOS, and the DBARV and DBALCARV groups showing no expression of eNOS. Key: NC: control (non-treated; ARV: cART treated; ALCARV: Alcohol + cART; DBARV: diabetic + cART; DBALCARV: diabetic + alcohol + cART.

4.1.17 TNF- alpha and Caspase 3 expression

Several techniques were tried to optimize TNF- alpha and Caspase 3 expression including adjusting primary antibody dilutions (1:50, 1:100, 1:1250, 1:500, 1:1000), comparing absent and present antigen retrieval in citrate buffer versus EDTA, adjusting time and concentration of blocking buffer (3% for 30 mins, 3% 1 hr, 5% 30 mins, 5% 1hr), changing ABC kit, secondary antibody and DAB. All attempts to optimize TNF- alpha and Caspase 3 expression were unsuccessful as shown in the images in figure 20 below.

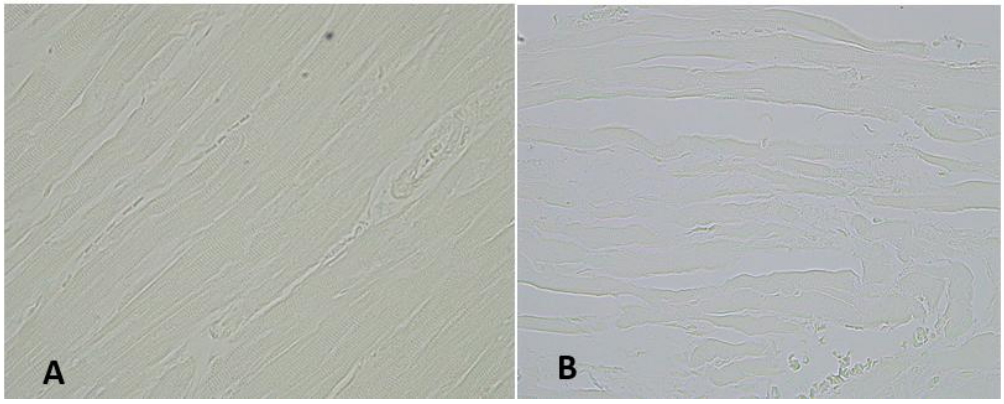

Figure 20 TNF-alpha and Caspase 3 non expression.

The non-expression of TNF-α (A) and Caspase-3 (B).

4.2 DIABETES AND ALCOHOL INTERACTION

4.2.1 Fasting glucose

The mean fasting glucose over the 12 weeks experimental period for alcohol, control, diabetes, and diabetes and alcohol groups are presented in Table 1 as mean ± SEM. The mean fasting glucose was significantly increased in DBALC and DB groups against NC group (Table 1, p=0.002 and 0.015 respectively). The ALC group was significantly decreased against DB group (Table 1, p=0.019), and DBALC group was significantly increased against ALC group (Table 1, p=0.002).

Table 1 Mean fasting glucose.

Significant difference in mean fasting glucose across groups.

Treatment groups	Mean Fasting glucose (mmol/L)
Control	5.1619 ± 0.06406
Alcohol	5.2095 ± 0.16687 $^{\theta}$
Diabetes	10.5179 ± 1.8907 *
Diabetes + Alcohol	12.568 ± 1.79175 $^{*\#}$

'*' represents a significant difference when compared to the NC group, '#' mean a significant difference in comparison to the ALC group, and 'θ' denotes a significant difference against the DB group. **Key:** NC= Control group (untreated), ALC = treated with alcohol, DB = (Diabetic group), and DBALC = diabetic animal treated with alcohol.

4.2.2 Surface area

The mean dorsal, ventral, and total surface area was determined for alcohol, control, diabetes, and diabetes and alcohol groups are presented in Table 2 as mean ± SEM and morphological images shown in figure 21. The mean dorsal surface area was significantly decreased in ALC and DBALC groups against NC group (Table 2, p=0.042 and 0.001 respectively). The DBALC group was also significantly decreased against DB and ALC groups (Table 2, p=0.008 and 0.005

respectively). The mean ventral surface area was significantly decreased in ALC and DBALC groups against NC group (Table 2, p=0.029 and 0.001 respectively). The DBALC group was also significantly decreased against the DB and ALC groups (Table 2, p=0.009 and 0.014 respectively). The mean total surface area was significantly decreased in ALC and DBALC groups against NC group (Table 2, p=0.033 and 0.001 respectively). The DBALC group was also significantly decreased against DB and ALC groups (Table 2, p=0.008 and 0.008 respectively). The heart surface appears shrunken with depressions in the ALC and DBALC groups, but morphological changes in atrium (arrows, Fig 21) of these groups are not clearly distinguishable.

Table 2 Surface Area

Significant difference in mean surface area across groups.

Treatment Group	Dorsal surface area (μm^2)	Ventral surface area (μm^2)	Total surface area (μm^2)
Control	222.865 ± 13.45294	223.938333 ± 12.91863	446.8033 ± 26.29238
Alcohol	192.5117 ± 8.31011 *****	188.795 ± 10.11812*****	381.3067 ± 17.91456*****
Diabetes	203.1467 ± 14.24206	201.453333 ± 14.01348	404.6 ± 28.10069
Diabetes + Alcohol	155.978 ± 8.20551 ***#θ**	156.662 ± 7.20353 ***#θ**	312.64 ± 15.22855***#θ**

'*' represents a significant difference when compared to the NC group, '#' mean a significant difference in comparison to the ALC group, and 'θ' denotes a significant difference against the DB group. Key: NC= Control group (untreated), ALC = treated with alcohol, DB = (Diabetic group), and DBALC = diabetic animal treated with alcohol.

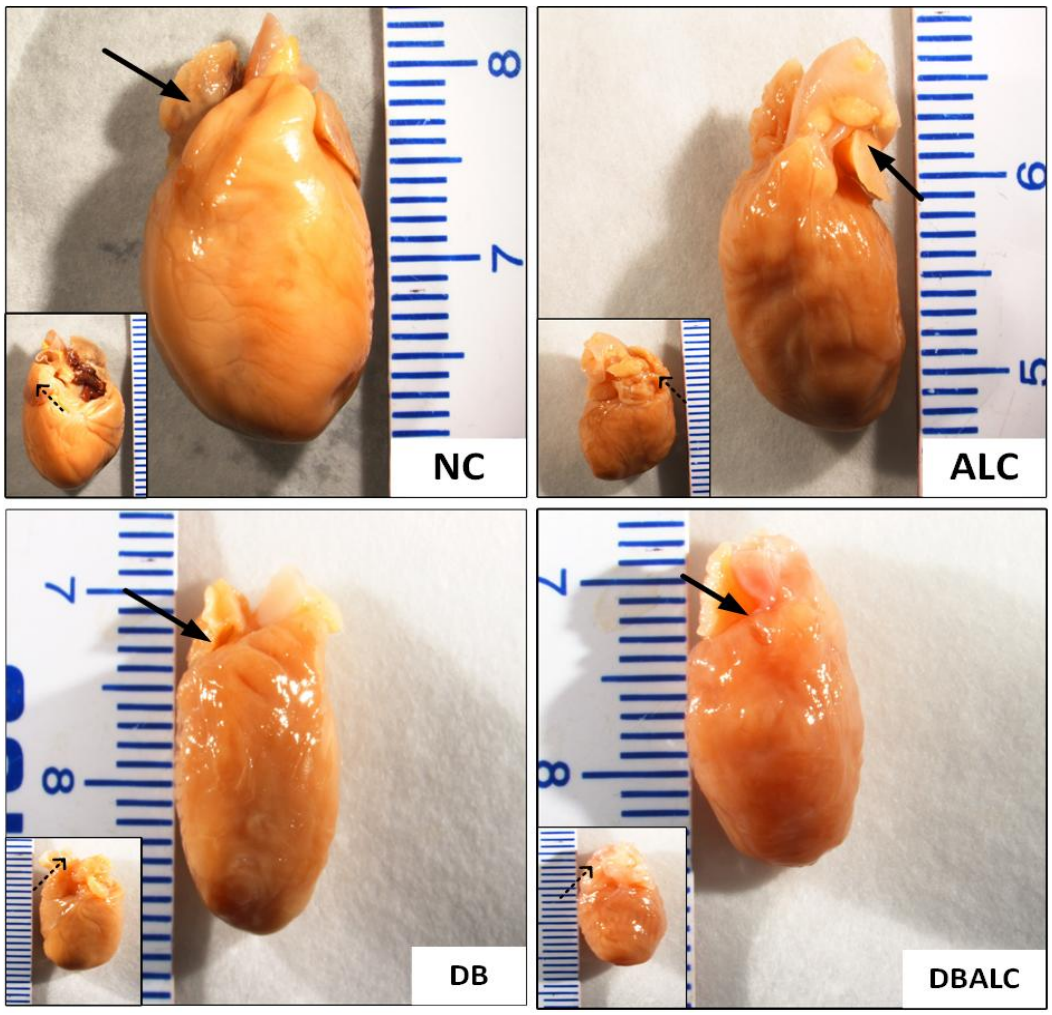

Figure 21 Mean surface area of the heart.

Black arrows: atrium: dorsal heart surface, broken arrow: atrium: ventral surface. Key: NC= Control group (untreated), ALC = treated with alcohol, DB = (Diabetic group), and DBALC = diabetic animal treated with alcohol.

4.2.3 Weight

The terminal body and heart weight of experimental animals were measured for alcohol, control, diabetes, and diabetes and alcohol groups, and presented in Table 3 as mean ± SEM.

Table 3 Body and heart weight

Significant difference in mean body and heart weight across groups.

Treatment groups	Body weight (g)	Heart Weight (g)	Body to Heart weight ratio
Alcohol	484.17 ± 16.21	1.55587 ± 0.101454 $^{\theta}$	315.07322 ± 13.92888
Control	514.67 ± 11.354	1.66542 ± 0.148496	322.09359 ± 30.1162
Diabetes	351.83 ± 25.37 $^{*\#}$	1.20375 ± 0.051581 $^{*\#}$	290.87448 ± 14.17306
Diabetes + Alcohol	342.83 ± 17.492 $^{*\#}$	1.06793 ± 0.02408 $^{*\#\theta}$	320.59668 ± 12.52004

'*' denotes a significant difference when compared to the NC group, '#' denotes a significant difference in comparison to the ALC group, and 'θ' denotes a significant difference against the DB group. Key: NC= Control group (untreated), ALC = treated with alcohol, DB = (Diabetic group), and DBALC = diabetic animal treated with alcohol.

The mean body weight in ALC group was significantly increased in ALC group against DB group (Table 3, p=0.001), significantly decreased in DB and DBALC groups against NC group (Table 3, p=0.001 in both groups) and significantly decreased in DBALC group against ALC group (Table 3, p=0.001).

4.2.4 Oxidative stress and cardiac muscle degeneration

The terminal serum MDA, GPx, and Troponin T and I were measured, and results are presented in Table 4 as mean ± SEM.

Table 4 MDA, GPx, Troponin I&T concentration

Significant difference in mean MDA, GPx, Troponin I&T across groups.

	MDA (µmol/gprotein)	GPx (µmol/L)	Troponin T (µmol/L)	Troponin I (µmol/L)
Control	0.01358681 ± 0.003113	58.23 ± 3.73049	36.048 ± 7.53214	74.6008 ± 5.26936
Alcohol	0.03300166 ± 0.004692*****	63.555 ± 1.03936	31,86367± 3.15072	74.552 ± 8.16457
Diabetes	0.0312297 ± 0.006165*****	66.4748 ± 5.27011	28,598 ± 8.14599	138.4582±11.27633***#**
Diabetes + Alcohol	0,017838903± 0.003409$^{\#\,\theta}$	44.1162±3.0645$^{*\#\theta}$	64.4392 ± 16.90913*	133,833 ± 16.86212*

'*' denotes a significant difference when compared to the NC group, '#' denotes a significant difference in comparison to the ALC group, and 'θ' denotes a significant difference against the DB group. Key: NC= Control group (untreated), ALC = treated with alcohol, DB = (Diabetic group), and DBALC = diabetic animal treated with alcohol.

The ALC and DB groups have a significantly higher mean MDA concentration against the NC group (p=0.009 and 0.034 respectively), while DBALC group is significantly decreased against DB and ALC groups (p=0.015 and 0.042 respectively). The GPx concentration is significantly lower in DBALC group against NC, ALC, and DB groups (p=0.019, 0.001, and 0.006 respectively). The DBALC significantly elevated troponin T concentration compared to control (p=0.39), while troponin I concentration is significantly higher in DB and DBALC against NC group (p=0.001), and significantly decreased in ALC group against DB group (p=0.001).

4.2.5 Coronary artery histomorphology

The coronary artery histomorphology changes in H&E (Fig. 22 A-D), Verhoeff Van Gieson (Fig. 22E-H), and Pentachrome stains (Fig. 22.1I-L), with varying morphologies represented. The tunica media thickness (double sided solid arrows, Fig. 22 A-D) and endothelial cells of tunica intima (arrowhead) are illustrated in H&E-stained images, and collagen fibres are represented in Verhoeff Van Gieson and Pentachrome stains (double sided broken arrow). The tunica media of the coronary artery was significantly thinner in ALC and DBALC groups against NC group (Table 5, p=0.026 and 0.023 respectively). The collagen percentage area fraction, as expressed in Van Gieson stain, is significantly lower in ALC, DB, and DBALC groups (Table 5, p=0.011, 0.039 and 0.044 respectively) against NC group. The elastic fibre percentage area fraction is significantly decreased in diabetes group against NC group (p=0.03). The collagen percentage area fraction, as observed in Pentachrome stain, is significantly increased in DBALC group against ALC group (Table 5, p=0.029). The muscle percentage area fraction was significantly decreased against DB group (Table 5, p=0.013). The collagen to elastic fibre ratio and collagen to muscle ratio both have no significant differences between groups.

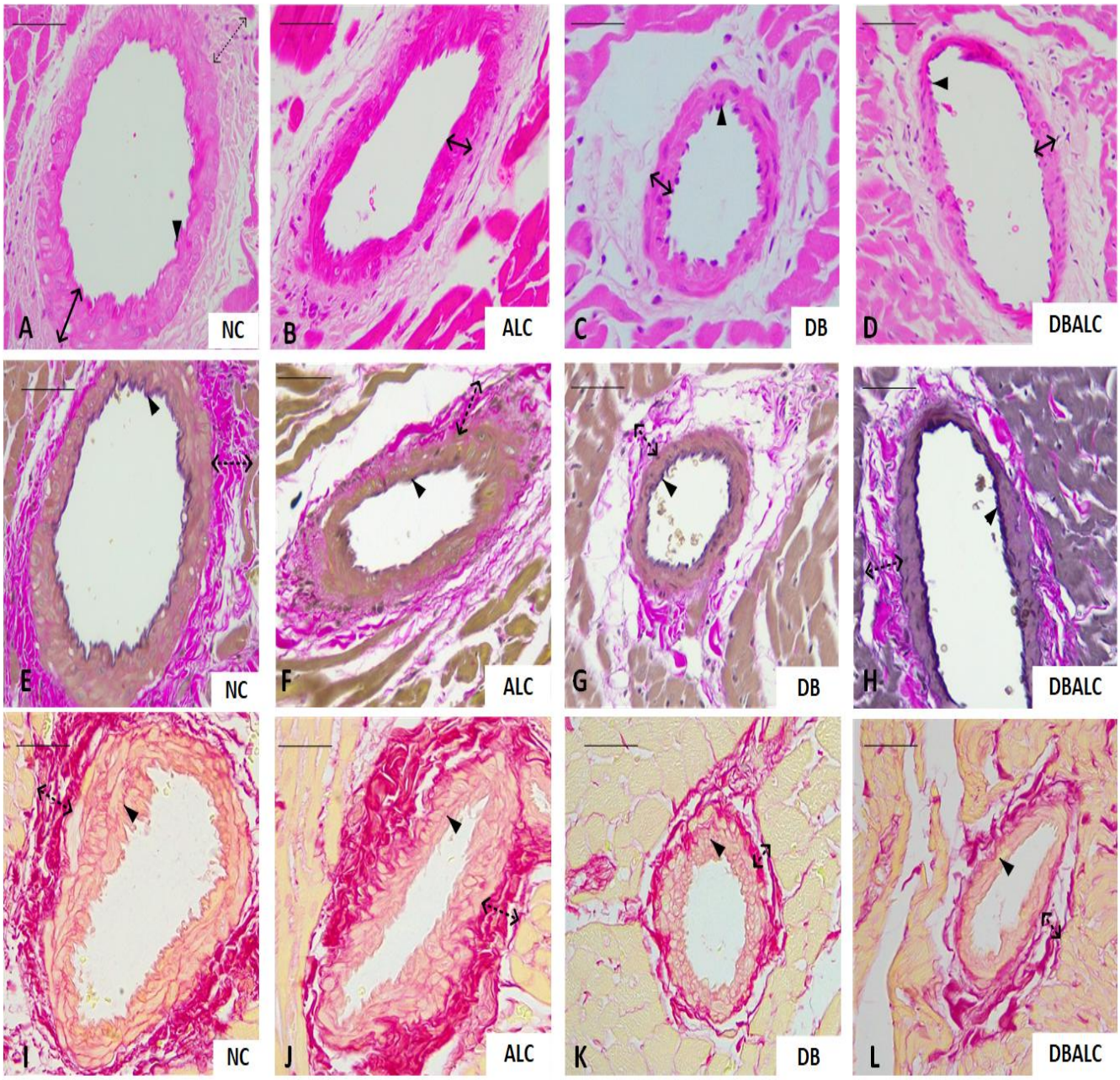

Figure 22 Coronary artery tunica media, collagen, smooth muscle, and elastic fibre profile

A-D) H&E stain, tunica media thickness (double-sided solid arrows), and the endothelial cells of the tunica intima (arrowhead). **E-H)** Verhoeff Van Gieson stain, collagen in pink/purple (double-sided broken arrows), elastic fibres in blue-black (arrowhead). **I-L)** Pentachrome stain, collagen in pink/purple (double-sided broken arrows), muscle fibres in blue-black (arrowhead). **Key**: NC= Control group (untreated), ALC = treated with alcohol, DB = (Diabetic group), and DBALC = diabetic animal treated with alcohol.

Table 5 Coronary Artery Histomorphology

	Tunica media Thickness (H&E) (µm)	Collagen (Van Gieson) (%)	Elastic Fibres (Van Gieson) (%)	Collagen to Elastic Fibre Ratio (Van Gieson)	Collagen (Pentachrome) (%)	Smooth muscle (Pentachrome) (%)	Collagen to smooth muscle ratio
Control	32.26 ± 2.956	20.576 ± 2.269	7.201 ± 1.167	0.359 ± 0.0518	27.149 ± 1.655	41.153 ± 3.860	1.572 ± 0.204
Alcohol	27.058 ± 1.126*	11.934 ± 2.269*	4.321 ± 1.343*	0.382 ± 0.115	24.269 ± 1.929	31.482 ± 4.249 θ	1.391 ± 0.288
Diabetes	24.366 ± 2.0058	13.786 ± 2.597*	4.321 ± 0.694*	0.364 ± 0.081	30.234 ± 3.615	48.149 ± 4.695	1.806 ± 0.368
Diabetes + Alcohol	23.280 ± 2.561*	12.757 ± 3.457*	5.349 ± 0.991	0.584 ± 0.163	35.376 ± 4.797 #	43.2106± 5.295	1.430 ± 0.335

Mean coronary artery tunica media thickness, collagen to elastic fibre ratio, and collagen to smooth muscle ratio across groups.

'*' denotes a significant difference when compared to the NC group, '#' denotes a significant difference in comparison to the ALC group, and 'θ' denotes a significant difference against the DB group. Key: NC= Control group (untreated), ALC = treated with alcohol, DB = (Diabetic group), and DBALC = diabetic animal treated with alcohol.

4.2.6 Aorta histomorphology

The histomorphology of aorta wall stained in H&E (Fig. 23A-D), Verhoeff Van Gieson (Fig. 23 E-H), and Pentachrome stain (Fig. 23I-L) respectively. The tunica media thickness (Fig. 23A-D, double sided solid arrows), tunica intima (Fig. 23A-D, broken arrows), and foam cells (Fig. 23C, encircled) are represented in H&E-stained images. Collagen fibres are presented in Verhoeff Van Gieson, and Pentachrome stained images (Fig. 23 E-L, double sided broken arrows), and smooth muscle fibres in Pentachrome stained images are represented by arrowhead. The thickness of the tunica media was significantly increased in ALC group against NC group (Table 6, p=0.013). The collagen percentage area fraction as observed in Van Gieson stain was significantly higher in the ALC group against NC and DB groups (Table 6, p=0.013 and 0.008 respectively), and significantly lower in DBALC group against the DB and ALC groups (Table 6, p=0.037 and 0.001 respectively). The collagen to elastic fibre ratio is significantly lower in DBALC group against the ALC group (Table 6, p=0.018). The collagen, muscle, collagen to muscle ratio, as well as elastic fibre percentage area fraction all have no significant difference across all groups.

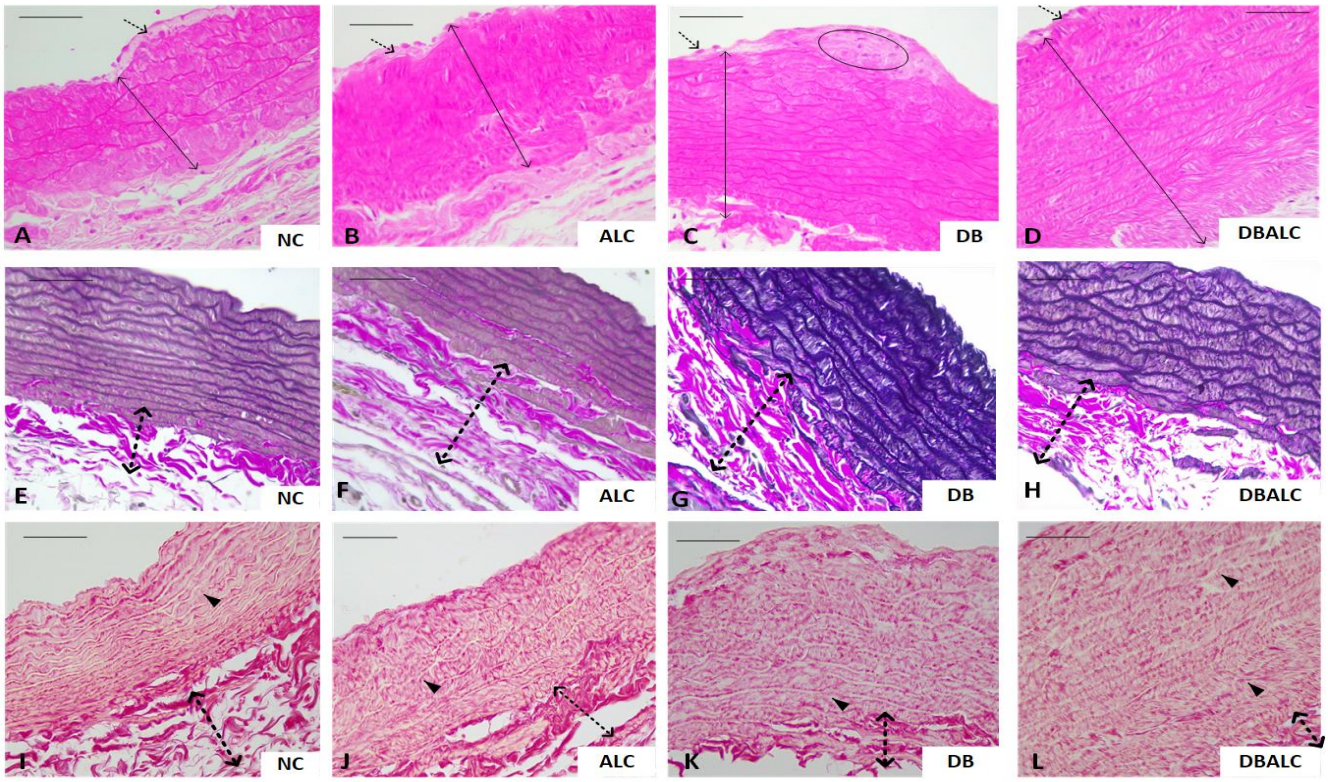

Figure 23 Aorta tunica media, collagen, smooth muscle, and elastic fibre profile

A-D) H&E stain, tunica media thickness (double sided solid arrows) and the endothelial cells of the tunica intima (arrowhead). **E-H)** Verhoeff Van Gieson stain, collagen in pink/purple (double sided broken arrows), elastic fibres in blue-black (arrowhead). **I-L)** Pentachrome stain, collagen in pink/purple (double sided broken arrows), muscle fibres in blue-black (arrowhead). Key: NC= Control group (untreated), ALC = treated with alcohol, DB = (Diabetic group), and DBALC = diabetic animal treated with alcohol.

Table 6 Aorta Histomorphology

Mean aorta tunica media thickness, collagen to elastic fibre ratio, and collagen to smooth muscle ratio across groups.

	Tunica Media Thickness (µm) (H&E)	% Collagen (Van Gieson)	% Elastic (Van Gieson)	% Collagen to Elastic Ratio (Van Gieson)	% Collagen area (Pentachrome)	% Smooth muscle area (Pentachrome)	% Collagen to smooth muscle ratio
Control	114.58 ± 4.644	16.872± 2.057	23.251 ± 1.870	0.774 ± 0.151	31.893± 6.45	40.741 ± 7.617	1.865 ± 1.266
Alcohol	141.209 ± 9.014 *****	23.868 ± 1.736$^{*\theta}$	19.753 ± 3.297	1.487 ± 0.386	32.305 ± 5.714	37.243 ± 5.661	1.525 ± 0.895
Diabetes	144.468 ± 15.767	17.284 ± 1.460	20.370 ± 4.165	1.225± 0.398	32.716 ± 6.195	40.329 ± 5.166	0.948 ± 0.24
Diabetes + Alcohol	157.238 ± 36.663	13.168 ± 1.449 $^{\theta\#}$	24.897 ± 2.218	0.538 ± 0.057$^{\#}$	28.601 ± 4.398	50.206 ± 5.349	0.641 ± 0.141

'*' denotes a significant difference when compared to the NC group, '#' denotes a significant difference in comparison to the ALC group, and 'θ' denotes a significant difference against the DB group. Key: NC= Control group (untreated), ALC = treated with alcohol, DB = (Diabetic group), and DBALC = diabetic animal treated with alcohol.

4.2.7 Atrial histomorphology

The atrium histomorphology in H&E (Fig. 24, A-D), and Pentachrome stain (Fig. 24, E-H), with varying morphologies were observed. The interstitial spaces (Fig. 24, asterisks) and interstitial cells (Fig. 24, encircled) were presented in H&E-stained images, and varying presentations of collagen fibres (broken arrows) across groups are shown. The atrial percentage area fraction represented by interstitial spaces in DBALC group is significantly higher against NC group (Table 7, p=0.031). The collagen percentage area fraction is significantly higher in DB and ALC groups against NC group (Table 7, p=0.034 and 0.007 respectively). The width of muscle at point of bifurcation was significantly lower in ALC group against NC and DB groups (Table 7, p=0.003 and 0.005), and significantly lower in DBALC group against the ALC group (Table 7, p=0.016). The waviness, collagen, and collagen to muscle percentage area fraction have no significant differences across all groups.

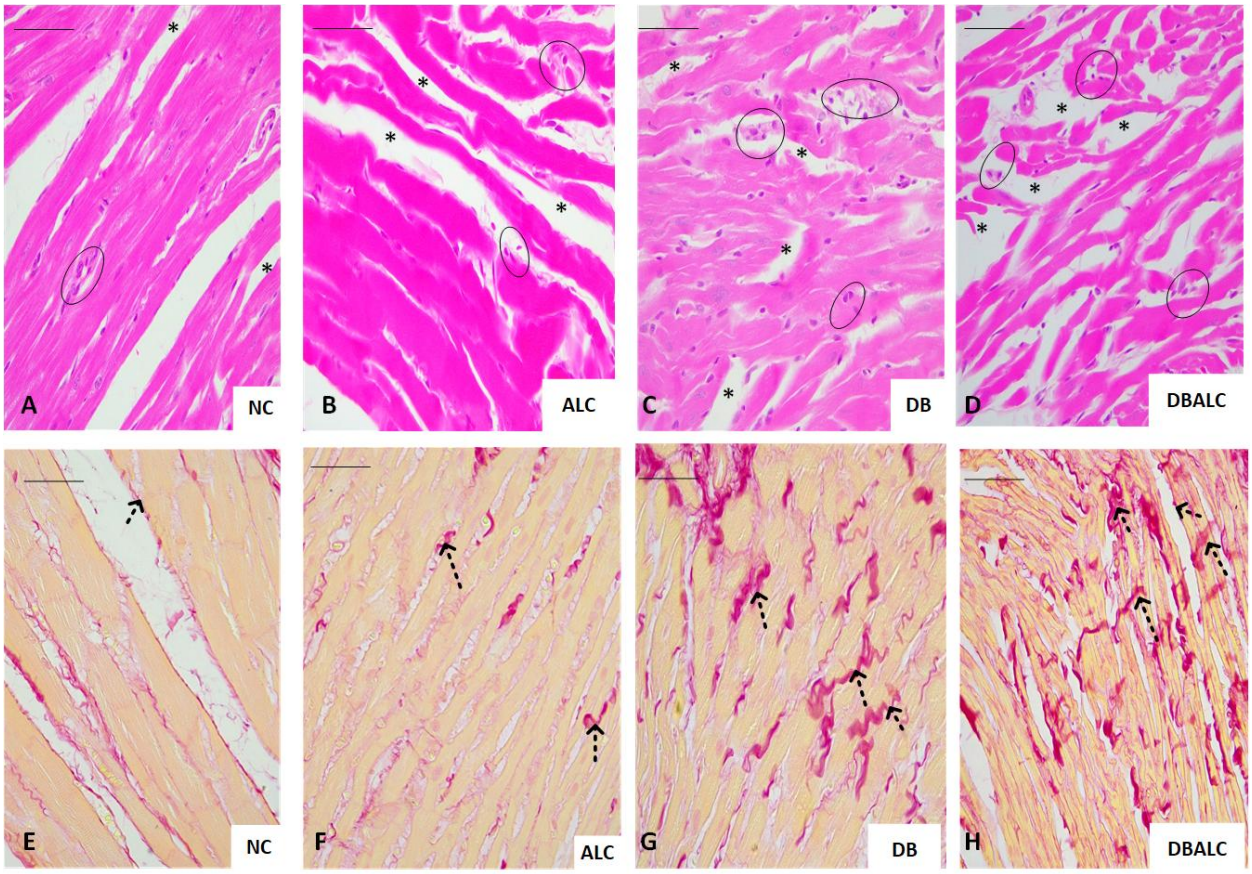

Figure 24 Atrial interstitial space, interstitial cells and cardiac myocyte to collagen profile

A-D) H&E stain, interstial cells (encircled), interstitial spaces (Fig. 24, asterisks). **E-H)** Pentachrome stain, collagen in pink/purple (broken arrows), muscle fibres in yellow to orange. Key: NC= Control group (untreated), ALC = treated with alcohol, DB = (Diabetic group), and DBALC = diabetic animal treated with alcohol.

Table 7 Atrial histomorphology

The results of the interstitial space percentage area fraction, collagen to muscle ratio, width of muscle fibre at the point of bifurcation and the score of waviness.

Treatment group	% Interstitial Space (H&E)	% Collagen	% Muscle	% Collagen to Muscle ratio	Muscle Bifurcation (µm)	Waviness Score
Alcohol	28.60±2.9	17.49 ± 1.66*	56.58 ± 4.49	3.40 ± 0.43	14.06 ± 0.92 *θ	1.1667 ± 0.21082
Control	21.81±3.54	10.08 ± 1.81	62.75 ± 7.32	8.81 ± 3.32	18.68 ± 0.98	1.5 ± 0.22361
Diabetes	28.60±4.03	16.66 ± 2.64*	53.29 ± 3.11	3.70± 0.68	20.07 ± 1.62	2 ± 0.2582
Diabetes + Alcohol	33.33±4.19 *	15.63 ± 3.82	53.49± 7.11	4.64± 1.31	17.212 ± 0.87#	1.8 ± 0.1633

'*' denotes a significant difference when compared to the NC group, '#' denotes a significant difference in comparison to the ALC group, and 'θ' denotes a significant difference against the DB group. Key: NC= Control group (untreated), ALC = treated with alcohol, DB = (Diabetic group), and DBALC = diabetic animal treated with alcohol.

4.2.8 Ventricle

The atrium is presented below, stained in H&E (Fig. 25A-D), and Pentachrome stains (Fig. 25E-H), with varying morphologies represented. The interstitial spaces (asterisks) and interstitial cells (encircled) are shown in H&E-stained images. The collagen fibres (broken arrows) are illustrated in Pentachrome stained images. The interstitial space percentage area fraction is significantly higher in DB group against NC group ($p=0.037$). The collagen percentage area fraction in ALC group is significantly lower in ALC group against NC and DBALC groups ($p<0.001$ and $p=0.03$ respectively), and significantly lower in DBALC group against ALC group ($p<0.001$). The muscle percentage area fraction is significantly lower in ALC and DB groups against NC group ($p<0.001$ and $p=0.038$ respectively), and significantly higher in DBALC group against ALC group ($p=0.04$). The collagen to muscle fibre ratio is significantly lower in ALC group against NC and DB groups ($p<0.001$ and $p=0.011$ respectively), and significantly higher in DBALC group against ALC group ($p<0.001$). The width of muscle fibre at bifurcation, and muscle waviness have no significant differences between groups.

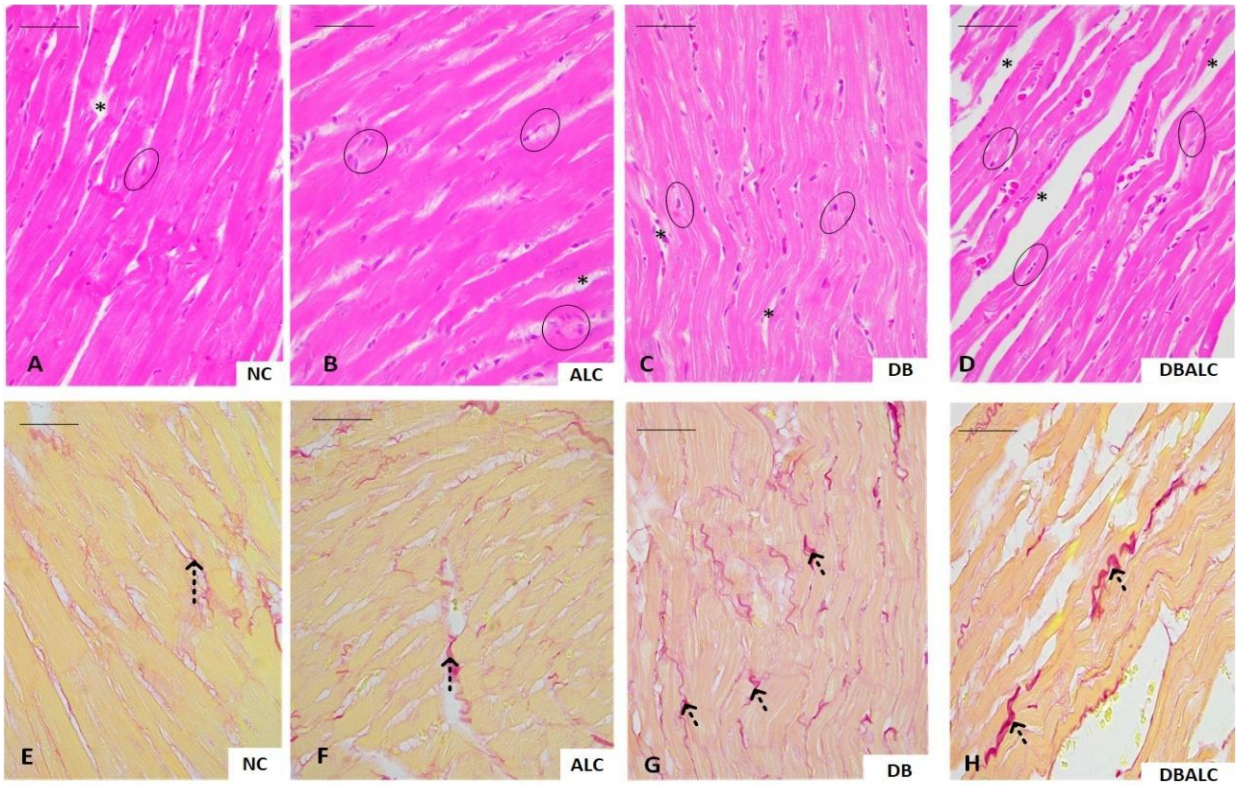

Figure 25 Ventricular interstitial space (asterisk), interstitial cell (encircled),and collagen profile (broken arrow).

Table 8 Ventricle

The results of the ventricular interstitial spaces percentage area fraction, collagen to muscle ratio, width of muscle fibre at the point of bifurcation, and score of waviness are presented in the table below.

	Interstitial Space (H&E) (%)	**Collagen percentage area fraction (%)**	**Muscle percentage area fraction (%)**	**Collagen to Muscle ratio**	**Muscle Bifurcation (µm)**	**Waviness score**
Alcohol	26.3379±1.61496	15.0208 ± 1.21034 *θ	50.4124 ± 3.17838 *****	3.4752 ± 0.41247 *θ	16.05 ± 1.19876	1.1667 ± 0.16667
Control	20.7822±3.45415	8.6421 ± 0.71279	75.7214 ± 4.92462	9.2466 ± 1.24713	16.7817 ± 1.34923	1 ± 0
Diabetes	29.2186±2.44159 *****	10.2882 ± 1.87686	60.2891 ± 6.04332 *****	6.7028 ± 1.12431	17.1808 ± 1.48217	1.3333 ± 0.21082
Diabetes + Alcohol	26.4202±3.05087	8.0248 ± 0.69474 #	64.4044 ± 6.46573 #	8.3452 ± 1.09935 #	19.259 ± 1.78537	1.4 ± 0.2

‘*’ denotes a significant difference when compared to the NC group, ‘#’ denotes a significant difference in comparison to the ALC group, and ‘θ’ denotes a significant difference against the DB group. Key: NC= Control group (untreated), ALC = treated with alcohol, DB = (Diabetic group), and DBALC = diabetic animal treated with alcohol.

4.2.9 Endothelial Nitric Oxide Synthase and C-Reactive Protein

The expression of CRP (Fig. 26A-H) and eNOS (Fig. 26I-P) are presented in their varying morphologies in epicardium and aorta. The NC group showed no presentation of CRP in both epicardium and aorta (Fig. 4.2.5A&E), while ALC (Fig. 26 B&F) and ARV (Fig. 26 C&G) groups expressed CRP in both nucleus (broken arrows) and myocyte (solid arrows) of epicardium and aorta. The DBALC group expressed more CRP in epicardium (solid arrows) (Fig. 26D) and also had some nuclear expression (broken arrows) in aorta (Fig. 26H). The NC group showed extensive expression of eNOS in epicardium (Fig. 26I) and aorta nucleus (Fig. 26M), with epicardium (solid arrows) of ALC group (Fig. 26J) showing less expression, and epicardia (solid arrows) of DB and DBALC groups (Fig. 26 K&L) showing little to no expression of eNOS. No eNOS is expressed in aorta of ALC, DB, and DBALC groups (Fig. 26 N, O, &P).

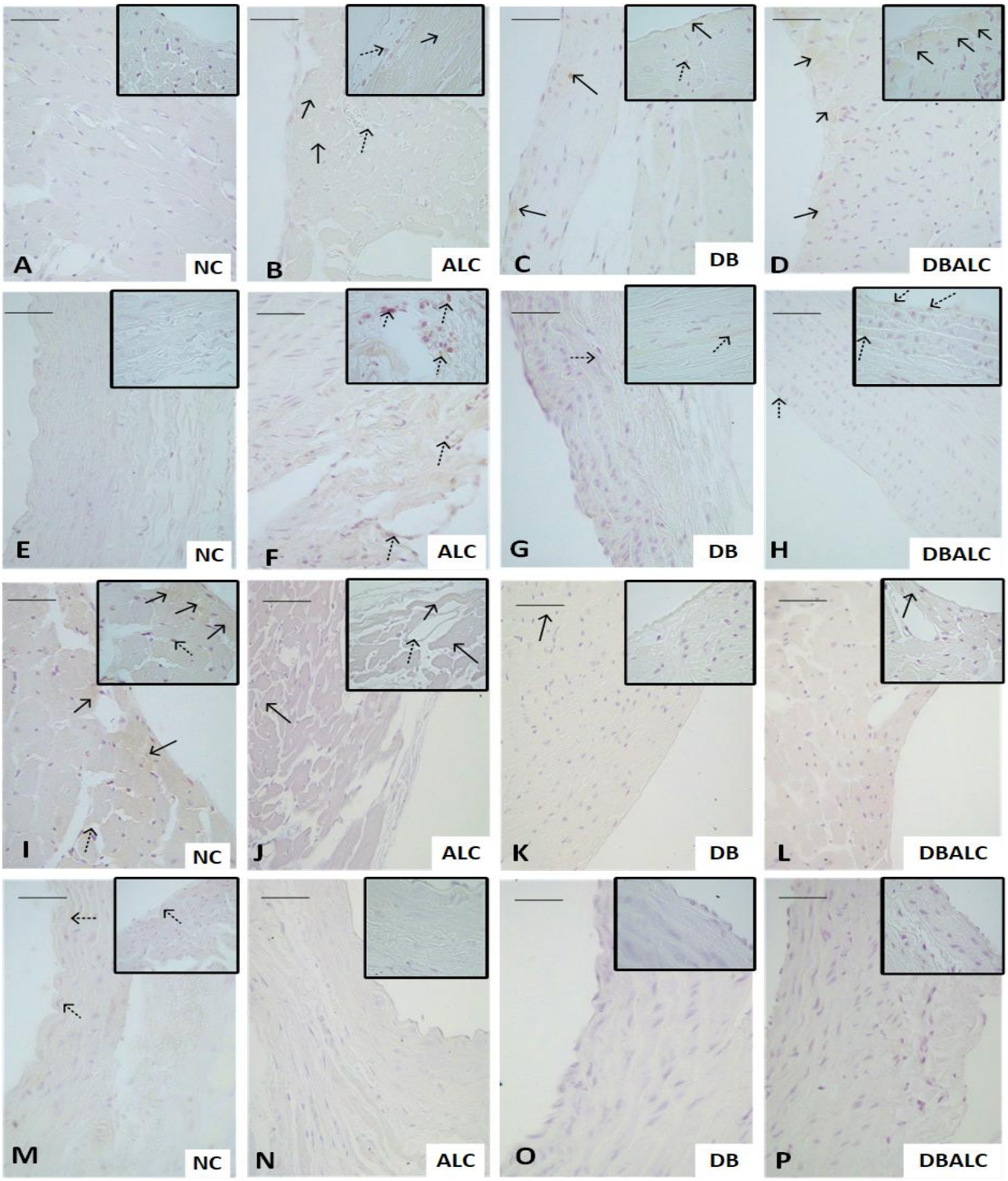

Figure 26 Endothelial Nitric Oxide Synthase and C-Reactive Protein

The expression of CRP (Fig. 4.2.5A-H), with the NC group showing no expression in both the epicardium (solid arrow) and the nucleus (broken arrow) of the aorta, the ALC group showing the most expression in both the epicardium (solid arrow) and nuclei of the aorta (broken arrows), and the DB and DBALC groups showing little to no expression and eNOS in both epicardium (solid arrows) and aorta (broken arrows). The expression of eNOS (Fig. 4.2.5I-P), with the NC group showing the most eNOS expression, in both the epicardium (solid arrows) and the nuclei in the aorta (broken arrows). The epicardium in the ALC, DB and DBALC groups showed little to no eNOS presentation (solid arrows), while the aorta in the ALC, DB and DBALC groups showed no eNOS presentation. Key: NC: control (non-treated; ARV: cART treated; ALCARV: Alcohol + cART; DBARV: diabetic + cART; DBALCARV: diabetic + alcohol + cART.

4.2.10 4.2.10 TNF- alpha and Caspase 3 expression

Several techniques were tried to optimize TNF- alpha and Caspase 3 expression including adjusting primary antibody dilutions (1:50, 1:100, 1:1250, 1:500, 1:1000), comparing absent and present antigen retrieval in citrate buffer versus EDTA, adjusting time and concentration of

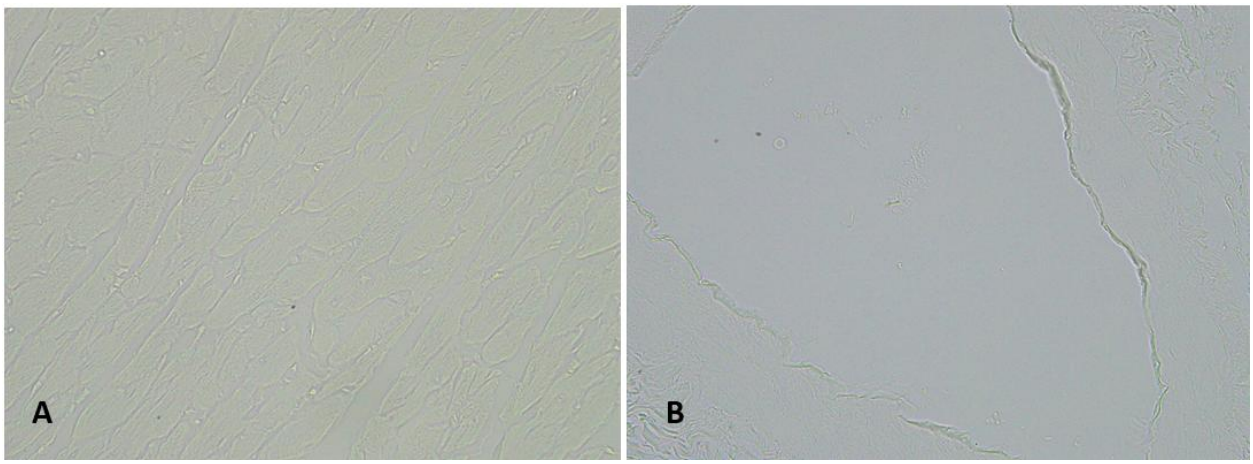

blocking buffer (3% for 30 mins, 3% 1 hr, 5% 30 mins, 5% 1hr), changing ABC kit, secondary.

Figure 27 TNF-alpha and Caspase 3 non expression.

The non-expression of TNF-α (A) and Caspase-3 (B).

CHAPTER 5

DISCUSSION AND CONCLUSIONS

This study was conducted to determine the cardiovascular toxicity effects that may arise due to alcohol use and sub-chronic cART regimes as PEP in diabetic individuals. The HIV naïve model used enables combinatorial effects to be studied by excluding possible confounding effects of HIV presence. The independent effects of cART, diabetes, and alcohol on the cardiovascular system have been well-researched

in HIV patients (Fernández-Solà, 2020b; Triposkiadis *et al.*, 2021; Batta *et al.*, 2023), but the combined effects of these parameters have not garnered much attention, especially in HIV naïve model. The results show elevated fasting glucose in diabetic groups (DB, DBALC, DBARV, and DBALCARV) with an attendant reduction in body weight and heart weight as reported in previous diabetic studies (Ioannou, Bryson and Boyko, 2007; Thrower and Bingley, 2014).

5.1 Independent cardiovascular effects of cART, diabetes, and alcohol

The cART treatment (ARV) induced oxidative stress (elevated GPx and reduced MDA), coronary artery inflammation (expression of CRP, non-expression of eNOS), tunic perturbations (increased elastic and decreased collagen fibers, ventricular atrophy (myocyte depletion and non-expression of eNOS) and increased atrial interstitial spaces, cells, and CRP expression. These observed cART effects corroborate with reports of cART-induced ROS imbalance with induced vascular inflammation and endothelial dysfunction (Jiang *et al.*, 2007; Steven *et al.*, 2019). Disruption of vascular and myocyte endothelium culminates in increased CRP signaling as a

downstream indicator of inflammation which has been associated with atrial fibrillation and ventricular atrophy (Eklund, 2009; Li *et al.*, 2022). Similarly, elevated Troponin I concentration observed with cART treatment is indicative of myocyte disassembling and is severally reported in association with myocardial necrosis and infarction (Potter, Hickman and Cullen, 2022). Consequently, cART treatment may induce ventricular muscle loss, and atrial thinning which could have led to significantly reduced total surface area of the heart recorded in cART group.

Additionally, alcohol treatment (ALC) induced elevated MDA levels, aorta inflammation (expression of CRP, non-expression of eNOS), elevated collagen in aorta, atrium, and ventricle combined with ventricular myocyte and coronary artery thinning (reduced tunica media and collagen). This potential for alcohol to induce fibrogenesis typically collagen type 1 to 3 has been previously reported (Soufen *et al.*, 2008). Our results indicate replacement fibrosis in the ventricle (decrease in myocyte with an increase in collagen) but reparative fibrosis (Vaideeswar *et al.*, 2014; Cunha *et al.*, 2022) in atrium and aorta, potentially due to pressure load induced by thinner dilated coronary vessels or/ and oxidative stress (Aragno *et al.*, 2008). Such myocardial effects of alcohol have been previously described as alcohol-dilated cardiomyopathy (Mirijello *et al.*, 2017).

Furthermore, diabetes condition (DB) independently elevates oxidants (MDA), aorta inflammation, endothelial dysfunction (shown by CRP expression and non-expression of eNOS), coronary artery dilation (indicated in reduced tunica media, collagen, and elastic fibres), and myocardial decline (indicated in atrial collagen deposition and ventricular myocyte loss with increased interstitial spaces). These results confirm reports of diabetes-induced oxidative stress and hyperglycemia (Thorand *et al.*, 2003) and cardiovascular inflammation (Assar, Angulo and Rodríguez-Mañas, 2016) facilitating depleted endothelial NOS production and mediation of

vasodilation. Our results show that diabetes induced pressure load due to coronary dilation may lead to an observed dilated ventricular atrophy and atrial fibrosis due to CRP expression as previously reported (Nemoto *et al.*, 2006; Nortamo *et al.*, 2017). Similarly, the recorded reduction in heart weight and elevated Troponin I observed in diabetes is reminiscent of diabetic dilated cardiomyopathy (Nellessen *et al.*, 2006).

5.2 Chemo-toxic effects of cART comorbidities with alcohol and diabetes on cardiovascular histopathology

Our results show that concomitant cART and ethanol treatment (ALCARV) mitigated the independent effects of both treatments on oxidative stress with elevation in both oxidants and antioxidants. This may arise due to the competition of cART and ethanol for cytochrome P which is utilized by both treatments for their intracellular signaling (Walubo, 2007; Doody *et al.*, 2017). We also report that the chemical interaction in ALCARV maintained ethanol-induced effects of coronary artery dilation and inflammation, aorta stiffening, atrial and ventricular fibrosis, and myocardial eNOS depletion. However, ALCARV did not induce myocardial CRP expression and serum Troponin I concentrations. This indicates that ALCARV interaction can induce cardiovascular perturbation in the absence of myocardial inflammation, which may not be detected in serum Troponin I which is often used in clinical diagnosis (Cerrato *et al.*, 2015; Piano, 2017).

On the other hand, cART treatment in diabetes (DBARV) maintains mostly the ART-induced effects of oxidative stress, inflammation with CRP expression (myocardial, interstitial, and coronary), and endothelial dysfunction with non-eNOS expression (myocardial and coronary). Additionally, DBARV increased atrial interstitial spaces and reduced the width of atrial myocyte bifurcation with an observed decrease in Troponin T but elevation in Troponin I higher than all

the other treated groups. This is consistent with reports of heightened Troponin I compared with Troponin T post-myocardial ischemia (Espinosa *et al.,* 2023). Although myocardial depletion and fibrosis are not reported in DBARV, the heightened myocardial and coronary inflammation and endothelial dysfunction reported compared to independent ARV and DB levels are major risk factors for the development of cardiovascular conditions (Joshi *et al.*, 2012; Kolluru, Bir and Kevil, 2012).

The multiple morbidity of cART, alcohol, and diabetes (DBALCARV) preserves the independent diabetic effect of increasing oxidant (MDA), and coronary artery dilation (tunica media and elastic fibre depletion). The results also show that DBALCARV upholds ALCARV effect of coronary artery inflammation, endothelial dysfunction, aorta stiffening, and replacement ventricular fibrosis. This indicates the cumulative vascular impediment by DBALCARV multiple morbidity. However, DBALCARV induces an additional effect of increased atrial interstitial cells, collagen deposition, and waviness of atrial myocytes coupled with reduced width of atrial myocyte bifurcation, indicative of histopathological changes described in atrial fibrillation (Weil and Ozcan, 2015). Furthermore, DBALCARV elevates Troponin T in contrast to Troponin I elevated in ARV and DBARV groups. This corroborates with reports of increased serum Troponin T levels in atrial fibrillation (Costabel, Burgos and Trivi, 2017).

5.3 Cardiovascular histopathology with alcohol use in diabetes

The interaction between alcohol treatment and diabetes (DBALC) reveals reduced antioxidants, aorta inflammation, coronary artery endothelial dysfunction, increased arterial interstitial spaces, and ventricular replacement fibrosis as previously reported (Vaideeswar *et al.*, 2014; Tsermpini, Plemenitaš Ilješ and Dolžan, 2022). Although these DBALC effects seem minimal compared to independent effects of ALC and DB, DBALC interaction records an elevation in both Troponin I

and Troponin T and could serve as an indicator of broad cardiovascular perturbations affecting the aorta, coronary artery, atrium, and ventricle simultaneously.

5.4 Conclusion

This study clearly shows that serum markers, and tissue-specific endothelial, inflammatory, and histological changes in cardiovascular system due to different combinations of diabetes, alcohol, and cART. One common factor that underpins all the treatments is presence of oxidative stress. This study demonstrates that myocyte, vascular inflammation and endothelial dysfunction in diabetes and its combination with cART treatment can induce elevated levels of serum Troponin I even in the absence of significant myocardial depletion. Similarly, cART, alcohol, and diabetes induce ventricular atrophy and fibrosis, atrial fibrillation, vascular inflammation, and endothelial dysfunction but only elevate Troponin T levels in serum. This should be taken into consideration in diagnosis and cardiovascular management of diabetic patients on cART PEP.

5.5 Recommendations for further studies

This study revealed that the combination of cART, alcohol, and diabetes in an HIV-naïve model induces oxidative stress and inflammation, leading to ventricular atrophy, atrial thinning, and fibrosis, with cardiovascular disturbances indicated by elevated cardiovascular biomarkers; Troponin T and I. This will be useful in the treatment of diabetic patients using PEP. Further investigation into the effects of all these factors on other organ systems would be useful in the holistic treatment of patients.

References

Abhilasha *et al.* (2021) 'Downregulation of interleukin-10 receptor (IL-10R) along with low serum IL-10 levels in newly diagnosed type 2 diabetes mellitus patients', *Gene Reports*, 24, p. 101251. Available at: https://doi.org/10.1016/j.genrep.2021.101251.

Alvarez Cooper, I. *et al.* (2020) 'Tumour Necrosis Factor in Neuroplasticity, Neurogenesis and Alcohol Use Disorder', *Brain Plasticity*, 6(1), pp. 47–66. Available at: https://doi.org/10.3233/BPL-190095.

Antony, I. *et al.* (2020) 'An Outlook on the Impact of HIV Infection and Highly Active Antiretroviral Therapy on the Cardiovascular System – A Review', *Cureus*, 12(11). Available at: https://doi.org/10.7759/cureus.11539.

Arackal, A. and Alsayouri, K. (2022) *Histology, Heart, StatPearls [Internet]*. StatPearls Publishing. Available at: https://www.ncbi.nlm.nih.gov/books/NBK545143/ (Accessed: 17 November 2022).

Aragno, M. *et al.* (2008) 'Oxidative Stress Triggers Cardiac Fibrosis in the Heart of Diabetic Rats', *Endocrinology*, 149(1), pp. 380–388. Available at: https://doi.org/10.1210/en.2007-0877.

Assar, M.E., Angulo, J. and Rodríguez-Mañas, L. (2016) 'Diabetes and ageing-induced vascular inflammation', *The Journal of Physiology*, 594(8), pp. 2125–2146. Available at: https://doi.org/10.1113/JP270841.

Bajpai, A. and Tilley, D.G. (2018) 'The Role of Leukocytes in Diabetic Cardiomyopathy', *Frontiers in Physiology*, 9, p. 1547. Available at: https://doi.org/10.3389/fphys.2018.01547.

Bastaki, S. (2005) 'Diabetes mellitus and its treatment', *Dubai Diabetes and Endocrinology Journal*, 13, pp. 111–134. Available at: https://doi.org/10.1159/000497580.

Batta, Y. *et al.* (2023) 'Direct and indirect cardiovascular and cardiometabolic sequelae of the combined anti-retroviral therapy on people living with HIV', *Frontiers in Physiology*, 14, p. 1118653. Available at: https://doi.org/10.3389/fphys.2023.1118653.

Bhatt, N.M. *et al.* (2015) 'Restoring redox balance enhances contractility in heart trabeculae from type 2 diabetic rats exposed to high glucose', *American Journal of Physiology. Heart and Circulatory Physiology*, 308(4), pp. H291-302. Available at: https://doi.org/10.1152/ajpheart.00378.2014.

Birkhoelzer, S.M., Cowan, E. and Guha, K. (2021) 'COVID-19: treatments and the potential for cardiotoxicity', *The British Journal of Cardiology*, 28(1), p. 7. Available at: https://doi.org/10.5837/bjc.2021.007.

Brien, S.E. *et al.* (2011) 'Effect of alcohol consumption on biological markers associated with risk of coronary heart disease: systematic review and meta-analysis of interventional studies', *BMJ*, 342, p. d636. Available at: https://doi.org/10.1136/bmj.d636.

Brunová, J. (2004) '[Endocrine diseases and diabetes]', *Casopis Lekaru Ceskych*, 143(8), pp. 507–511.

Cerrato, E. *et al.* (2015) 'Cardiovascular disease in HIV patients: from bench to bedside and backwards', *Open Heart*, 2(1), p. e000174. Available at: https://doi.org/10.1136/openhrt-2014-000174.

Cheng, D.M. *et al.* (2009) 'Alcohol consumption and lipodystrophy in HIV-infected adults with alcohol problems', *Alcohol (Fayetteville, N.Y.)*, 43(1), pp. 65–71. Available at: https://doi.org/10.1016/j.alcohol.2008.09.004.

Cheung, N. and Wong, T.Y. (2008) 'Diabetic retinopathy and systemic vascular complications', *Progress in Retinal and Eye Research*, 27(2), pp. 161–176. Available at: https://doi.org/10.1016/j.preteyeres.2007.12.001.

Chia, P.Y., Teo, A. and Yeo, T.W. (2020) 'Overview of the Assessment of Endothelial Function in Humans', *Frontiers in Medicine*, 7, p. 542567. Available at: https://doi.org/10.3389/fmed.2020.542567.

Costabel, J.P., Burgos, L.M. and Trivi, M. (2017) 'The Significance Of Troponin Elevation In Atrial Fibrillation', *Journal of Atrial Fibrillation*, 9(6), p. 1530. Available at: https://doi.org/10.4022/jafib.1530.

da Cunha, G.H. *et al.* (2020) 'Diabetes mellitus in people living with HIV/AIDS: prevalence and associated risk factors', *AIDS care*, 32(5), pp. 600–607. Available at: https://doi.org/10.1080/09540121.2019.1695727.

Cunha, P.S. *et al.* (2022) 'The Atrium in Atrial Fibrillation – A Clinical Review on How to Manage Atrial Fibrotic Substrates', *Frontiers in Cardiovascular Medicine*, 9. Available at: https://doi.org/10.3389/fcvm.2022.879984.

Cupido, J. (2021) *The Demand for Alcohol in South Africa during the National Lockdown*, *International Society of Substance Abuse Professionals*. Available at: https://www.issup.net/knowledge-share/publications/2021-02/demand-alcohol-south-africa-during-national-lockdown (Accessed: 9 February 2023).

Dong, J. and Chen, H. (2018) 'Cardiotoxicity of Anticancer Therapeutics', *Frontiers in Cardiovascular Medicine*, 5, p. 9. Available at: https://doi.org/10.3389/fcvm.2018.00009.

Doody, E.E. *et al.* (2017) 'Ethanol metabolism by alcohol dehydrogenase or cytochrome P450 2E1 differentially impairs hepatic protein trafficking and growth hormone signaling', *American Journal of Physiology. Gastrointestinal and Liver Physiology*, 313(6), pp. G558–G569. Available at: https://doi.org/10.1152/ajpgi.00027.2017.

Dubé, M.P. *et al.* (2008) 'Effects of HIV Infection and Antiretroviral Therapy on the Heart and Vasculature', *Circulation*, 118(2), pp. e36–e40. Available at: https://doi.org/10.1161/CIRCULATIONAHA.107.189625.

Ehehalt, F. *et al.* (2015) 'Blood Glucose Homeostasis in the Course of Partial Pancreatectomy – Evidence for Surgically Reversible Diabetes Induced by Cholestasis | PLOS ONE', *PLOS ONE*, 10(8). Available at: https://doi.org/10.1371/journal.pone.0134140.

Eklund, C.M. (2009) 'Chapter 5 Proinflammatory cytokines in CRP baseline regulation', in *Advances in Clinical Chemistry*. Elsevier (Advances in Clinical Chemistry), pp. 111–136. Available at: https://doi.org/10.1016/S0065-2423(09)48005-3.

Espinosa, A.S. *et al.* (2023) 'Differences between cardiac troponin I vs. T according to the duration of myocardial ischaemia', *European Heart Journal. Acute Cardiovascular Care*, 12(6), pp. 355–363. Available at: https://doi.org/10.1093/ehjacc/zuad017.

Felaco, M. *et al.* (2001) 'Endothelial Nitric Oxide Synthase (eNOS) Expression and Localization in Healthy and Diabetic Rat Hearts', *Annals of Clinical & Laboratory Science*, 31(2), pp. 179–186.

Fernández-Solà, J. (2020a) 'The Effects of Ethanol on the Heart: Alcoholic Cardiomyopathy', *Nutrients*, 12(2), p. 572. Available at: https://doi.org/10.3390/nu12020572.

Fernández-Solà, J. (2020b) 'The Effects of Ethanol on the Heart: Alcoholic Cardiomyopathy', *Nutrients*, 12(2), p. 572. Available at: https://doi.org/10.3390/nu12020572.

Foster, P. *et al.* (2019) 'Circulating levels of cardiac troponin T are associated with coronary noncalcified plaque burden in HIV-infected adults: a pilot study', *International journal of STD & AIDS*, 30(3), pp. 223–230. Available at: https://doi.org/10.1177/0956462418800873.

Frati, G. *et al.* (2017) 'An overview of the inflammatory signalling mechanisms in the myocardium underlying the development of diabetic cardiomyopathy', *Cardiovascular Research*, 113(4), pp. 378–388. Available at: https://doi.org/10.1093/cvr/cvx011.

Funderburg, N.T. and Mehta, N.N. (2016) 'Lipid Abnormalities and Inflammation in HIV inflection', *Current HIV/AIDS reports*, 13(4), pp. 218–225. Available at: https://doi.org/10.1007/s11904-016-0321-0.

Funk, S.D., Yurdagul, A. and Orr, A.W. (2012) 'Hyperglycemia and Endothelial Dysfunction in Atherosclerosis: Lessons from Type 1 Diabetes', *International Journal of Vascular Medicine*, 2012, p. e569654. Available at: https://doi.org/10.1155/2012/569654.

Galley, H.F. and Webster, N.R. (2004) 'Physiology of the endothelium', *British Journal of Anaesthesia*, 93(1), pp. 105–113. Available at: https://doi.org/10.1093/bja/aeh163.

Graves, D.T. and Kayal, R.A. (2008) 'Diabetic complications and dysregulated innate immunity', *Frontiers in Bioscience: A Journal and Virtual Library*, 13, pp. 1227–1239. Available at: https://doi.org/10.2741/2757.

Hadi, H.A.R. and Suwaidi, J.A. (2007) 'Endothelial dysfunction in diabetes mellitus', *Vascular Health and Risk Management*, 3(6), pp. 853–876.

Hammarsten, O. *et al.* (2018) 'Possible mechanisms behind cardiac troponin elevations', *Biomarkers*, 23(8), pp. 725–734. Available at: https://doi.org/10.1080/1354750X.2018.1490969.

Hijmering, M.L. *et al.* (2007) 'Binge drinking causes endothelial dysfunction, which is not prevented by wine polyphenols: a small trial in healthy volunteers', *The Netherlands Journal of Medicine*, 65(1), pp. 29–35.

Hong, S.-W. *et al.* (2015) 'High-risk drinking is associated with a higher risk of diabetes mellitus in Korean men, based on the 2010–2012 KNHANES', *Alcohol*, 49(3), pp. 275–281. Available at: https://doi.org/10.1016/j.alcohol.2015.02.004.

Howard, A.A., Arnsten, J.H. and Gourevitch, M.N. (2004) 'Effect of alcohol consumption on diabetes mellitus: a systematic review', *Annals of Internal Medicine*, 140(3), pp. 211–219. Available at: https://doi.org/10.7326/0003-4819-140-6-200403160-00011.

Huff, T., Boyd, B. and Jialal, I. (2022) 'Physiology, Cholesterol', in *StatPearls*. Treasure Island (FL): StatPearls Publishing. Available at: http://www.ncbi.nlm.nih.gov/books/NBK470561/ (Accessed: 21 November 2022).

Husain, N.E. *et al.* (2017) 'Diabetes, metabolic syndrome and dyslipidemia in people living with HIV in Africa: re-emerging challenges not to be forgotten', *HIV/AIDS (Auckland, N.Z.)*, 9, pp. 193–202. Available at: https://doi.org/10.2147/HIV.S137974.

Hvidtfeldt, U.A. *et al.* (2010) 'Alcohol Intake and Risk of Coronary Heart Disease in Younger, Middle-Aged, and Older Adults', *Circulation*, 121(14), pp. 1589–1597. Available at: https://doi.org/10.1161/CIRCULATIONAHA.109.887513.

Iakunchykova, O. *et al.* (2020) 'Evidence for a Direct Harmful Effect of Alcohol on Myocardial Health: A Large Cross- Sectional Study of Consumption Patterns and Cardiovascular Disease Risk Biomarkers From Northwest Russia, 2015 to 2017', *Journal of the American Heart Association*, 9(1), p. e014491. Available at: https://doi.org/10.1161/JAHA.119.014491.

Imhof, A. and Koenig, W. (2003) 'Alcohol inflammation and coronary heart disease', *Addiction Biology*, 8(3), pp. 271–277. Available at: https://doi.org/10.1080/13556210310001602176.

International Diabetes Foundation (2021) 'IDF Diabetes Atlas | Tenth Edition'. Available at: https://diabetesatlas.org/ (Accessed: 22 November 2022).

Ioannou, G.N., Bryson, C.L. and Boyko, E.J. (2007) 'Prevalence and trends of insulin resistance, impaired fasting glucose, and diabetes', *Journal of Diabetes and its Complications*, 21(6), pp. 363–370. Available at: https://doi.org/10.1016/j.jdiacomp.2006.07.005.

Jankowski, J. *et al.* (2021) 'Cardiovascular Disease in Chronic Kidney Disease', *Circulation*, 143(11), pp. 1157–1172. Available at: https://doi.org/10.1161/CIRCULATIONAHA.120.050686.

Jia, G. and Sowers, J.R. (2021) 'Hypertension in Diabetes: An Update of Basic Mechanisms and Clinical Disease', *Hypertension*, 78(5), pp. 1197–1205. Available at: https://doi.org/10.1161/HYPERTENSIONAHA.121.17981.

Joshi, M.S. *et al.* (2012) 'Increased myocardial prevalence of C-reactive protein in human coronary heart disease: Direct effects on microvessel density and endothelial cell survival', *Cardiovascular pathology : the official journal of the Society for Cardiovascular Pathology*, 21(5), pp. 428–435. Available at: https://doi.org/10.1016/j.carpath.2011.12.003.

Julg, B. and Bogner, J.R. (2008) 'Atripla^{TM} – HIV therapy in one pill', *Therapeutics and Clinical Risk Management*, 4(3), pp. 573–577.

Kolluru, G.K., Bir, S.C. and Kevil, C.G. (2012) 'Endothelial Dysfunction and Diabetes: Effects on Angiogenesis, Vascular Remodeling, and Wound Healing', *International Journal of Vascular Medicine*, 2012, p. 918267. Available at: https://doi.org/10.1155/2012/918267.

Kovacs, L. *et al.* (2021) 'Chronic Exposure to HIV-Derived Protein Tat Impairs Endothelial Function via Indirect Alteration in Fat Mass and Nox1-Mediated Mechanisms in Mice',

International Journal of Molecular Sciences, 22(20), p. 10977. Available at: https://doi.org/10.3390/ijms222010977.

Kovacs, L., Kress, T.C. and Belin de Chantemèle, E.J. (2022) 'HIV, Combination Antiretroviral Therapy, and Vascular Diseases in Men and Women', *JACC: Basic to Translational Science*, 7(4), pp. 410–421. Available at: https://doi.org/10.1016/j.jacbts.2021.10.017.

Laonigro, I. *et al.* (2009) 'Alcohol abuse and heart failure', *European Journal of Heart Failure*, 11(5), pp. 453–462. Available at: https://doi.org/10.1093/eurjhf/hfp037.

Lehrke, M. and Marx, N. (2017) 'Diabetes Mellitus and Heart Failure', *The American Journal of Cardiology*, 120(1, Supplement), pp. S37–S47. Available at: https://doi.org/10.1016/j.amjcard.2017.05.014.

Li, X. *et al.* (2022) 'C-reactive protein and atrial fibrillation: Insights from epidemiological and Mendelian randomization studies', *Nutrition, Metabolism and Cardiovascular Diseases*, 32(6), pp. 1519–1527. Available at: https://doi.org/10.1016/j.numecd.2022.03.008.

Marincowitz, C. *et al.* (2019) 'Vascular endothelial dysfunction in the wake of HIV and ART', *The FEBS Journal*, 286, pp. 1256–1270. Available at: https://doi.org/10.1111/febs.14657.

Masenga, S.K. *et al.* (2020) 'Hypertension and Metabolic Syndrome in Persons with HIV', *Current Hypertension Reports*, 22(10), p. 78. Available at: https://doi.org/10.1007/s11906-020-01089-3.

Mbanya, J.C.N. *et al.* (2010) 'Diabetes in sub-Saharan Africa', *The Lancet*, 375(9733), pp. 2254–2266. Available at: https://doi.org/10.1016/S0140-6736(10)60550-8.

McCalister, A. *et al.* (2015) 'Excess Alcohol Consumption and Cardiac Fibrosis', *The FASEB Journal*, 29(S1), p. LB604. Available at: https://doi.org/10.1096/fasebj.29.1_supplement.lb604.

Melhuish, A. and Lewthwaite, P. (2018) 'Natural history of HIV and AIDS', *Medicine*, 46(6), pp. 356–361. Available at: https://doi.org/10.1016/j.mpmed.2018.03.010.

Minzer, S., Losno, R.A. and Casas, R. (2020) 'The Effect of Alcohol on Cardiovascular Risk Factors: Is There New Information?', *Nutrients*, 12(4), p. 912. Available at: https://doi.org/10.3390/nu12040912.

Mirijello, A. *et al.* (2017) 'Alcoholic cardiomyopathy: What is known and what is not known', *European Journal of Internal Medicine*, 43, pp. 1–5. Available at: https://doi.org/10.1016/j.ejim.2017.06.014.

Mirza, S. *et al.* (2012) 'Type 2-Diabetes is Associated With Elevated Levels of TNF-alpha, IL-6 and Adiponectin and Low Levels of Leptin in a Population of Mexican American: A Cross-Sectional Study', *Cytokine*, 57(1), pp. 136–142. Available at: https://doi.org/10.1016/j.cyto.2011.09.029.

Mohan, M. *et al.* (2021) 'Left Ventricular Hypertrophy in Diabetic Cardiomyopathy: A Target for Intervention', *Frontiers in Cardiovascular Medicine*, 8. Available at: https://www.frontiersin.org/articles/10.3389/fcvm.2021.746382 (Accessed: 16 November 2022).

Moncada, S. and Higgs, A. (1993) 'The L-arginine-nitric oxide pathway', *The New England Journal of Medicine*, 329(27), pp. 2002–2012. Available at: https://doi.org/10.1056/NEJM199312303292706.

Morojele, N.K. *et al.* (2006) 'Alcohol use and sexual behaviour among risky drinkers and bar and shebeen patrons in Gauteng province, South Africa', *Social Science & Medicine (1982)*, 62(1), pp. 217–227. Available at: https://doi.org/10.1016/j.socscimed.2005.05.031.

Mpinganjira, M.G. *et al.* (2023) 'Association of alcohol use and multimorbidity among adults aged 40 years and above in rural South Africa', *Scientific Reports*, 13(1), p. 7807. Available at: https://doi.org/10.1038/s41598-023-35018-6.

Nellessen, U. *et al.* (2006) 'Serial analysis of troponin I levels in patients with ischemic and nonischemic dilated cardiomyopathy', *Clinical Cardiology*, 29(5), pp. 219–224. Available at: https://doi.org/10.1002/clc.4960290510.

Nemoto, O. *et al.* (2006) 'Left Ventricular Dysfunction and Remodeling in Streptozotocin-Induced Diabetic Rats', *Circulation Journal*, 70(3), pp. 327–334. Available at: https://doi.org/10.1253/circj.70.327.

Ng, F. (2016) 'Diabetes-associated cardiac fibrosis: Cellular effectors, molecular mechanisms and therapeutic opportunities', *Journal of molecular and cellular cardiology*, 90. Available at: https://doi.org/10.1016/j.yjmcc.2015.12.011.

Noflatscher, M. *et al.* (2020) 'Association of Food and Alcohol Consumption with Peripheral Atherosclerotic Plaque Volume as Measured by 3D-Ultrasound', *Nutrients*, 12(12), p. 3711. Available at: https://doi.org/10.3390/nu12123711.

Nortamo, S. *et al.* (2017) 'Association of sST2 and hs-CRP levels with new-onset atrial fibrillation in coronary artery disease', *International Journal of Cardiology*, 248, pp. 173–178. Available at: https://doi.org/10.1016/j.ijcard.2017.07.022.

Odegaard, A.O. *et al.* (2016) 'Oxidative stress, inflammation, endothelial dysfunction and incidence of type 2 diabetes', *Cardiovascular Diabetology*, 15, p. 51. Available at: https://doi.org/10.1186/s12933-016-0369-6.

Osuji, F.N. *et al.* (2018) 'The effects of highly active antiretroviral therapy on the serum levels of pro-inflammatory and anti-inflammatory cytokines in HIV infected subjects', *Journal of Biomedical Science*, 25(1), pp. 1–8. Available at: https://doi.org/10.1186/s12929-018-0490-9.

Piano, M.R. (2017) 'Alcohol's Effects on the Cardiovascular System', *Alcohol Research : Current Reviews*, 38(2), p. 219.

Piano, M.R. *et al.* (2020) 'Effects of Alcohol on the Cardiovascular System in Women', *Alcohol Research : Current Reviews*, 40(2), p. 12. Available at: https://doi.org/10.35946/arcr.v40.2.12.

Polsky, S. and Akturk, H.K. (2017) 'Alcohol Consumption, Diabetes Risk, and Cardiovascular Disease Within Diabetes', *Current Diabetes Reports*, 17(12), p. 136. Available at: https://doi.org/10.1007/s11892-017-0950-8.

Potter, J.M., Hickman, P.E. and Cullen, L. (2022) 'Troponins in myocardial infarction and injury', *Australian Prescriber*, 45(2), pp. 53–57. Available at: https://doi.org/10.18773/austprescr.2022.006.

Rafieian-Kopaei, M. *et al.* (2014) 'Atherosclerosis: Process, Indicators, Risk Factors and New Hopes', *International Journal of Preventive Medicine*, 5(8), pp. 927–946.

Raghavan, S. *et al.* (2019) 'Diabetes Mellitus–Related All- Cause and Cardiovascular Mortality in a National Cohort of Adults', *Journal of the American Heart Association*, 8(4), p. e011295. Available at: https://doi.org/10.1161/JAHA.118.011295.

Randell, P. and Moyle, G. (2009) 'Antiretroviral therapy with heart', *American Journal of Therapeutics*, 16(6), pp. 579–584. Available at: https://doi.org/10.1097/MJT.0b013e318192116f.

Rodriguez, A. *et al.* (2015) 'Alcohol and Apoptosis: Friends or Foes?', *Biomolecules*, 5(4), pp. 3193–3203. Available at: https://doi.org/10.3390/biom5043193.

Ross, M.H. (2018) *Histology: a text and atlas: with correlated cell and molecular biology*. 8th edition. Philadelphia: Wolters Kluwer.

Roth, G.A. *et al.* (2020) 'Global Burden of Cardiovascular Diseases and Risk Factors, 1990–2019', *Journal of the American College of Cardiology*, 76(25), pp. 2982–3021. Available at: https://doi.org/10.1016/j.jacc.2020.11.010.

Sapuła, M. *et al.* (2022) 'Impact of Combined Antiretroviral Therapy on Metabolic Syndrome Components in Adult People Living with HIV: A Literature Review', *Viruses*, 14(1), p. 122. Available at: https://doi.org/10.3390/v14010122.

Schwinger, R.H.G. (2021) 'Pathophysiology of heart failure', *Cardiovascular Diagnosis and Therapy*, 11(1), pp. 263–276. Available at: https://doi.org/10.21037/cdt-20-302.

Segre, C.A.W. *et al.* (2015) 'Troponin in diabetic patients with and without chronic coronary artery disease', *BMC Cardiovascular Disorders*, 15(1), p. 72. Available at: https://doi.org/10.1186/s12872-015-0051-z.

Sena, C.M. *et al.* (2018) 'Vascular Oxidative Stress: Impact and Therapeutic Approaches', *Frontiers in Physiology*, 9, p. 1668. Available at: https://doi.org/10.3389/fphys.2018.01668.

Serhiyenko, V.A. and Serhiyenko, A.A. (2018) 'Cardiac autonomic neuropathy: Risk factors, diagnosis and treatment', *World Journal of Diabetes*, 9(1), pp. 1–24. Available at: https://doi.org/10.4239/wjd.v9.i1.1.

Sert, N.P. du *et al.* (2020) 'Reporting animal research: Explanation and elaboration for the ARRIVE guidelines 2.0', *PLOS Biology*, 18(7), p. e3000411. Available at: https://doi.org/10.1371/journal.pbio.3000411.

Sharif, S. *et al.* (2021) 'Low-grade inflammation as a risk factor for cardiovascular events and all-cause mortality in patients with type 2 diabetes', *Cardiovascular Diabetology*, 20(1), p. 220. Available at: https://doi.org/10.1186/s12933-021-01409-0.

Shikuma, C.M. *et al.* (2011) 'Change in High-Sensitivity C-Reactive Protein Levels Following Initiation of Efavirenz-Based Antiretroviral Regimens in HIV-Infected Individuals', *AIDS Research and Human Retroviruses*, 27(5), pp. 461–468. Available at: https://doi.org/10.1089/aid.2010.0154.

Simó, R. *et al.* (2019) 'Diabetic retinopathy as an independent predictor of subclinical cardiovascular disease: baseline results of the PRECISED study', *BMJ Open Diabetes Research and Care*, 7(1), p. e000845. Available at: https://doi.org/10.1136/bmjdrc-2019-000845.

Smarr, B.L. *et al.* (2017) 'Sex differences in variability across timescales in BALB/c mice', *Biology of Sex Differences*, 8, p. 7. Available at: https://doi.org/10.1186/s13293-016-0125-3.

Soccal, R.M. *et al.* (2016) 'Nitric oxide levels in HIV-infected, untreated patients and HIV-infected patients receiving antiretroviral therapy', *Biomedicine & Pharmacotherapy*, 79, pp. 302–307. Available at: https://doi.org/10.1016/j.biopha.2016.02.027.

Soufen, H.N. *et al.* (2008) 'Collagen content, but not the ratios of collagen type III/I mRNAs, differs among hypertensive, alcoholic, and idiopathic dilated cardiomyopathy', *Brazilian Journal of Medical and Biological Research*, 41, pp. 1098–1104. Available at: https://doi.org/10.1590/S0100-879X2008001200009.

Steven, S. *et al.* (2019) 'Vascular Inflammation and Oxidative Stress: Major Triggers for Cardiovascular Disease', *Oxidative Medicine and Cellular Longevity*, 2019, p. e7092151. Available at: https://doi.org/10.1155/2019/7092151.

Sun, J. *et al.* (2021) 'Hyperglycaemia-associated Caspase-3 predicts diabetes and coronary artery disease events', *Journal of internal medicine*, 290(4), p. 855. Available at: https://doi.org/10.1111/joim.13327.

Taylor, A.M. and Bordoni, B. (2022) 'Histology, Blood Vascular System', in *StatPearls*. Treasure Island (FL): StatPearls Publishing. Available at: http://www.ncbi.nlm.nih.gov/books/NBK553217/ (Accessed: 17 November 2022).

Thorand, B. *et al.* (2003) 'C-Reactive Protein as a Predictor for Incident Diabetes Mellitus Among Middle-aged Men: Results From the MONICA Augsburg Cohort Study, 1984-1998', *Archives of Internal Medicine*, 163(1), pp. 93–99. Available at: https://doi.org/10.1001/archinte.163.1.93.

Thrower, S.L. and Bingley, P.J. (2014) ‘What is type 1 diabetes?’, *Medicine*, 42(12), pp. 682–686. Available at: https://doi.org/10.1016/j.mpmed.2014.09.003.

Tirziu, D. and Simons, M. (2008) ‘Endothelium-driven myocardial growth or nitric oxide at the crossroads’, *Trends in cardiovascular medicine*, 18(8), pp. 299–305. Available at: https://doi.org/10.1016/j.tcm.2009.01.002.

Toda, N. and Ayajiki, K. (2010) ‘Vascular Actions of Nitric Oxide as Affected by Exposure to Alcohol’, *Alcohol and Alcoholism*, 45(4), pp. 347–355. Available at: https://doi.org/10.1093/alcalc/agq028.

Tran, N. *et al.* (2022) ‘Endothelial Nitric Oxide Synthase (eNOS) and the Cardiovascular System: in Physiology and in Disease States’, *American journal of biomedical science & research*, 15(2), pp. 153–177.

Triposkiadis, F. *et al.* (2021) ‘Diabetes Mellitus and Heart Failure’, *Journal of Clinical Medicine*, 10(16), p. 3682. Available at: https://doi.org/10.3390/jcm10163682.

Tsermpini, E.E., Plemenitaš Ilješ, A. and Dolžan, V. (2022) ‘Alcohol-Induced Oxidative Stress and the Role of Antioxidants in Alcohol Use Disorder: A Systematic Review’, *Antioxidants*, 11(7), p. 1374. Available at: https://doi.org/10.3390/antiox11071374.

UNAIDS (2022) *Fact sheet - Latest global and regional statistics on the status of the AIDS epidemic.*, *UNAIDS*. Available at: https://www.unaids.org/en/resources/documents/2022/UNAIDS_FactSheet (Accessed: 22 November 2022).

Urschel, K. and Cicha, I. (2015) ‘TNF-α in the cardiovascular system: from physiology to therapy’, *International Journal of Interferon, Cytokine and Mediator Research*, 7, pp. 9–25. Available at: https://doi.org/10.2147/IJICMR.S64894.

Vaideeswar, P. *et al.* (2014) ‘Cardiac pathology in chronic alcoholics: A preliminary study’, *Journal of Postgraduate Medicine*, 60(4), p. 372. Available at: https://doi.org/10.4103/0022-3859.143958.

Vandormael, A. *et al.* (2019) ‘Declines in HIV incidence among men and women in a South African population-based cohort’, *Nature Communications*, 10(1), p. 5482. Available at: https://doi.org/10.1038/s41467-019-13473-y.

Vitoria, M. *et al.* (2018) ‘The transition to dolutegravir and other new antiretrovirals in low-income and middle-income countries: what are the issues?’, *AIDS (London, England)*, 32(12), pp. 1551–1561. Available at: https://doi.org/10.1097/QAD.0000000000001845.

Volpe, C.M.O. *et al.* (2018) ‘Cellular death, reactive oxygen species (ROS) and diabetic complications’, *Cell Death & Disease*, 9(2), p. 119. Available at: https://doi.org/10.1038/s41419-017-0135-z.

Walubo, A. (2007) ‘The role of cytochrome P450 in antiretroviral drug interactions’, *Expert Opinion on Drug Metabolism & Toxicology*, 3(4), pp. 583–598. Available at: https://doi.org/10.1517/17425225.3.4.583.

Wang, M. *et al.* (2022) ‘Endothelial Dysfunction and Diabetic Cardiomyopathy’, *Frontiers in Endocrinology*, 13. Available at: https://www.frontiersin.org/articles/10.3389/fendo.2022.851941 (Accessed: 16 November 2022).

Wang, S. and Ren, J. (2018) 'Role of autophagy and regulatory mechanisms in alcoholic cardiomyopathy', *Biochimica et Biophysica Acta (BBA) - Molecular Basis of Disease*, 1864(6, Part A), pp. 2003–2009. Available at: https://doi.org/10.1016/j.bbadis.2018.03.016.

Watanabe, L.M. *et al.* (2016) 'Influence of HIV infection and the use of antiretroviral therapy on selenium and selenomethionine concentrations and antioxidant protection', *Nutrition*, 32(11), pp. 1238–1242. Available at: https://doi.org/10.1016/j.nut.2016.03.024.

Wei, J. *et al.* (2022) 'Preliminary evidence for the presence of multiple forms of cell death in diabetes cardiomyopathy', *Acta Pharmaceutica Sinica B*, 12(1), pp. 1–17. Available at: https://doi.org/10.1016/j.apsb.2021.08.026.

Weil, B.R. and Ozcan, C. (2015) 'Cardiomyocyte Remodeling in Atrial Fibrillation and Hibernating Myocardium: Shared Pathophysiologic Traits Identify Novel Treatment Strategies?', *BioMed Research International*, 2015, p. 587361. Available at: https://doi.org/10.1155/2015/587361.

Wilson, H.I. and Mapesi, H. (2020) 'Rollout of dolutegravir-based antiretroviral therapy in sub-Saharan Africa and its public health implications', *The Pan African Medical Journal*, 37, p. 243. Available at: https://doi.org/10.11604/pamj.2020.37.243.25512.

Wilson, R.D. and Islam, Md.S. (2012) 'Fructose-fed streptozotocin-injected rat: an alternative model for type 2 diabetes', *Pharmacological Reports*, 64(1), pp. 129–139. Available at: https://doi.org/10.1016/S1734-1140(12)70739-9.

Wu, D. and Cederbaum, A.I. (2003) 'Alcohol, Oxidative Stress, and Free Radical Damage', *Alcohol Research & Health*, 27(4), pp. 277–284.

Xu, S. *et al.* (2021) 'Endothelial Dysfunction in Atherosclerotic Cardiovascular Diseases and Beyond: From Mechanism to Pharmacotherapies', *Pharmacological Reviews*. Edited by Q. Ma, 73(3), pp. 924–967. Available at: https://doi.org/10.1124/pharmrev.120.000096.

Yan, L. (2018) 'Redox imbalance stress in diabetes mellitus: Role of the polyol pathway - Yan - 2018 - Animal Models and Experimental Medicine - Wiley Online Library', *Animal Models and Experimental Medicine*, 1(1), pp. 7–13. Available at: https://doi.org/10.1002/ame2.12001.

APPENDICES

1. Silane coated slides

1. Immerse slides in 3% 3-aminopropyltriethoxysilane (APES) in acetone	30 minutes
2. Rinse in 2 x acetone	
3. Rinse in distilled water	
4. Leave to dry at room temperature	Overnight
5. Store at 4ºC	± 2 months

2. Haematoxylin and Eosin stain

Dewax and Hydrate

1. Dewax in xylene	2 x 10 minutes
2. Immerse in 100% ethanol for	2 x 10 dips
3. Immerse in 95% ethanol for	1 x 10 dips

4. immerse in 70% ethanol for	1 x 10 dips
5. Wash in running water for	1 minute
Nuclear Staining	
6. Stain in Meyer's Haematoxylin	12 minutes
7. Wash in running tap water	5 minutes
8. Differentiate in 1% acid alcohol for 1 dip	
9. Wash in running tap water	5 minutes
10. Stain in Scott's tap water for	5 minutes
11. Wash in running tap water	5 minutes
Cytoplasmic staining	
12. Stain in Eosin	12 minutes
13. Rinse in tap water.	
Dehydrate and mount	
14. Immerse in 70% ethanol	10 dips
15. Immerse in 95% ethanol	10 dips
16. Immerse in 100% ethanol	2 x 10 dips
17. Immerse in xylene	2 x 10 dips
18. Mount in Entellen	

3. Modified Verhoeff Van Gieson stain

Solutions

Modified Verhoeff working elastic solution

3 parts 3% Haematoxylin in 95% alcohol

2 parts 2% ferric chloride in 100ml distilled water

1 part Lugol's iodine

Lugol's Iodine

Lugol's Iodine	1g
Potassium Iodide	2g
Distilled water	100ml

Van Gieson solution

Saturated Picric Acid	100ml
1% aqueous Acid Fuchsin	18ml
Distilled water	100ml

Method:

Dewax and Hydrate

1. Dewax in xylene	2 x 10 minutes
2. Immerse in 100% ethanol for	2 x 10 dips

3. Immerse in 95% ethanol for	1 x 10 dips
4. immerse in 70% ethanol for	1 x 10 dips
5. Wash in running water for	5 minute

Staining

6. Stain in modified Verhoeff working elastic solution	7 minutes
7. Wash in running tap water	1 minute
8. Differentiate in 0.4% aqueous Ferric Chloride	1 minute

* Check differentiation microscopically

9. Wash in running tap water	5 minutes
10. Counterstain in Van Gieson solution	1 minute

Dehydrate and mount

11. Immerse in 70% ethanol	5 dips
12. Immerse in 95% ethanol	5 dips
13. Immerse in 100% ethanol	2 x 10 dips
14. Immerse in xylene	2 x 10 dips

15. Mount in Entellen

4. Modified Pentachrome stain

Solutions

6% Nitric acid in Distilled water

0.5% Toluidine blue in Distilled water

0.1% Picrosirius staining solution (0.5g Sirius red dissolved in 500ml distilled water, saturated in picric acid)

Method

Dewax and Hydrate

1. Dewax in xylene	2 x 10 minutes
2. Immerse in 100% ethanol for	2 x 10 dips
3. Immerse in 95% ethanol for	1 x 10 dips
4. immerse in 70% ethanol for	1 x 10 dips
5. Wash in running water for	5 minutes

Staining

6. Pre-treat with 6% Nitric acid	5 minutes
7. Stain with toluidine blue solution	5 minutes
8. Rinse in distilled water	
9. Stain with Picrosirius solution	5 minutes
10. Rinse in distilled water	

Dehydrate and mount

11. Immerse in 70% ethanol	5 dips

12. Immerse in 95% ethanol	5 dips
13. Immerse in 100% ethanol	2 x 10 dips
14. Immerse in xylene	2 x 10 dips

15. Mount in Entellen

5. Immunohistochemistry

Immunohistochemistry Solutions

10Mm Sodium Citrate Buffer pH 6

Tri Sodium citrate (dehydrate)	2.9g
Distilled water	1000ml
0.3% Triton X	3ml

Mix to dissolve sodium citrate and adjust pH to 6 with 1M HCl.

1M Phosphate Buffer pH 7.4

NaCl	16g
Na_2HPO_4	3.5g
KCl	0.4g
KH_2PO_4	0.4g
Distilled water	2000g

Mix to dissolve and adjust pH to 7.4 with 1M HCl.

Normal goat serum

PBS	100µl
Normal goat serum	3µl

Make up enough for the number of slides used.

Primary antibody

3% Normal goat serum	1000 µl
Secondary antibody	1 µl

Make up enough for the number of slides used.

Secondary antibody

3% Normal goat serum	1000 µl
Secondary antibody	1 µl

Make up enough for the number of slides used.

ABC

25µl A + 25µl B + 1.25ml PBS. Make up 30 minutes before use.

DAB working solution

a) In a clean bijou bottle measure out 1mg DAB (0.001g). To this, add Tris HCl and mix well.
b) In a separate tube, add:

    29µl cold distilled water

1µl hydrogen peroxide (100%)

Add 20µl of solution b) to DAB sol a).

IHC Method for 5µl paraffin sections

Day 1

1. Deparaffinize sections in xylene for	2x 10 minutes
2. Rehydrate sections through graded alcohols	
3. Wash slides in running water	5 minutes
4. Antigen retrieve sections in Citrate buffer pH 6 in water bath at 60ºC	Overnight

Day 2

5. Allow sections to cool to room temperature for	20 minutes
6. Rinse slides in PBS	1 x 5 minutes
7. Block endogenous peroxide with 2% H_2O_2 in methanol.	15 minutes
8. Wash slides in PBS pH 7.4	3 x 5minutes
9. Incubate with 5% normal goat serum (100µl per slide) at room temperature	30 minutes
10. Tap serum off slides. DO NOT WASH	
11. Incubate with primary antibody at 4ºC	Overnight

Day 3

12. Allow sections to reach room temperature	
13. Wash in PBS pH 7.4	3 x 5 minutes
14. Incubate in biotinylated secondary antibody	30 minutes

***MAKE UP ABC**

15. Wash in PBS pH 7.4	3 x 5 minutes
16. Incubate in ABC (make up ABC 30 minutes before use)	30 minutes
17. Wash in PBS pH 7.4	3 x 5 minutes
18. Incubate with DAB working solution	5 minutes
19. Rinse in running tap water	5 minutes
20. Counterstain with diluted Haematoxylin	15 seconds

21. Dehydrate through graded alcohols, clear in xylene, and mount with Entellen.

***Negative control: replace the primary antibody with normal goat serum.**

6. ImageJ Analysis

1. Grid plugin with cell counter tool

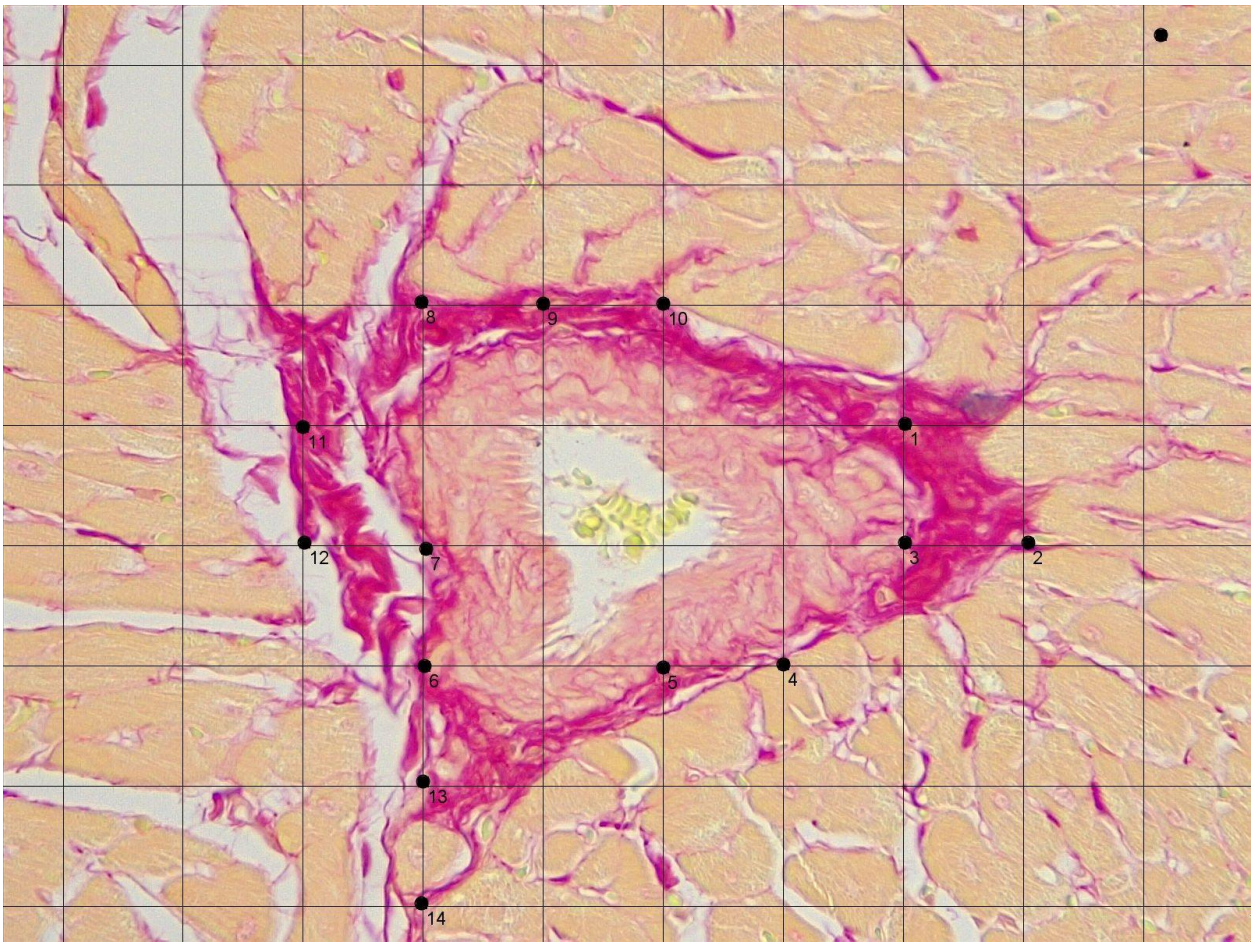

2. Straight line tool

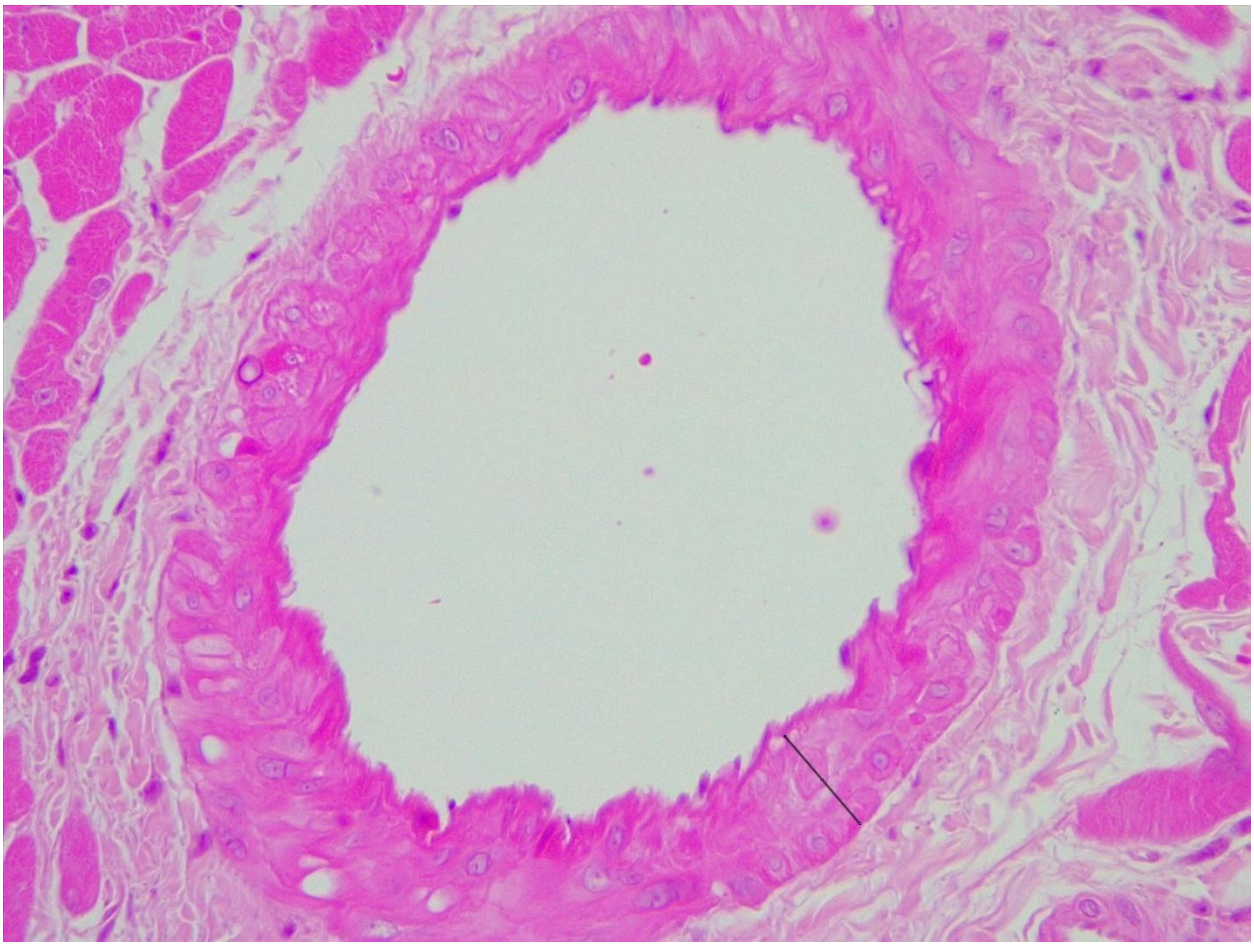

7. Ethical Clearance

AREC 2017 M&E

Please note that only typewritten applications will be accepted.

UNIVERSITY OF THE WITWATERSRAND
ANIMAL RESEARCH ETHICS COMMITTEE
MODIFICATIONS AND EXTENSIONS TO EXPERIMENTS

a. Name: Prof Ejikeme Mbajiorgu
Staff number: A

b. School and email address: Anatomical Sciences, Ejikeme.mbajiorgu@wits.ac.za

c. Experiment to be modified / extended

Original AESC number	2018	011	58C
Other M&Es :			04

d. Project Title: CHARACTERIZATION OF STREPTOZOTOCIN INDUCED DIABETIC MALE SPRAGUE-DAWLEY RATS WITH CHRONIC ALCOHOL INTAKE AND ANTIRETROVIRAL THERAPY.

		No.	Species
e.	Number and species of animals originally approved:	120	*Sprague- Dawley rats*
f.	Number of additional animals previously allocated on M&Es:	N/A	
g.	Total number of animals allocated to the experiment to date:	107	
h.	Number of animals used to date:	107	

i. Specific modification ~~/ extension requested~~:

Change of Permit or PI:

a. 1.This was a group research project which I initiated and accepted three of my students who enrolled (Dr I Eguvoen, Ms Jaclyn Johnson and Mr Vaughan) in the project. Jaclyn has completed her PhD, Dr Eguvoen and Mr Vaughan (SMU staff) has moved to SMU.

b. 2. However, the ethics permit was issued on the name of DR. I Eguvoen, Student ID 0616737M, who is finalizing his thesis analysis at SMU.

c. 3. But, I have admitted two new master's students to continue the work on other tissues that I collected during the experiment.

d. In other to facilitate their studies, I am therefore requesting for the ethics permit to be transferred to my name as the original PI to enable the use of the tissues collected for further studies without hindrance.

Inclusion of MSc students

a. Inclusion of **Mcebo Zwane** (student number; 1473425) and **Mmotong Mahloko** (student number; 1863024) as co-workers for their M.Sc. degree projects in the School Anatomical Sciences.

b. The students will use the heart, lungs, vascular tissue, and blood samples already harvested from the study for the purpose of a M.Sc. degree with Prof Ejikeme Mbajiorgu and Dr Jaclyn Asouzu Johnson as supervisors.

c. The student will use already harvested tissue for the study of treatment effects on organs, which does not involve any new animal, treatment or extra use of the WRAF facility.

j. Motivation for modification / extension:

This will enable this student, **Mcebo Zwane** (student number; 1473425) and **Mmotong Mahloko** (student number; 1863024) to use the tissue and avoid wasting this tissue, extra-funding and thereby maximising the use of the animals in the study as approved.

Date: 30/11/2022 Signature:

RECOMMENDATIONS

Extension of the study until the 31 December 2023.
Approval for the transfer of the study to Prof. Mbajiorgu as the PI.
Approval for the inclusion of MSc students; M. Zwane and M. Mahloko as co-workers on the protocol, and to access the described, stored tissue samples for in vitro analysis.

Date:18 December 2022 Signature:

Deputy Chair, AREC